DYNAMIC RELIABILITY USING ENTRY-TIME APPROACH

FOR MAINTENANCE OF NUCLEAR POWER PLANTS

A Dissertation

by

SHUWEN WANG

Submitted to the Office of Graduate Studies of
Texas A&M University
in partial fulfillment of the requirements for the degree of

DOCTOR OF PHILOSOPHY

May 2008

Major Subject: Nuclear Engineering

DYNAMIC RELIABILITY USING ENTRY-TIME APPROACH

FOR MAINTENANCE OF NUCLEAR POWER PLANTS

A Dissertation

by

SHUWEN WANG

Submitted to the Office of Graduate Studies of
Texas A&M University
in partial fulfillment of the requirements for the degree of

DOCTOR OF PHILOSOPHY

Approved by:

Chair of Committee,   Paul Nelson
Committee Members, Marvin L. Adams
                                 Martin A. Wortman
                                 Guergana P. Petrova
Head of Department,   Raymond Juzaitis

May 2008

Major Subject: Nuclear Engineering

ABSTRACT

Dynamic Reliability Using Entry-time Approach for

Maintenance of Nuclear Power Plants. (May 2008)

Shuwen Wang, B.S., Shanghai Jiao Tong University;

M.E., Texas A&M University

Chair of Advisory Committee: Dr. Paul Nelson

Entry-time processes are finite-state continuous-time jump processes with transition rates depending only on the two states involved in transition, the calendar time, and the most recent arrival time, which is termed as *entry-time*.

The entry-time processes have the potential to provide a significantly greater range of applicability and flexibility than traditional reliability tools for case studies related to equipment and components in nuclear power plants.

In this dissertation, the finite difference approximation of the integrodifferential Chapman-Kolmogorov equations for the entry-time processes was developed, and then it was verified by application to some hypothetical examples that are solved by alternative means, either (semi-)analytically or via simulation.

To demonstrate the ability of entry-time model to applications in nuclear power plants for a RIAM based scenario, the entry-time approach is applied to the maintenance of main generators in nuclear power using the data from INPO-EPIX database. In this application, both reliability and financial performances acquired using the entry-time

approaches corresponding to different maintenance policies are presented and discussed to help make maintenance decisions for the plant management.

The ability of the EPIX database to provide time-dependent failure rates is demonstrated and the techniques for extraction of failure rates from the database for main generators are also discussed.

ACKNOWLEDGEMENTS

First, I would like to thank my advisor Dr. Paul Nelson for his support during my study at Texas A&M University and especially during the work of the dissertation.

I would like to thank all other professors on my committee: Dr. Marvin Adams, Dr. Martin Wortman and Dr. Guergana Petrova for their advice and valuable suggestions in finishing the dissertation.

I would like to thank Mr. Ernie Kee, from STP, for his generous help and support for both my work and dissertation.

I also would like to thank INPO for their generous help with the EPIX database, especially the help from Mr. Glenn Masters.

Finally, I would like to thank my wife, Yana, for her love and continuous support during the work of the dissertation.

TABLE OF CONTENTS

LIST OF TABLES

Page

LIST OF FIGURES

Page

Page

CHAPTER I

INTRODUCTION

The objective of the research underlying this dissertation was to develop, assess and demonstrate applicability of a novel reliability methodology, centered about what we term as "entry-time processes," that has the potential to provide a significantly greater range of applicability and flexibility than traditional reliability tools for case studies related to equipment and components in nuclear power plants.

The essential idea of the entry-time methodology is to expand traditional finite-state Markov models, whose application to equipment reliability and maintenance issues for nuclear power plants is well known [1], by appending "entry time" (the time at which the system entered its present finite state) as an additional continuous state variable. This extension permits reliability issues for equipment having time-dependent failure rates, or more generally time-dependent transition rates between arbitrarily defined finite states, to be treated via Markov models. See Chapter II below for further details.

The inclusion of entry time as a state variable leads to Chapman-Kolmogorov equations that have an integrodifferential form (cf. also Chapter II below), in contrast to the linear system of ordinary differential equations that constitute the Chapman-Kolmogorov equations for a finite-state Markov model. It is well known (e.g., [2]) that the neutron transport equation is also an instance of such an integrodifferential Chapman-Kolmogorov equation. In recognition of this analogy, we propose here to

---

This dissertation follows the style of Reliability Engineering and System Safety.

solve the Chapman-Kolmogorov equations in the reliability application by adapting discrete algorithms of the type widely employed in neutron transport theory (cf. Chapter III below). By contrast, DeVooght and Smidts [3] employed Monte Carlo methods for the solution of their prototypical state-transition equations when modeling safety-related considerations in nuclear power plants. The entry-time process is flexible in definition of states, i.e. the definition of states can be changed according to different modeling requirements. Last, but not least, the capability of allowing tracking of probabilities of "intermediate" events (e.g. states of a given system other than "failure" and "running") can help to make management decisions on preventive and corrective maintenance, and to develop systematic policies related to enhancement of system or component reliability.

The entry-time methodology has particular potential for incorporation into case studies supporting plant planning, and related case studies, including such matters as the effects of component aging and the scheduling of inspections, tests and planned preventive maintenance activities. This potential is demonstrated in Chapter V below, in application to an economically significant reactor subsystem, here selected as the main generator system. The potential for this sort of application can only be further enhanced by obtaining improved estimates of equipment failure rates through first-principles consideration of the underlying causes of failure. Nonetheless, extraction of failure rates from limited amounts of data, for specific systems, structures and components (SSCs), appears likely, for the foreseeable future, to be one of the more difficult aspects of applying any methodology for quantitatively analyzing equipment reliability issues. In this dissertation these issues are treated in Chapter IV.

In a speech given by Nuclear Regulatory Commission (NRC) Chairman Dale E. Klein, it mentions that "…In fact, I think it can be safely said that the Nuclear Renaissance has officially begun …[4]". With the fast growing nuclear business and developing nuclear technology, nuclear energy has been more competitive comparing to coal and gas energy. While many factors have contributed to this competitive resurgence of nuclear energy, two of the central causes are a remarkable improvement in unit capacity factors and a significant trend toward power upratings [5]. Many changes in the overall economic/regulatory setting have provided the motivation for these industry-wide changes, and many improvements in industry practice have contributed to their enablement. The general philosophy underlying these improvements is a proactive approach to simultaneous and objective consideration of both financial and engineering factors so as to support management decisions directed toward increasing overall energy output while ensuring plant safety. This philosophical approach has become symbolized by the term "asset management." As such it is embodied in the RIAM (Risk-informed Asset Management) concept [6] that has been aggressively pursued by STPNOC (South Texas Plant Nuclear Operating Company), the complementary NAM (Nuclear Asset/Risk Management) program [7] of EPRI, and the Nuclear Asset Management task force of the Nuclear Electric Institute (NEI). As one of the important parts of the RIAM programs, Life Cycle Management (LCM) is becoming the standard to measure plant excellence [8]. In the report prepared by Gregor and Chockie (also see [8]), different aging management programs including LCM are summarized. Among all the programs, EPRI developed Aging Management Tools for mechanical and structural equipment to

provide guidance to the plant licensees; also EPRI initiated the Preventive Maintenance (PM) project to develop an industry consensus of best practices for maintenance and aging management. The Institute of Nuclear Power Operations (INPO) led the development of an equipment reliability guide (AP-913) that incorporated the PM basis, LCM and Reliability Centered Maintenance (RCM) programs. Other similar research has been done in US Department of Energy (DOE) and NRC. In particular, NRC has done some License Renewal (LR) research to investigate the aging degradation of safety-related equipments and later the safety requirements for LR were made mandatory requirements as part of the regulations. The relationship of various industry and NRC programs is shown in Figure 1 [8].

Asset management has been identified, in the context of nuclear power, as the practice of resource allocation and risk management at all levels of an electricity-generating company to create maximum value and profitability to stakeholders. Liming and Grantom (see also [6]) define risk-informed asset management as follows: "RIAM is a process by which analysts review historical performance and develop logic models and data analyses to predict critical decision support figures-of-merit (or metrics) for generating station managers and electric utility company objectives. These metrics include, but are not limited to: profitability, projected revenue, projected costs, asset value, safety, power production availability, efficiency and others. These authors continue to clarify that RIAM "complements and integrates existing activities like PRA, preventive maintenance optimization (PMO), life cycle management (LCM), and nuclear asset management (NAM) methodologies." The importance of proactively managing

plant assets can only be increased by the current NRC movement away from traditional prescriptive regulations, in favor of performance-based implementation of risk-based regulations [9].
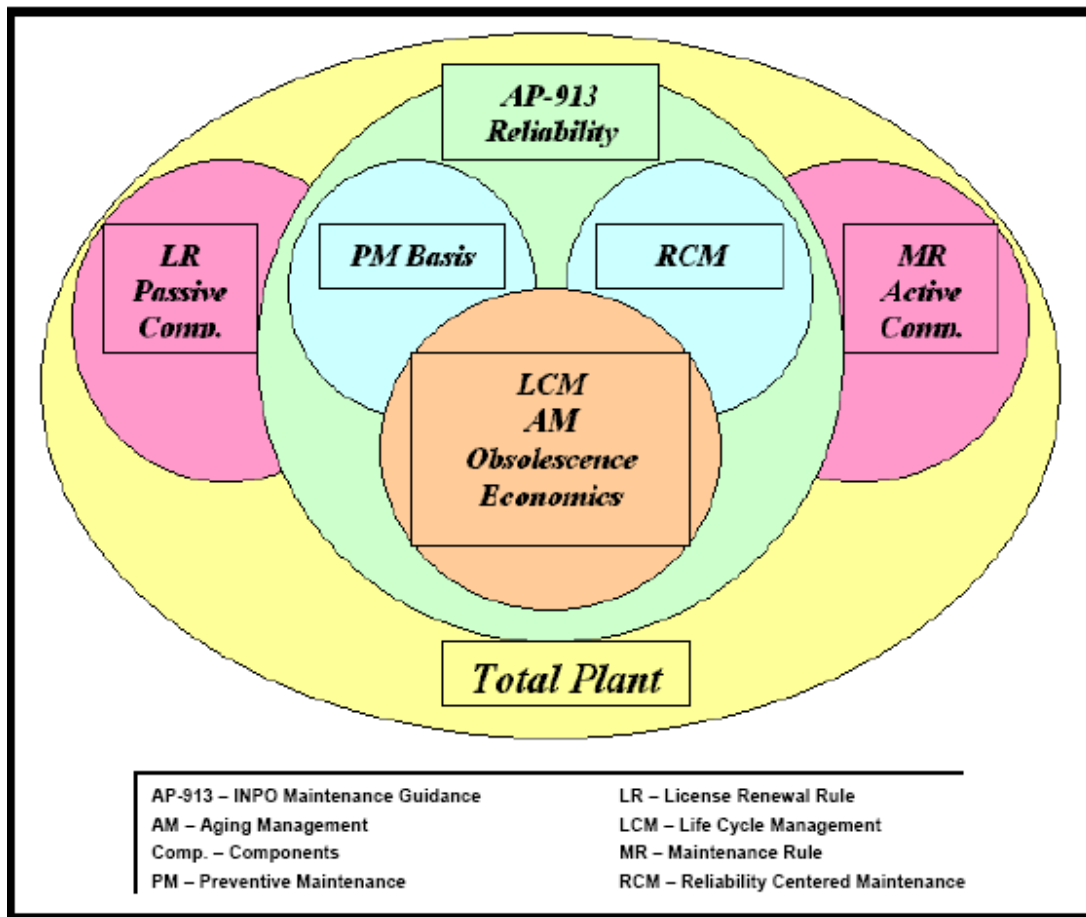
Figure 1. The relationship of aging management programs [8]

In the current nuclear industry, a lot of effort (as summarized in [10]) has been put into the development of applicable models that can be used to enhance power-plant performance, such as increasing power output, or decreasing cost while still meeting the

required safety objective. EPRI and its user group are building new Generation Risk Assessment (GRA) [11] models based on the existing PRA models. GRA models provide a systematic approach to estimating how equipment reliability relates to the risk of future lost generation from trips and derates and to prioritizing components and systems based on their importance to productivity. Others such as the reliability group at Comanche Peak nuclear power plant are doing some SPV (Single Point Vulnerability) analysis to all the key components in nuclear systems so that they can focus on increasing the reliability performance of those key components in order to optimize nuclear-power-plant safety/economic performance. No matter what methods or models are used, they have the same goal, which is simultaneous and objective consideration of both financial and engineering factors so as to support management decisions directed toward increasing overall energy output while ensuring plant safety.

The above applications tend generically to fall within the area of reliability and maintenance. Within the general area of reliability and maintenance, such practices as proactive in-service inspection, testing and preventive maintenance of plant components and subsystems, of course with due regard for safety-based regulatory constraints, have played a major role in the industry-wide performance improvements cited in the preceding section. The importance of in-service inspection, testing and preventive maintenance can only be increased by the current Nuclear Regulatory Commission (NRC) movement away from traditional prescriptive regulations, in favor of performance-based implementation of risk-based regulations.

Many of the generic applications have motivated some of the developments of asset management techniques and tools for nuclear applications, and in turn have been the subject of applications of these techniques and tools. However, almost all the current applications are based on constant failure rate assumptions, which arises problems when dealing with aging and degradation phenomena in safety-significant nuclear power plant equipments [12]. Therefore, it's important to find new approaches in Nuclear Asset Management (NAM) and Risk-informed Asset Management (RIAM) which can not only meet the risk-based requirement but also solve the aging and degradation phenomena which normally bring time-dependent failure rates or transition rates. The proposed methodology "entry-time process" will give a new approach in the application of risk-based nuclear asset management. On the one hand, the entry-time process solves the time-dependent transition rates related problems in the current Nuclear Asset Management (NAM) and Risk-informed Asset Management (RIAM) applications. On the other hand, this process can support management decisions directed toward increasing overall reliability while still meeting the economic demands in order to maximize the plant output and minimizing costs related to maintenance and plant enhancement. Also it may provide a new methodology for applications in PRA and GRA in nuclear power plants to include time-dependent features based on the existing models.

In the past two decades, a number of methods such as Probabilistic Risk Assessment (PRA), Markov models (cf. [1]), simulation [13] and other methods for risk assessment of dynamic systems [14] have been used to evaluate SSC (System, Structure and Component) reliability in NPP (Nuclear Power Plants) to ensure NPP safety. Among all

these models, PRA model is one of the most popular models that are being used in nuclear industry. However, the assumption of constant failure rates in the PRA model has restricted the application of this model at a certain level [15]. It has been proved that aging is an important factor in NPP component failure such as piping system rapture [16]. It is clear that failure due to aging is not constant; rather, by definition aging is the phenomena of a failure rate that increases with time, at least until further actions such as repair or replacement are taken. To solve this problem, we need to find a new methodology that incorporates aging effects and maintenance policies into the existing PRA model and further with the new GRA model, which are on the current forefront of developments in the nuclear industry, to achieve better results for system reliability/risk assessment and to support management decisions directed toward increasing overall energy output while ensuring plant safety objectives continue to be met. There are some jobs done (such as [17]) to incorporate aging effects into PRA, similarly, the dynamic reliability parameters generated by the entry-time approach at the system level can be used as input to the static PRA and GRA models to incorporate preventive maintenance policies and aging affects.

In this dissertation, the objective of developing, verifying and applying the entry-time approach is accomplished as follows: In Chapter II the entry-time model is defined, the corresponding integrodifferential Chapman-Kolmogorov equations are developed, and a discrete algorithm for their solution is developed. In Chapter III the discrete algorithm is verified by application to some hypothetical examples that are solved by alternative means, either (semi-)analytically or via simulation. After that, the entry-time

approach is applied to a real filed NPP application in a RIAM based scenario using the data from INPO-EPIX database followed by possible applications of the entry-time approach to PRA and GRA model in NPP in Chapter V. Also the applicability of the EPIX database is proved in Chapter IV. More specifically, in Chapter IV the time-dependent failure rates, i.e. aging effects are extracted from the EPIX database for some general components such as rotors and circuit breakers to show the applicability of the database in aging analysis, then the time-dependent failure rates for the main generator system are extracted using different schemes for the application in Chapter V. Chapter V mainly focuses on the application of the entry-time model to maintenance of the main generator system in nuclear power plants. In this chapter, both the reliability performance and the financial performance of the system are analyzed based on different preventive maintenance policies. Also possible applications of the entry-time approach to PRA and GRA model in NPP is given at the end of this chapter.

CHAPTER II

ENTRY-TIME PROCESSES

The primary objective of this chapter is to establish the basics of entry-time processes, and of one approach to their computational use in modeling reliability issues. In Section 2.1 we outline the fundamentals of entry-time processes, as a particular type of stochastic process. This culminates in the generalized state-transition equations (Equations (8) and (9) below), whose computational solution is the essence of the novel methodology proposed and developed in this dissertation. A particular discrete algorithm for the computational solution of the generalized state-transition equations is outlined in Section 2.2. This algorithm will provide the basis for much of the subsequent usage of entry-time models to study reliability issues in nuclear power plants.

2.1 Fundamentals

The treatment of this section is intended to follow the traditions of stochastic processes, as viewed within the field of applied probability. See [18] and [19] for examples of the fundamentals of stochastic processes, as so viewed.

Given a simple marked point process [20], the *entry time* associated to calendar time t is defined as the most recent arrival time; symbolically $\tau(t) = \tau_{N(t)}$, where N is the associated counting process. The mark values will commonly be referred to as "states", and denoted by "k".

Definition: An *entry-time process* is a random marked point process $\Psi : \Omega \rightarrow \mathbf{M}$, where Ω is the underlying probability space, M is the space of all simple marked point processes having some fixed finite mark space, say *K=1:I*, and the rates $\lambda_{ij}(\tau, t)$ of transition from mark *j* to mark *i* are specified as a function of calendar time *t* and entry time $\tau := \tau(t) \leq t$. Here the entry time is the time at which the process attained mark *j*, given that it has that mark at calendar time *t*.

In the application to reliability the value of the associated mark, at calendar time *t*, is some characterization of the state of the equipment of interest, in terms of its functionality at that time. Henceforth we will therefore use the term "state" rather than "mark."

An entry-time process is not a finite-state Markov process, because of the dependence of the transition rates on the entry time (generically denoted here as τ), which is no later than the calendar time (*t*). If one augments the state space by the entry time, there results a Semi-Markov process, with associated Chapman-Kolmogorov equations [21], termed here as *generalized state-transition equations*. We now wish to develop those equations, in some detail.

Given an entry-time process, we take as our immediate objective to find a determined system of equations whose solution would provide the time-dependent *state probabilities*,

$$P_i(t) := \Pr\left\{ k_{N(t)} = i \right\}, \text{ for all } i \in 1:I \text{ and } t > 0, \tag{1}$$

from the known transition rates, and a known initial distribution of states, say

$$P_i(0) := \Pr\{k_0 = i\} = P_i^{(0)}, i \in 1:I. \tag{2}$$

Our approach does not (immediately) lead to a set of determined equations in which the state probabilities appear per se as the unknown dependent variable. Rather that role is played by the entry-time state probabilities,

$$P_i^{(1)}(\tau, t) := \Pr\left[\{N(t) = N(\tau)\} \cap \{k_{N(t)} = i\} \right] \tag{3}$$

However, note that $P_i^{(1)}(t) = P_i^{(1)}(t,t)$ so that (approximations to) the entry-time state probabilities entail approximations to the state probabilities.

In the following we first obtain the integrodifferential state-transition equations on the basis of the assumption that the transition rates are known. Then we observe that these integrodifferential equations can be reinterpreted to permit the concept of more general (e.g., time-certain) transitions.

Let $0 \leq \tau \leq t$. Then $P_i^{(1)}(\tau, t)$ is the probability that at (calendar) time t the system had entry time occurring on or before τ, with associated state i. This happens if and only if at time t the entry time is either 0 or some τ', $0 < \tau' \leq \tau$. The probability of the former is $P_i^{(1)}(0,t)$. The latter happens if and only if the system transitions into state i at or prior to τ, and does not subsequently transition out at or prior to time t. If $0 < \tau'' < \tau'$, then the probability that at time τ' the system has entry time in $d\tau''$ at τ'', with associated mark j, is $D_1 P_j^{(1)}(\tau'', \tau')d\tau'' + o(d\tau'')$. (Here, and throughout, D_i denotes the partial derivative with respect to the ith argument, while "o" and "O" respectively denote quantities that approach zero fast than or no slower than their arguments.) Given this, the probability that a transition to state i occurs during $d\tau'$ at τ' is $\lambda ij(\tau', \tau') d\tau' + o(d\tau')$. Thus the

probability of a transition from state j with entry time in $d\tau''$ at τ'' to state i with entry time in $d\tau'$ at τ' is

$$D_1 P_j^{(1)}(\tau'',\tau')\lambda_{ij}(\tau'',\tau')d\tau'd\tau'' + o(d\tau'')O(d\tau') + o(d\tau')O(d\tau'').$$

If we now sum over all states j, and pass to the limiting integral in the usual fashion, then we find

$$N_i^+(\tau,t) = \sum_{j=1}^{I}\int_0^{\tau}\int_0^{\tau'}\lambda_{ij}(\tau'',\tau')D_1 P_j^{(1)}(\tau'',\tau')\, d\tau''d\tau' + \sum_{j=1}^{I}\int_0^{\tau}\lambda_{ij}(0,\tau')P_j^{(1)}(0,\tau')d\tau' \qquad (4)$$

as the relative frequency of transitions into state i with associated entry times $\tau \le t$. Here the last term is the contribution due to transitions from systems in their initial state, and therefore not included in the transitions counted within the double integral.

To obtain the net contribution of such transitions to $P_i^{(1)}(\tau,t)$ it is necessary to subtract the relative frequency of transitions into state i that occur after time 0 and at or prior to time τ and that are followed by subsequent transitions that occur at or prior to time t. Considerations similar to the above lead to the computation of that frequency as

$$N_i^-(\tau,t) = \sum_{j=1}^{I}\int_0^{\tau}\int_{\tau''}^{t}\lambda_{ji}(\tau'',\tau')D_1 P_i^{(1)}(\tau'',\tau')\, d\tau'd\tau'' = \sum_{j=1}^{I}\int_0^{t}\int_0^{\min\{\tau',\tau\}}\lambda_{ji}(\tau'',\tau')D_1 P_i^{(1)}(\tau'',\tau')\, d\tau''d\tau'. (5)$$

If we combine all of these results, we then obtain

$$P_i^{(1)}(\tau,t) = P_i^{(1)}(0,t) + N_i^+(\tau,t) - N_i^-(\tau,t), \qquad (6)$$

or

$$P_i^{(1)}(\tau,t) = P_i^{(1)}(0,t) + \sum_{j=1}^{I}\int_0^{\tau}\int_0^{\tau'}\lambda_{ij}(\tau'',\tau')D_1 P_j^{(1)}(\tau'',\tau')\, d\tau''d\tau' + \sum_{j=1}^{I}\int_0^{\tau}\lambda_{ij}(0,\tau')P_j^{(1)}(0,\tau')\, d\tau' -$$

$$\sum_{j=1}^{I}\int_0^{t}\int_0^{\min\{\tau',\tau\}}\lambda_{ji}(\tau'',\tau')D_1 P_i^{(1)}(\tau'',\tau')\, d\tau''d\tau' + P_i^{(1)}(0,t). \qquad (7)$$

The (initial form of) the integrodifferential equations we are seeking are obtained by differentiating Equation(7). If Equation (7) is differentiated with respect to t, the result is

$$D_2 P_i^{(1)}(\tau,t) = \frac{\partial P_i^{(1)}}{\partial t}(\tau,t) = -\sum_{j=1}^{I}\int_0^{\tau} \lambda_{ji}(\tau',t) D_1 P_i^{(1)}(\tau',t)\, d\tau' - \left\{\sum_{j=1}^{I} \lambda_{ji}(0,t)\right\} P_i^{(1)}(0,t), \qquad (8)$$

where we have used $\dfrac{\partial P_i^{(1)}}{\partial t}(\tau,t) = -\left\{\sum_{j=1}^{I} \lambda_{ji}(0,t)\right\} P_i^{(1)}(0,t).$ Similarly, if in Equation (7) we

set $\tau=t$, and differentiate the result with respect to t, then we obtain

$$D_1 P_i^{(1)}(t,t) + D_2 P_i^{(1)}(t,t) = \frac{\partial P_i^{(1)}}{\partial \tau}(t,t) + \frac{\partial P_i^{(1)}}{\partial t}(t,t) = \sum_{j=1}^{I}\int_0^{t} \lambda_{ij}(\tau',t) D_1 P_j^{(1)}(\tau',t)\, d\tau' +$$

$$\sum_{j=1}^{I} \lambda_{ij}(0,t) P_j^{(1)}(0,t) - \sum_{j=1}^{I}\int_0^{t} \lambda_{ji}(\tau',t) D_1 P_i^{(1)}(\tau',t)\, d\tau' - \left\{\sum_{j=1}^{I} \lambda_{ji}(0,t)\right\} P_i^{(1)}(0,t). \qquad (9)$$

Equations (8) and (9) are the desired initial form of the integrodifferential equation. Now we generalize these by noting that the integrals on the right-hand side can be written as Riemann-Stieltjes integrals [22]. The corresponding equations are

$$D_2 P_i^{(1)}(\tau,t) = \frac{\partial P_i^{(1)}}{\partial t}(\tau,t) = \sum_{j=1}^{I}\int_0^{\tau} D_1 P_i^{(1)}(\tau',t)\, d_{\tau'} \Lambda_{ji}(\tau',t) - \left\{\sum_{j=1}^{I} \lambda_{ji}(0,t)\right\} P_i^{(1)}(0,t), \qquad (10)$$

and

$$D_1 P_i^{(1)}(t,t) + D_2 P_i^{(1)}(t,t) = \frac{\partial P_i^{(1)}}{\partial \tau}(t,t) + \frac{\partial P_i^{(1)}}{\partial t}(t,t)$$

$$= -\sum_{j=1}^{I}\int_0^{t} D_1 P_j^{(1)}(\tau',t)\, d_{\tau'} \Lambda_{ij}(\tau',t) + \sum_{j=1}^{I} \lambda_{ij}(0,t) P_j^{(1)}(0,t)$$

$$+\sum_{j=1}^{I}\int_0^{t} D_1 P_i^{(1)}(\tau',t)\, d_{\tau'} \Lambda_{ji}(\tau',t) - \left\{\sum_{j=1}^{I} \lambda_{ji}(0,t)\right\} P_i^{(1)}(0,t), \qquad (11)$$

where the integrators are the (nonnegative and nonincreasing in τ) *cumulative transition functions*

$$\Lambda_{ij}(\tau,t) = \int_{\tau}^{t} \lambda_{ij}(\tau',t)\, d\tau'.$$

Interpretation of these integrators is discussed below, but now we focus on the use of them to incorporate delta functions in the transition rates, through (positive) jump discontinuities in the integrators. However, then the integrals on the right-hand sides of these equations need not exist, in the Riemann-Stieltjes sense. We finesse this issue as follows. First, we assume that for any fixed t, each integrator has at most finitely many discontinuities in τ, say $\{\tau_k\} = \{\tau_k(t)\}$, for each fixed t. Then we compute a typical integral in (10) or (11) by summing over the intervals of continuity; e.g.,

$$\int_{0}^{\tau} D_1 P_i^{(1)}(\tau',t)\, d_{\tau'}\Lambda_{ji}(\tau',t) = \sum_{k} \int_{\tau_k}^{\tau_{k+1}} D_1 P_i^{(1)}(\tau',t)\, d_{\tau'}\Lambda_{ji}(\tau',t). \tag{12}$$

We then assume that for each fixed t the derivatives are piecewise continuous in τ, with only simple jump discontinuities, and interpret the values of these derivatives at the endpoints of each of the integrals on the right as the limits from the interior of the interval. Finally, we normalize the integrators by the assumption that they are continuous from the right in τ. With these conventions the integrands and integrators on the right-hand side of Equation (12) never have a simultaneous discontinuity, so each of these constituent integrals is well-defined in the Riemann-Stieltjes sense. As the net effect of all of these conventions is to evaluate delta-function (i.e., atomic) contributions

to the transition rates as the left limit of the integrand, we shall term them collectively as the *left-atomic convention*.

This convention permits incorporation of policies that can be represented as time-certain events in the entry or sojourn times. (For example, systems incorporated before the year 2000 will be immediately replaced, or systems will be replaced once they reach five years of age.) Time-certain events in calendar time or that affect the initial distribution of states can similarly be incorporated on an ad hoc basis. It would be of some interest to develop an even further generalized version of Equations (10) or (11) that formally incorporates all of these possibilities; however, that is outside the scope of the present work.

Note that if the transition rates depend only on the sojourn time, then they are given by

$$\lambda_{ij}(\tau,t) = \frac{f_{ij}(t-\tau)}{1 - \sum_{i'=1}^{I} F_{ij}(t-\tau)} = \frac{f_{ij}(t-\tau)}{S_j(t-\tau)}, \ t \geq \tau,$$

where $f_{ij}(s)$ is the *probability density* function for transitions from state j to state i at sojourn time s, and

$$F_{ij}(s) := \int_0^s f_{ij}(s') \, ds', \ S_j(s) := 1 - \sum_{i'=1}^{I} F_{i'j}(s).$$

are respectively the cumulative transition probability from state j to state i after sojourn time s, and the survival probability in state j after sojourn time s. In this case, the cumulative transition functions satisfy

$$\Lambda_{ij}(\tau,t) = \int_{\tau}^{t} \frac{f_{ij}(t-\tau')}{1-\sum_{i'=1}^{I} F_{ij}(t-\tau')} \, d\tau', \ t \geq \tau.$$

In the case that only one f_{ij} is nonzero, with say i and j respectively representing failed and operating states, the preceding integral can be evaluated as

$$\Lambda_{ij}(\tau,t) = -\ln\left[1 - F(t-\tau)\right] = H(t-\tau),$$

where $F(s) = F_{ij}(s)$ is the *cumulative probability* of failure prior to sojourn time s, and

$$H(s) := -\ln \ S(s) \ = -\ln \ S_{ij}(s)$$

is often termed as the *cumulative hazard* function. In this context the survival function $S(s)$ is commonly termed reliability function, and denoted $R(s)$.

The cumulative transition functions Λ_{ij} are thus a generalization, to multistate competing-process stochastic models, of the common hazard function. While the cumulative transition functions are nonnegative, they are not probabilities, hence need not be bounded above by one. They share this property with the transition rates and probability density functions, in contrast to the cumulative transition probabilities, survival probabilities and reliabilities.

2.2 Discrete Algorithm

In this section we develop a finite-difference methodology for approximate solution of the generalized state transition Equations (10) and (11) of the preceding section.

Figure 2 depicts the first quadrant of the $(\tau, t,)$-plane. The $P_i(\tau, t)$ are sought in the relevant region $t > \tau$, overlaid by a mesh of square cells of dimension $\Delta t \times \Delta t$, for some positive value of Δt. We use m and n respectively as discrete surrogates for τ and t, τ_m

$=m\Delta t$ and $t_n=n\Delta t$.   The objective is to obtain computational approximations

$P_i^{(m,n)} \approx P_i(m\Delta t, n\Delta t).$ We use the notations

$$C_{mn} = \left\{(\tau,t): \tau_m \leq \tau \leq \tau_{m+1}, t_n \leq t \leq t_{n+1}\right\},$$

for $m \leq n$, and $T_n = C_{nn} \bigcap \{(\tau,t): t \geq \tau\}.$
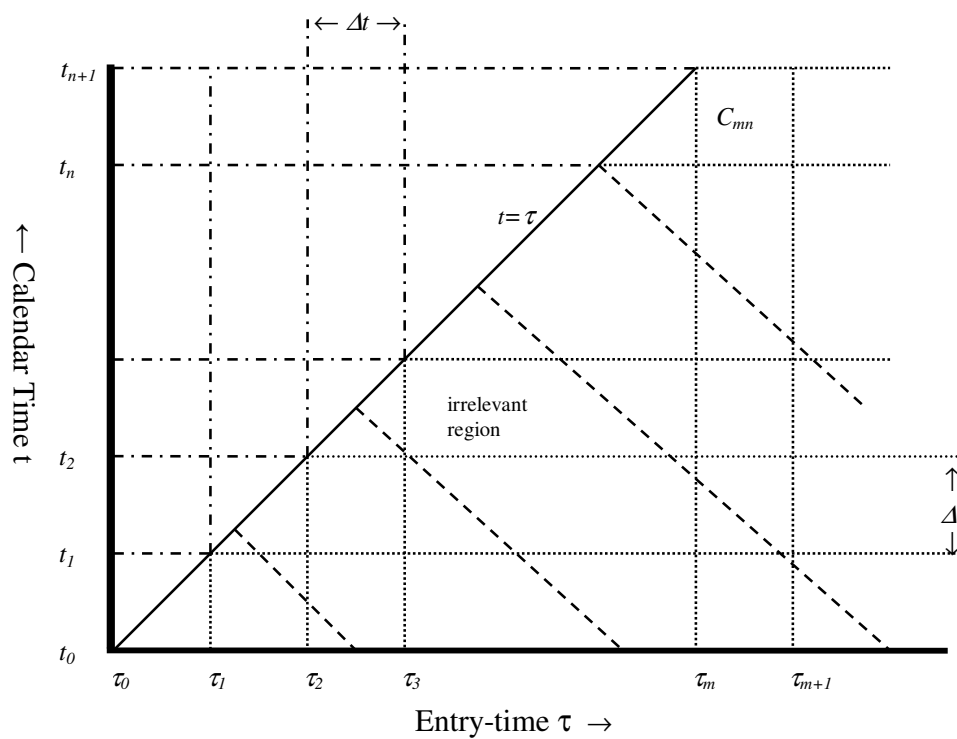
Figure 2. The computational grid for entry-time process

We begin by evaluating Equation (10) at $\tau_m=m\Delta t$, and then integrating the resulting

equation on t, from $t=t_n$ to $t=t_{n+1}$, for some $n>m$. The result is

$$P_i^{(1)}(\tau_m,t_{n+1}) - P_i^{(1)}(\tau_m,t_n) = \sum_{j=1}^{I}\left\{\sum_{m'=0}^{m-1}\iint_{C_{m'n}} D_1 P_i^{(1)}(\tau',t)\,d_{\tau'}\Lambda_{ji}(\tau',t)\,dt - \int_{t_n}^{t_{n+1}}\lambda_{ji}(0,t)P_i^{(1)}(0,t)\,dt\right\}. \quad (13)$$

If we similarly integrate Equation (11) from $t=t_n$ to $t=t_{n+1}$, the result is

$$P_i^{(1)}(t_{n+1},t_{n+1}) - P_i^{(1)}(t_n,t_n) = -\sum_{j=1}^{I}\left\{\sum_{m'=0}^{m-1}\iint_{C_{m'n}} D_1 P_j^{(1)}(\tau',t)\,d_{\tau'}\Lambda_{ij}(\tau',t)\,dt + \iint_{T_n} D_1 P_j^{(1)}(\tau',t)\,d_{\tau'}\Lambda_{ij}(\tau',t)\,dt - \right.$$

$$\left.\int_{t_n}^{t_{n+1}}\lambda_{ij}(0,t)P_j^{(1)}(0,t)\,dt\right\} + \sum_{j=1}^{I}\left\{\sum_{m'=0}^{m-1}\iint_{C_{m'n}} D_1 P_i^{(1)}(\tau',t)\,d_{\tau'}\Lambda_{ji}(\tau',t)\,dt + \iint_{T_n} D_1 P_i^{(1)}(\tau',t)\,d_{\tau'}\Lambda_{ji}(\tau',t)\,dt - \right. \quad (14)$$

$$\left.\int_{t_n}^{t_{n+1}}\lambda_{ji}(0,t)P_i^{(1)}(0,t)\,dt\right\}.$$

Equations (13) and (14) are exact, but not directly useful. We seek computational approximations to these, in terms of the $P_i^{(m,n)}$, so that the latter are determined from these approximating equations. The choices made in this pursuit are dictated by simplicity, as consistent with the goal of initial tests of the computational entry-time approach to dynamic reliability. If utility of this approach is established, then more sophisticated and efficient approximations can be subsequently pursued.

In Equation (13) we obtain a finite-difference approximation, by introducing the following approximations:

1) Throughout t is replaced by t_n, except that in the argument of the integrators Λ_{ij} and the transition rates λ_{ij} it is replaced by t_{n+1}. Note that these replacements remove the t dependence in the integrands and integrators, so that the integrals over t effectively become multiplication by Δt. (The resulting computational method is explicit, because of the replacement of t by t_n in the unknown entry-time probabilities.)

2) Within the integral over the partial derivative is replaced by the corresponding difference quotient,

$$D_1 P_i^{(1)}(\tau', t_n) \rightarrow \frac{P_i^{(1)}(\tau_{m'+1}, t_n) - P_i^{(1)}(\tau_{m'}, t_n)}{\Delta t}.$$

3) Values of the entry-time state probabilities at an arbitrary grid point, say $(\tau, t) = (\tau_m, t_n)$, are replaced by the corresponding computational approximation,

4) The remaining integral over τ' is explicitly evaluated,

$$\int_{\tau_{m'}}^{\tau_{m'+1}} d_{\tau'} \Lambda_{ji}(\tau', t_{n+1}) = \Lambda_{ji}(\tau_{m'+1}, t_{n+1}) - \Lambda_{ji}(\tau_{m'}, t_{n+1}).$$

The result of these manipulations is

$$P_i^{(m,n+1)} = P_i^{(m,n)} - \Delta t \sum_{j=1}^{I} \lambda_{ji}(0, t_n) P_i^{(0,n)} - \sum_{m'=0}^{m-1} \sum_{j=1}^{I} \left[P_i^{(m'+1,n)} - P_i^{(m',n)} \right] \left[\Lambda_{ji}(\tau_{m'}, t_{n+1}) - \Lambda_{ji}(\tau_{m'+1}, t_{n+1}) \right],$$
$$i = 1:I, m = 0:n-1, n = 0:N-1.$$

$$(15)$$

where $T=N\Delta t$ is some *terminal time*. In Equation (14) we make similar replacements, and further neglect the integrals over the triangular regions T_n. The result is

$$P_i^{(n+1,n+1)} = P_i^{(n,n)} + \Delta t \left\{ \sum_{j=1}^{I} \left[\lambda_{ij}(0, t_n) P_j^{(0,n)} - \lambda_{ji}(0, t_n) P_i^{(0,n)} \right] \right\} +$$
$$\sum_{m'=0}^{n-1} \sum_{j=1}^{I} \left\{ \left[P_j^{(m'+1,n)} - P_j^{(m',n)} \right] \left[\Lambda_{ij}(\tau_{m'}, t_{n+1}) - \Lambda_{ij}(\tau_{m'+1}, t_{n+1}) \right] - $$
$$\left[P_i^{(m'+1,n)} - P_i^{(m',n)} \right] \left[\Lambda_{ji}(\tau_{m'}, t_{n+1}) - \Lambda_{ji}(\tau_{m'+1}, t_{n+1}) \right] \right\}, i = 1:I, n = 0:N-1.$$

$$(16)$$

Equations (15) and (16) are used, along with the initial conditions, to obtain $P_i^{(m,n)}$ and $P_i^{(m,m)}$. $P_i^{(m,m)}$ is the state probability that we are after at time $t=m\Delta t$. The

detailed procedure is as follows. The $P_i^{(0,0)}$ are given by $P_i^{(0,0)} = P_i(0,0) = P_i^{(0)}$ (the initial conditions). For $m = 0$ and $n = 0$ the only unknowns in the I Equation (15) are the I unknowns $P_i^{(0,1)}$. These unknowns appear linearly, and each is only one of these equations, so that the solution is explicit. With the $P_i^{(0,1)}$ known, Equations (16) for $m = 1$ and $n = 1$ are a system of I linear equations in the I unknowns $P_i^{(1,1)}$, and can be solved accordingly. This pattern repeats for a sequentially increasing values of $n = 2, 3, ..., N$. First Equations (15) are solved, as a diagonal linear system of I equations in as many unknowns (the $P_i^{(m,n+1)}$) for each value of n, in order of increasing $m = 0, 1, 2, ... n$. Then Equations (16) give the I unknowns $P_i^{(n+1,n+1)}$.

Experience with particle transport suggests that conservation and nonnegativity of probability are two desirable properties of computational approximations. It is seen from Equation (16) that the above method delineated above satisfies

$$\sum_{i=1}^{I} P_i^{(n+1,n+1)} \equiv \sum_{i=1}^{I} P_i^{(n,n)}$$

so that probability is conserved (up to roundoff error in the computations). The example in Chapter III shows this scheme need not produce nonnegative probabilities, but also suggests the manner in which this fails is relatively harmless.

Explicit methods typically have first-order accuracy, so that

$$\left| P_i^{(m,n)} - P_i^{(1)}(\tau, t) \right| = O(\Delta t)$$

Where m and n vary with the time step so that $m\Delta t$ and $n\Delta t$ remain fixed, at τ and t, respectively. We verify this in details in Chapter III.

In the approximations made above, there is some arbitrariness in the discretization choices, especially in the first step (see above label (1) in the assumption part). By using a backward time approximation for calendar time in the probabilities and a forward approximation in the transition rates and integrators, it removes the t dependence in the integrands and integrators, so that the integrals over t effectively become multiplication by Δt.

This deterministic computational solution method for the computational solution of the generalized state-transition equations will be used, in the following chapter, to apply the entry-time processes to some test examples. First, the entry-time approach is applied to a semianalytically solvable example and compare to the semianalytic solutions of the example. Following that, the entry-time approach is compared to simulation. Once the computational algorithm is thus verified, it will then be employed in subsequent chapters for purposes of exploring the application of entry-time processes to asset management for nuclear power plants.

CHAPTER III

VERIFICATION OF THE DISCRETE ALGORITHM

The purpose of this chapter is to verify the computational method developed in Chapter II, by some hypothetical examples. In Section 3.1, a semianalytically solvable four-state example is given, and the discrete algorithm is compared to its semianalytic solutions. The discrete methodology is compared to simulation for a three-state example in Section 3.2. In the last section of this chapter, an RIAM base application of this methodology is given to show the potential application of entry-time processes to asset management for nuclear power plants.

The work described in this chapter is closely based on work co-written by the author and P Nelson (see [23] for details). More detailed analysis is given in this dissertation than in the journal paper.

3.1 A Semianalytically Solvable Example

The purpose of this section is to verify the computational method developed in the preceding section, by comparing its performance to the (nearly) analytic solution of a simple three-state problem contrived to lend itself to such a solution. The example and its semianalytic solution are formulated in Section 3.1.1. Computational results via the finite-difference method developed in the preceding Chapter II are described in Section 3.1.2.

3.1.1 Formulation and Semianalytic Solution

Consider a component that can be in four states:

State 1: In service, as received from the manufacturer;

State 2: Out of service for repair;

State 3: In service, as a refurbished unit;

State 4: Out of service, for salvage.

Failures of manufacturer equipment are assumed to be distributed cumulatively as the Weibull distribution,

$$W(\tau;\alpha_1,\beta_1) := 1 - \exp(-(\tau/\alpha_1)^{\beta_1}),$$

for appropriate values of α_1 and β_1. Once a manufacturer component fails it enters state 2, where it is refurbished in 0.1 years. It then returns to service as a refurbished component. Failures of refurbished components are distributed as $W(\tau;\alpha_2,\beta_2)$, where presumably $\alpha_1 \leq \alpha_2$ and $\beta_1 \leq \beta_2$. Once a refurbished component fails no further repairs are attempted, so it is sent to salvage.

It is well known that Weibull distribution is commonly used in reliability field because it is convenient as a model for various physics phenomena and it has a clear physical sense as a distribution of external values [24]. However, the traditional Weibull distribution widely used in reliability analysis can only model monotone increasing or decreasing failure rate functions. For many complex systems, the failure rate function exhibits a bathtub shape. The bathtub shape of equipment failure rate changes with time is given in Figure 3. At the early stage of operation, also known as the burn-in period, failure rate decreases rapidly as manufacturing and construction defects are repaired (this

phenomena is also called "infant mortality"). As the system stabilizes the failure rate levels off. This second stage is called the useful life period and during this stage failure rate increases slowly. As equipment wears out, the degradation becomes dominant, and the failure rate increases. This third stage is called the wear-out period. If all three stages of FR vs. time are plotted, the curve resembles a bath-tub. This bathtub curve of Figure 3 summarizes the life-time aging of equipment or component [25].
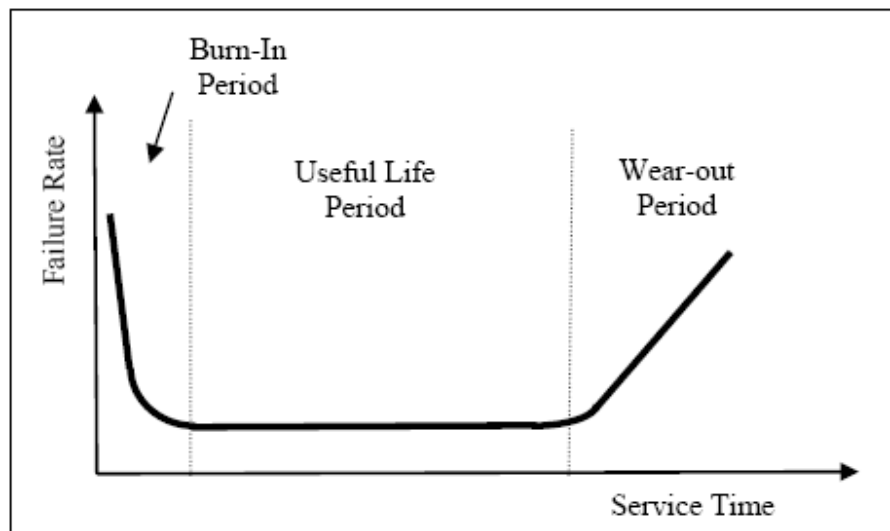
Figure 3. Bathtub curve failure rate

A modified three-parameter Weibull model is introduced in [26] to capture the bathtub shape failure rate for some components. Another way to capture the bathtub shape failure rate by Weibull distribution is to use a "weighted sum of Weibull distributions",

$$F(t) = w \times W(t, \alpha_1, \beta_1) + (1-w) \times W(t, \alpha_2, \beta_2)$$

where w is a weighted parameter and $W(t;\alpha,\beta) := 1 - \exp(-(\tau/\alpha)^\beta)$. Here we have $\beta_1 < 1$ so that the first term captures the infant mortality and $\beta_2 > 1$ so that the second term captures the aging effects.

Hence the corresponding failure rate is:

$$\lambda(t) = \frac{w f_1(t) + (1-w) f_2(t)}{1 - F(t)}$$

where $f_1(t) = \dfrac{dW(t,\alpha_1,\beta_1)}{dt}$ and $f_2(t) = \dfrac{dW(t,\alpha_2,\beta_2)}{dt}$.

For example, here we take $\alpha_1 = \alpha_2 = 20.0, \beta_1 = 0.5, \beta_2 = 6.0$ and $w = 0.5$ so that the failure distribution is equally weighted between the two distributions. Figure 4 shows the bathtub failure rate plot using the above parameters.

For this example equipment, the appropriate initial conditions are $P(0) = \begin{pmatrix} 1 & 0 & 0 & 0 \end{pmatrix}$. We know from the statement of the problem that the only way the equipment transits out of State 1 is when it is out of service for repair (State 2) and the failures of equipment are defined by the Weibull distribution $W(\tau;\alpha_1,\beta_1) := 1 - \exp(-(\tau/\alpha_1)^{\beta_1})$. Therefore, for $t \geq t_0 \geq 0$, the probability that the equipment is in State 1 is given by:

$$P_1(t,t_0) = 1 - W(t;\alpha_1,\beta_1) = \exp(-(t/\alpha_1)^{\beta_1}),$$

Similarly, the probability that the equipment is in State 2 is given as follows:

$$P_2(t,t_0) = W(t_0;\alpha_1,\beta_1) - W((t - .1 \wedge t_0) \vee 0; \alpha_1,\beta_1) , \ (\wedge = \text{``min''}, \vee = \text{``max''}),$$

where $W(t_0; \alpha_1, \beta_1)$ is the probability system transits into State 2 and $W((t-.1 \wedge t_0) \vee 0; \alpha_1, \beta_1)$ gives the probability system transits out State 2.
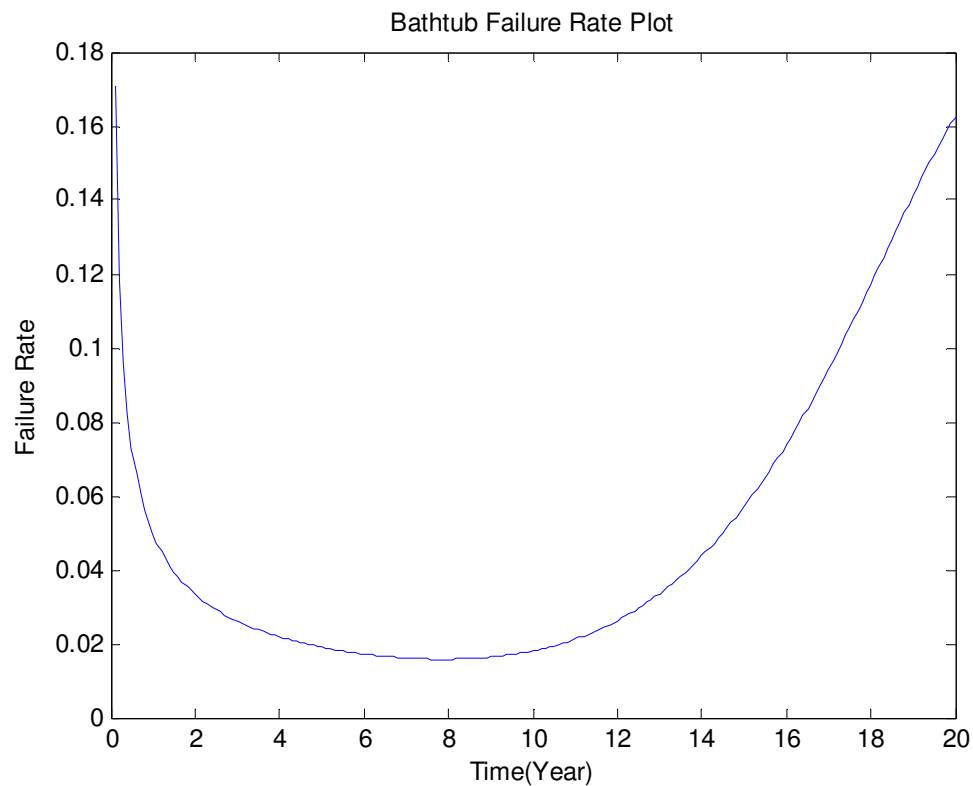
Figure 4. Bathtub failure rate plot using "weighted sum of Weibull distributions"

It is a little bit complex for the calculation of probabilities system is in States 3 and 4. It is clear from the definition of states that $P_3(t, t_0) = 0$ and $P_4(t, t_0) = 0$ when $t < 0.1$ because there is no transition from State 3 and hence no transition from State 3 to State 4. When $t \geq 0.1$, both P_3 and P_4 involve quadratures (definite integrals) of analytic functions as shown below:

$$P_3(t,t_0) = \int_{.1}^{\min\{t,t_0+.1\}} W'(s-.1;\alpha_1,\beta_1)\left[1-W(t-s;\alpha_2,\beta_2)\right] \, ds,$$

$$P_4(t,t_0) = \int_{.1}^{\min\{t,t_0+.1\}} W'(s-.1;\alpha_1,\beta_1)W(t-s;\alpha_2,\beta_2) \, ds$$

Hence, the corresponding solutions are ($\wedge$ = "min", $\vee$ = "max"), for $t \geq t_0 \geq 0$,

$$P_1(t,t_0) = 1 - W(t;\alpha_1,\beta_1) = \exp(-(t/\alpha_1)^{\beta_1}),$$

$$P_2(t,t_0) = W(t_0;\alpha_1,\beta_1) - W((t-.1\wedge t_0)\vee 0;\alpha_1,\beta_1) =$$
$$\begin{cases} W(t_0;\alpha_1,\beta_1), \ t \leq .1, \\ W(t_0;\alpha_1,\beta_1) - W(t-.1;\alpha_1,\beta_1), \ 0 < t-.1 \leq t_0, \\ 0, \ t_0 < t-.1, \end{cases}$$
$$= \exp\left(-\left(((t-.1\wedge t_0)\vee 0)/\alpha_1\right)^{\beta_1}\right) - \exp\left(-\left(t_0/\alpha_1\right)^{\beta_1}\right),$$

$$P_3(t,t_0) = \begin{cases} 0, \ t < .1, \\ \int_{.1}^{\min\{t,t_0+.1\}} W'(s-.1;\alpha_1,\beta_1)\left[1-W(t-s;\alpha_2,\beta_2)\right] \, ds, \ t \geq .1, \end{cases}$$

and

$$P_4(t,t_0) = \begin{cases} 0, \ t < .1, \\ \int_{.1}^{\min\{t,t_0+.1\}} W'(s-.1;\alpha_1,\beta_1)W(t-s;\alpha_2,\beta_2) \, ds, \ t \geq .1, \end{cases}^{.}$$

where

$$W'(\tau;\alpha,\beta) := \frac{dW}{d\tau}(\tau;\alpha,\beta).$$

The solutions for P_1 and P_2 are analytic. Those for P_3 and P_4 involve quadratures of analytic functions. Those quadratures are easily carried out computationally (see

Section 3.1.2 for details). In that sense the entire solution is known semianalytically. The finite-difference method of the preceding section will now be tested against this semianalytic benchmark.

3.1.2 Computational Results

As discussed in the preceding section that the solutions for P_3 and P_4 involve quadratures of analytic functions. Here in this section those quadratures are carried out computationally via MatLab implementation (see Appendix F for details). For each t, when evaluating the quadratures, $\Delta s = 0.0001$ is applied in the MatLab code. To check the accuracy of the evaluated quadratures using $\Delta s = 0.0001$, $\Delta s = 0.0005, 0.001$ are also applied to the code for comparison. Table 1 shows the different values for P_3 and P_4 evaluated at some time points.

Table 1

Comparison of $P_3(t)$ and $P_4(t)$ for different $\triangle s$

T	$P_3(t)$ $\triangle s$=0.0001	$P_3(t)$ $\triangle s$=0.0005	$P_3(t)$ $\triangle s$=0.001	$P_4(t)$ $\triangle s$=0.0001	$P_4(t)$ $\triangle s$=0.0005	$P_4(t)$ $\triangle s$=0.001
0.5	0.14844	0.14859	0.14878	0.032866	0.032899	0.032940
1	0.23108	0.23118	0.23132	0.13133	0.13138	0.13146
2	0.23719	0.23724	0.23731	0.37610	0.37619	0.37629
3	0.17955	0.17958	0.17962	0.58591	0.58600	0.58612
4	0.12204	0.12205	0.12207	0.73572	0.73582	0.73594
5	0.07884	0.07885	0.07887	0.83488	0.83983	0.83511
6	0.049601	0.049607	0.049614	0.89808	0.89818	0.89831

From the above table we can see that the computational results of the semianalytic solution are believed to be accurate to (at least) three digits as presented.

For this section the parameters of the preceding section were taken as $\alpha_1 = 0.5$, $\alpha_2 = 1.0$, $\beta_1 = 1.0$ and $\beta_2 = 1.25$. From the definition of transition rates and cumulative transition rates from Section 2.1, we can easily get the corresponding nonzero transition rates and cumulative transition rates for the above system. The transition rates and cumulative transition functions are

$$\lambda_{21}(\tau, t) = \frac{W'(t - \tau; \alpha_1, \beta_1)}{1 - W(t - \tau; \alpha_1, \beta_1)},$$

$$\lambda_{32}(\tau, t) = \frac{\delta(t - \tau)}{H(t - \tau)},$$

$$\lambda_{43}(\tau, t) = \frac{W'(t - \tau; \alpha_2, \beta_2)}{1 - W(t - \tau; \alpha_2, \beta_2)},$$

$$\Lambda_{21}(\tau, t) = -\ln\left[1 - W(t - \tau; \alpha_1, \beta_1)\right],$$

$$\Lambda_{32}(\tau, t) = \begin{cases} 0, \tau \geq t - .1, \\ \infty, \tau < t - .1, \end{cases}$$

$$\Lambda_{43}(\tau, t) = -\ln\left[1 - W(t - \tau; \alpha_2, \beta_2)\right].$$
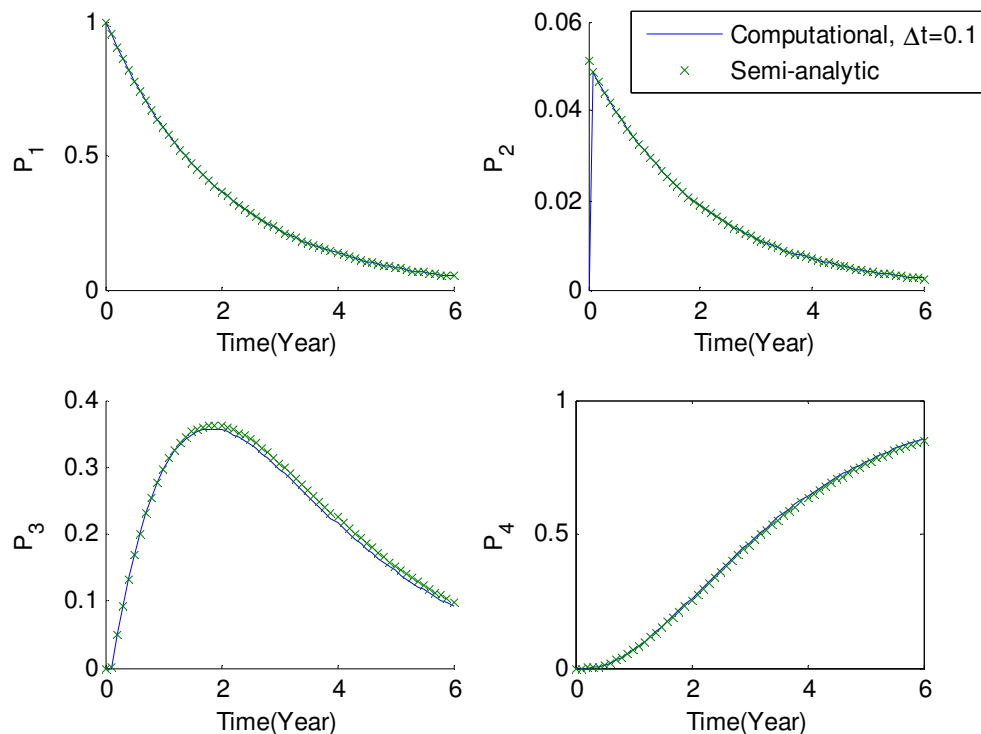
Figure 5. Comparison of computed probabilities to the semianalytic solution

The first six years of the corresponding solutions are shown in Figure 5, with the semianalytic solution of the preceding section plotted as the discrete points (x's), and the computational results, with $\Delta t = 0.1$, plotted as the solid lines in the same figure. The computational approximation is practically identical to the semianalytic solution, although some discrepancy is graphically distinguishable, especially in the state probabilities P_3 and P_4, at the later (calendar) times. These results are for a relatively small time step, but results for larger time steps are totally unviable, because they fail to capture any transfers from state 2 to state 3. This is because at these larger time steps all

such transfers are contained mathematically in the terms corresponding to the integrals over the triangular regions that were neglected in the computational method of the preceding section. Methods presumably could be produced that are not subject to this failing, but the objective of the present chapter is to verify and understand the specific method of Chapter II.

The computational errors in the state probabilities, as compared to the semianalytic solution (believed to be accurate to the magnitude of 10-3) are plotted in Figure 6. To see the trends of error changes with decreasing time step, three groups of error data are shown in that figure, with $\triangle t$=0.1, 0.02 and 0.025 (plotted as blue lines, discrete points and red lines respectively). It can be seen clearly from Figure 6 that, the error decreases with decreasing time step. The errors are in the order of 10^{-3} ~ 10^{-4} for P_1, P_3 and P_4. Because of the sudden jump in P_2, from 0 to around 0.05 at time t=0, the errors in P_2 at the first few time points are relatively larger. Therefore, it is not easy to see the order of accuracy from the plot for $\triangle P_2$, however, a detailed study of the error data (as shown in Table 2. Please note here that only $\triangle P_2(t)$ and $\triangle P_4(t)$ are given due to limited space of the table, and the results for $\triangle P_1(t)$ and $\triangle P_3(t)$ are similar) for $\triangle P_2$ shows that the order of the errors is around 10^{-4} ~ 10^{-5}. This means that the finite-difference methodology of Chapter II has very good accuracy, compared to the results from semianalytic results. This provides the desired verification of the finite-difference methodology of Chapter II.
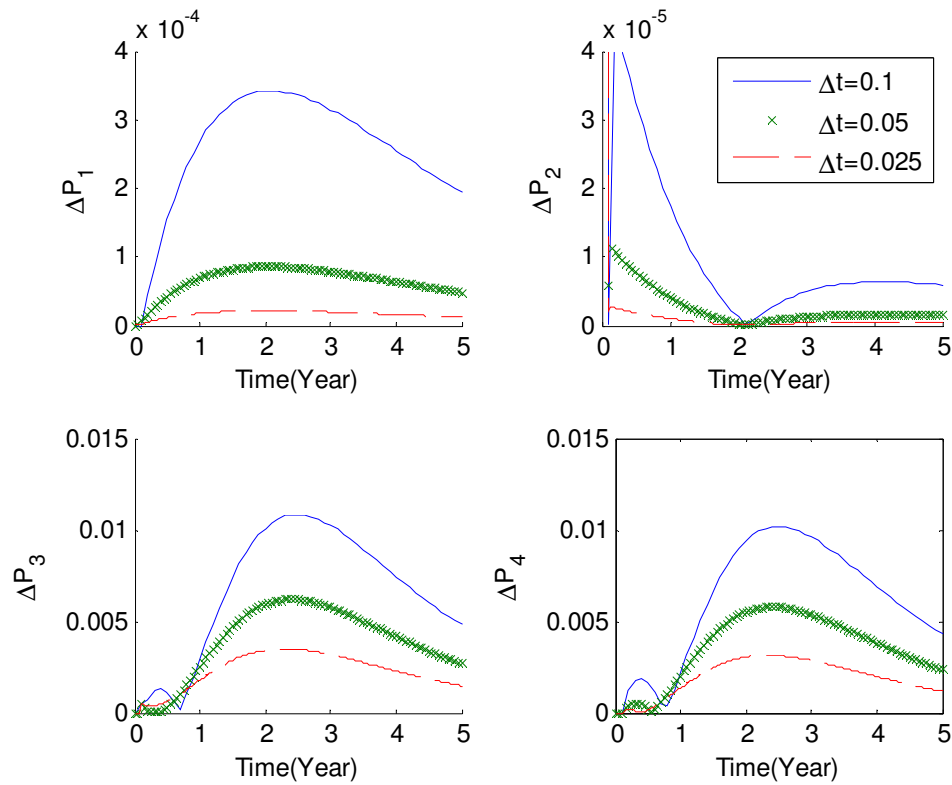
Figure 6. Plots of error for each state, as compared to the semianalytic solution

Table 2

Comparison of $\triangle P_2(t)$ and $\triangle P_4(t)$ for different $\triangle t$

t	$\triangle P_2(t)$			$\triangle P_4(t)$		
	$\triangle t = 0.1$	$\triangle t = 0.05$	$\triangle t = 0.025$	$\triangle t = 0.1$	$\triangle t = 0.05$	$\triangle t = 0.025$
1	0.1745e-4	0.0409e-4	0.0099e-4	0.0022	0.0020	0.0014
2	0.0117e-4	0.0020e-4	0.0004e-4	0.0094	0.0055	0.0030
3	0.0493e-4	0.0125e-4	0.0032e-4	0.0096	0.0054	0.0029
4	0.0637e-4	0.0159e-4	0.0040e-4	0.0069	0.0038	0.0020
5	0.0588e-4	0.0146e-4	0.0036e-4	0.0043	0.0024	0.0012

Results relevant to detailed computational accuracy appear in Figure 7. Here $\varepsilon(P_i)$ is the computational error in the state probability P_i, as compared to the semianalytic solution (believed to be accurate to three digits represented in the error as discussed early in this section), and for the time step indicated in the plots. The corresponding order of accuracy $n(P_i)$ is defined as

$$n(P_i) := \frac{\ln\left[\varepsilon_p(P_i)/\varepsilon(P_i)\right]}{\ln 2},$$

where ε_p is the corresponding error at the preceding time step. It is shown from the plots that the values for ΔP_1 and ΔP_2 clearly cluster toward two and the values for ΔP_3 and ΔP_4 go toward one (also shown in Table 3). This confirms the order one accuracy anticipated in Section 2.2. The sudden changes in ΔP_2 is most likely due to the error accumulation/ cancellation during the calculation, further study of the reason is not addressed here.
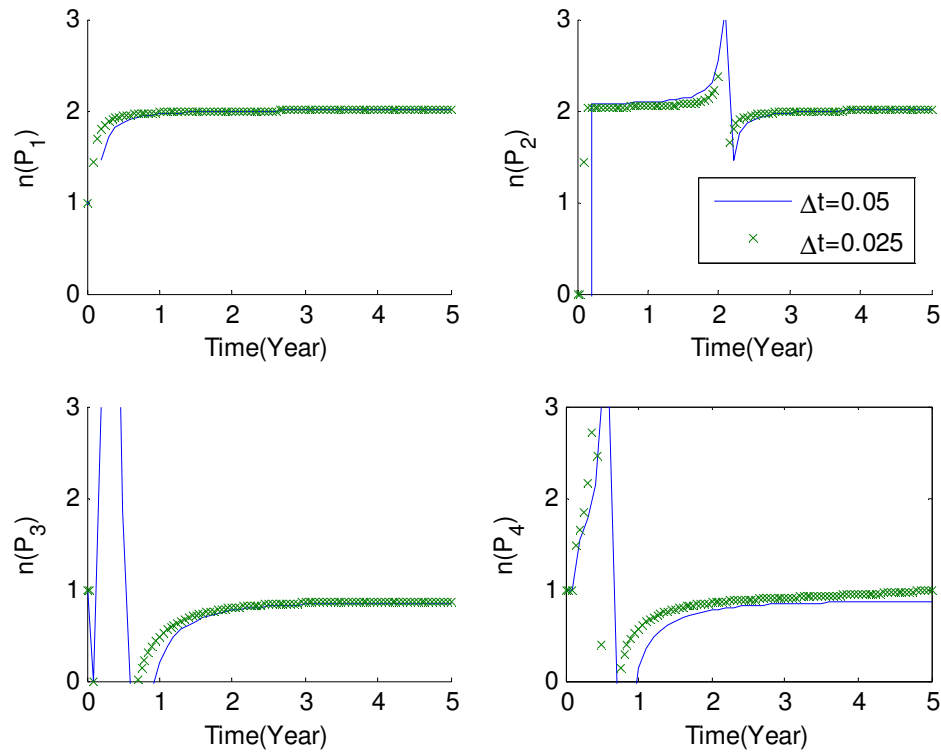
Figure 7. Plots of order of accuracy for each state

Table 3

Order of accuracy for the discrete algorithm in this example

t	$n(P_1(t))$		$n(P_2(t))$		$n(P_3(t))$		$n(P_4(t))$	
	$\triangle t =0.05$	$\triangle t$ =0.025	$\triangle t$ =0.05	$\triangle t$ =0.025	$\triangle t$ =0.05	$\triangle t$ =0.025	$\triangle t$ =0.05	$\triangle t$ =0.025
1	1.9579	1.9801	2.0940	2.0473	0.2122	0.4793	0.1419	0.5673
2	1.9937	1.9969	2.5501	2.3649	0.7672	0.7980	0.7746	0.8535
3	2.0018	2.0008	1.9759	1.9885	0.8306	0.8529	0.8400	0.9092
4	2.0034	2.0016	2.0029	2.0014	0.8399	0.8660	0.8569	0.9436
5	2.0025	2.0011	2.0080	2.0039	0.8370	0.8677	0.8720	0.9934

We take these results, as regards both accuracy and order of accuracy, as providing confirmation of the correctness of the finite-difference method of Chapter II, and of its MatLab implementation that is the fundamental source of the computational results presented throughout this dissertation.

Please note here that in the above example the system does not allow "state reentry", which means that once the system leaves a state, it never comes back to the same state. However, in some scenario, it is often required to have a state reentry. For example, when a system is replaced after it gets into the "failure state" from the "normal running state", it can come back to "normal running state" and this procedure can be repeated. In the next section, an example that permits state reentry is constructed and the computational results from the entry-time approach are compared to simulations.

3.2 A Simplified Computational Example, with Comparison to Simulation

This section is devoted to a hypothetical three-state example that permits state reentry. Computational results from the above methodology are compared to simulations.

The three-state example is formulated in Section 3.2.1. In Section 3.2.2 we apply to the three-state example the MatLab finite-difference code used to obtain the results described in the preceding section, and we verify this application by comparison against (differential and integral) results obtained from simulation.

3.2.1 Formulation

The characteristics of the three-state example are:

- The three states are "in-service (1)," "out of service for preventive maintenance (PM) (state 2)," and "out-of-service for corrective maintenance (CM) (state 3)."

- The transition rate from 1 to 3 is defined by an annual failure rate of .05 + 0.2s, where s is "time in service" (sojourn time in state 1). (This simulates aging effects, but not infant mortality.)

- The transition rate from state 1 to state 2 is defined by a policy of completely replacing systems after they have been in service for a "replacement period" T_r. The value of this parameter is not specified, because we take the issue associated with this example as determination of the preferred choice of the replacement period. This is similar to issues that arise in both life-cycle management [27] and optimization of preventive maintenance [28] in NPPs.

- The transition rate from 2 to 1 is defined by the fact that systems can be completely replaced within $t_p = 0.2$ years, provided the outage is planned so that replacement equipment can be ordered and on hand when the outage occurs.

- The transition rate from state 3 to state 1 is defined by the fact that it requires $t_c = 0.4$ years to replace the system, if the outage is not planned, so that replacement equipment must be specially ordered.

- There are no transitions, in either direction, between states 2 and 3.

The graphical relationships among the three states can be seen in Figure 8 where PM Period $t_p = 0.2$ years and CM Period $t_c = 0.4$ years.
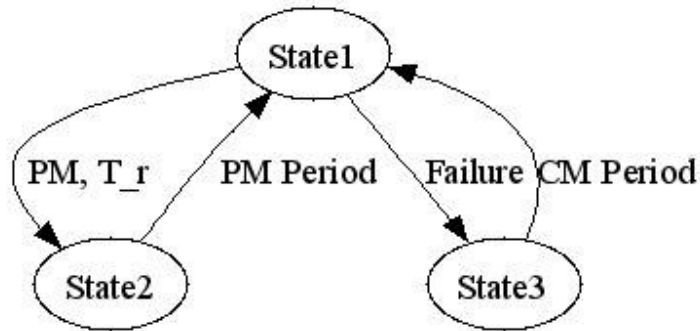
Figure 8. Relationships of states for the example of Section 3.2.1

3.2.2 Verification

Similar to the solutions of transition rates in the Section 3.1.2, from the definition of transition rates and cumulative transition rates from Section 2.1, for this three-state example the nonzero values of λ_{ij} and Λ_{ij} are:

$$\lambda_{21}(\tau,t) = \delta(t-\tau-T_r), \ \lambda_{31}(\tau,t) = .05+0.2(t-\tau),$$
$$\lambda_{12}(\tau,t) = \delta(t-\tau-.2), \ \lambda_{13}(\tau,t) = \delta(t-\tau-.4)$$

and

$$\Lambda_{21}(\tau,t) = H_+(t-\tau-T_r), \ \Lambda_{31}(\tau,t) = .05(t-\tau)+0.1(t-\tau)^2,$$
$$\Lambda_{12}(\tau,t) = H_+(t-\tau-.2), \ \Lambda_{13}(\tau,t) = H_+(t-\tau-.4).$$

Here H_- is the Heaviside step function with $H_-(0)=0$, as consistent with the left-atomic convention (see Section 2.1).
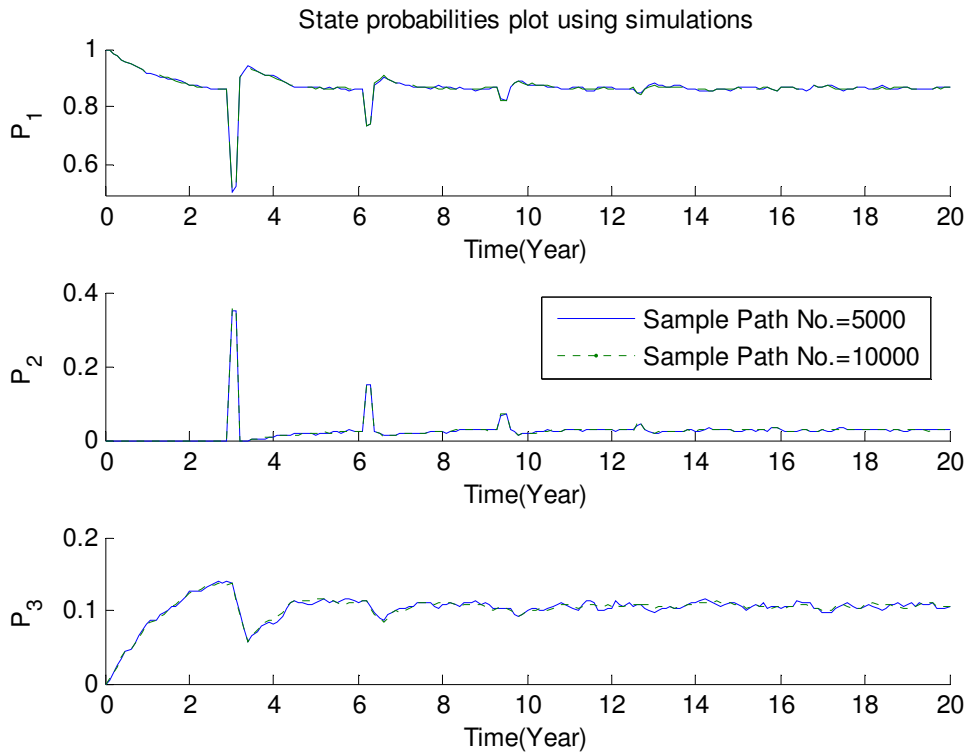
Figure 9. State probabilities plot from simulations

In Figure 9 we plot, over an operating period of 20 years, the time-dependent state probabilities, for a replacement period of $T_r = 3$ years, as obtained from 10,000 sample paths (green solid line) and 5,000 sample paths (blue dashed line) respectively, and $\Delta t = 0.1$ years. It is clear to see from the plots that results obtained from simulations using different number of sample paths agree with each other with only small differences.

In Table 4, the yearly averaged probability differences for two simulations

$$\frac{1}{T}\int_0^T \Delta P_i(t)\, dt = \frac{1}{T}\int_0^T \left(P_i(t)_{10,000} - P_i(t)_{5,000} \right) dt, \quad i = 1,2,3$$

are given. As we can see from the table that the integral quantities of the probability difference of results obtained from simulation using different number of sample paths are at a magnitude of 10^{-4}, and this gives us a sense of accuracy of the simulation methods using 10,000 sample paths. Therefore, the results obtained from simulation using 10,000 sample paths will be used as a standard in comparison with the results obtained from the entry-time process calculations.

Table 4

Mean annual probability differences for two simulations

t	2	4	6	8	10	16	20
$\frac{1}{T}\int_0^T \Delta P_1(t)\,dt$	5.49e-4	9.09e-4	6.99e-4	3.79e-4	8.80e-4	7.10e-4	2.90e-4
$\frac{1}{T}\int_0^T \Delta P_2(t)\,dt$	0	1.38e-3	1.60e-4	1.10e-4	2.39e-4	5.00e-4	1.89e-4
$\frac{1}{T}\int_0^T \Delta P_3(t)\,dt$	5.50e-4	4.69e-4	5.40e-4	2.70e-4	6.40e-4	2.09e-4	4.79e-4

In Figure 10 we plot, over an operating period of 20 years, the computed time-dependent state probabilities, for a replacement period of $T_r = 3$ years. The solid blue lines represent simulation results, as obtained from 10,000 sample paths, and $\Delta t = 0.1$ years. In the following we treat this as a standard for assessing the above finite-difference method. However, these simulation results contain some high-frequency small-amplitude variations that presumably represent stochastic effects (noise), even with this number of sample paths. (These effects are most visible in Figure 10 as the

high-frequency oscillations in P_3.) Significantly smaller numbers of sample paths lead to similar effects, with larger amplitudes in the oscillations (see the plots in Figure 9 for example of this phenomenon).
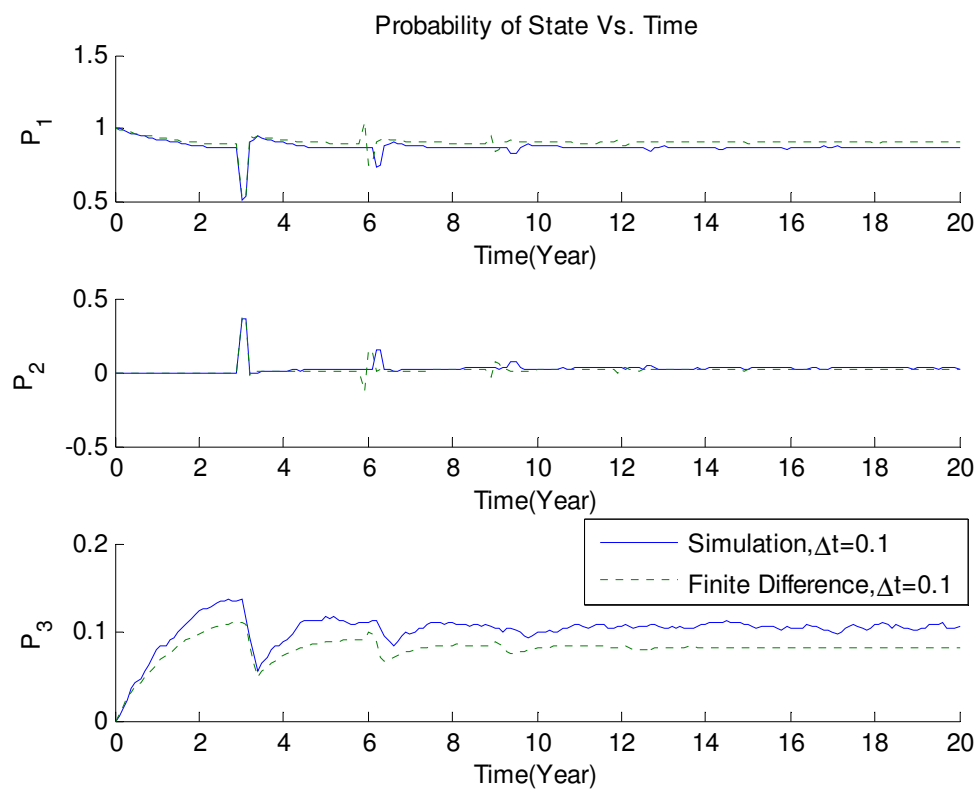
Figure 10. Comparison of state probabilities using same time step

The finite-difference results from step size $\Delta t = 0.1$ years appear in Figure 10 as discontinuous green lines. These are grossly similar to the corresponding simulation (blue line), but there are noteworthy differences:

1) The finite-difference results for P_1 (operating) and P_2 (PM) agree well (to graphical accuracy) with the simulations, away from the PM spikes that occur, with decreasing amplitude, approximately at multiples of three years. However, at or near these PM spikes there are two significant differences:

   (a) The expected spikes (downward jump in P_1 and upward jump in P_2) are, except for the first, somewhat larger for the finite-difference solution than for the simulation.

   (b) In the finite-difference solution the expected jumps approximately at multiples of three years are preceded by unexpected precursors consisting of smaller jumps in the opposite direction. There is no indication of these precursors in the simulation. In the case of P_1 (P_2) this "false" spike is even greater than one (respectively, less than zero).

2) The finite-difference results for P_3 (corrective maintenance) are consistently slightly lower and later than the corresponding simulation results.

We now explore the sources of these differences.

If the simulation results are a reliable standard, then it is a reasonable hypothesis that these effects are due to discretization error. Figure 11 displays results intended to test this hypothesis. The solid blue lines in this figure represents the results of the same simulation as described in conjunction with Figure 10, except now with a sampling period of $\Delta t = 0.05$ years. The data points themselves are not plotted, in order to minimize the graphical clutter. This, along with the higher sampling frequency, makes even more apparent the low-amplitude high-frequency noise mentioned above. The

dashed green lines and solid red lines in Figure 11 represent the corresponding finite-difference results, with time steps of respectively $\Delta t = 0.10$ and $\Delta t = 0.05$ years.
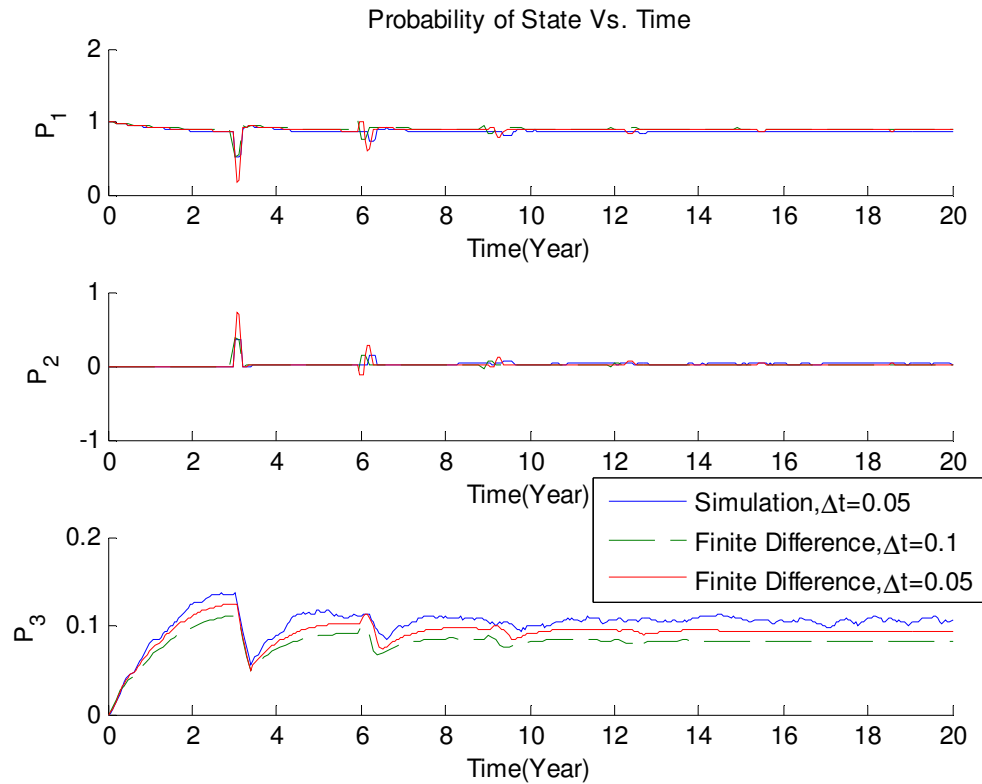
Figure 11. Comparison of state probabilities using different time steps

The general agreement between the finite-difference and simulation results becomes better as the time step is reduced in the finite-difference method; in particular, the finite-difference results for state P_3 (corrective maintenance) are becoming larger as the time step decreases, and therefore in better general agreement with the simulation results, to the extent that can be judged by the apparent persistent noise in the corresponding

simulation results. This provides some confirmation that effect 2) above stems from discretization error in the finite-difference results.

However, the effects labeled (1) above do not seem to disappear, or even moderate, as the time step is decreased. If one studies individual data points in the finite-difference results, the following structure emerges. The excessive magnitude in the expected PM spikes (past the first) occurs as *a single data point*, regardless of the size of the time step, and that point is located at the earliest time within the expected spike.

The remaining data in the expected PM spike take values in about the expected range. Likewise the false precursor occurs as a single data point, which invariably is located at a time of $t_p = 0.2$ years prior to the initial time of the expected PM spike.

We believe these two phenomena are related, and stem from the following considerations. One can consider the finite-difference approximations (15) and (16) as a discrete time Markov model, provided the "discrete transition coefficients,"

$$\lambda_{ij}(0,t_n) \text{ and } \Lambda_{ij}(\tau_m,t_{n+1}) - \Lambda_{ij}(\tau_{m+1},t_{n+1})$$

satisfy

$$\sum_{i=1}^{I} \lambda_{ij}(0,t_n) \leq 1 \text{ and } \sum_{i=1}^{I} \left[\Lambda_{ij}(\tau_m,t_{n+1}) - \Lambda_{ij}(\tau_{m+1},t_{n+1}) \right] \leq 1, \tag{17}$$

identically in *i*, *m* and *n* so that these coefficients can be interpreted as *bona fide* probabilities. For the example of this section the constraining inequality (17) fails for $j = 1$ (operating state) and $t_{n+1} - \tau_{m+1} = t_p = 0.2$ years, because then

$$\Lambda_{2j}(\tau_m,t_{n+1}) - \Lambda_{2j}(\tau_{m+1},t_{n+1}) = 1, \text{ and } \Lambda_{3j}(\tau_m,t_{n+1}) - \Lambda_{3j}(\tau_{m+1},t_{n+1}) > 0,$$

the latter because there is some probability a system entering the operating state between times τ_m and τ_{m+1}, and further remaining in that state until time t_n, will require corrective maintenance some time between t_n and t_{n+1}. The pathological consequences of this phenomenon are particularly amplified when a preceding discontinuity occurred between the two entry times (i.e., between τ_m and τ_{m+1}), which corresponds to time T_r following both beginning and end of the preceding PM spikes. These correspond respectively to the times of the false precursors and of the points of excessive magnitude in the expected PM spikes.

We choose here to accept these clearly incorrect results (probabilities less than zero and greater than one), because in the limit $\Delta t \to 0$ the effect of these false values becomes negligible in computing the integral quantities that are ultimately of real interest in applications[1]. (See the following section.) Further, we do not attempt to develop ad hoc "fix ups" to deal with these phenomena, notwithstanding that they are cosmetic liabilities, because they tend to cancel each other in computation of integral quantities (see the results in Table 5). It would be of some interest to develop a fix based on renormalization of the discrete transition coefficients described above, but we shall not pursue that here.

Some comparative instances, finite differences versus simulation, of integral quantities (mean annual residence time in each of the three states, over a 20 year operating period (terminal time)) are shown in Table 5. For the finite-difference

---

[1] In this respect these phenomena bear some resemblance to the well-known Gibbs' phenomenon.

approximation the integral providing the mean annual residence time was evaluated by means of the trapezoidal rule, with the probabilities as determined from the finite-difference approximation, and with a time step of 0.1 years. For the (10,000 sample path) simulation the integral was similarly evaluated, except the probabilities of a given state at time t were computed as the fraction of the selected sample paths in that state at that time.

The baseline (topmost) entries under the finite-difference columns in Table 5 are the residence times as obtained with a time step of $\Delta t = 0.10$ years. These agree with the simulation results to more-or-less two digits of accuracy. The parenthetical results underneath were obtained by extrapolating to zero time step, under the assumption of first-order accuracy, these baseline results along with the corresponding results with a time step of 0.2 years. This extrapolation adds at least an additional digit of accuracy, in comparison to the simulation results. This adds further confidence that the finite-difference method of Chapter II is both correct, and has been correctly implemented in the MatLab code of Appendix F.

Table 5

Mean annual residence times, as a function of the replacement period

Replacement period	$\frac{1}{T}\int_0^T P_1(t)\,dt$, FD: $\Delta t = .1(\Delta t \to 0)$	$\frac{1}{T}\int_0^T P_1(t)\,dt$, simulation	$\frac{1}{T}\int_0^T P_2(t)\,dt$, FD: $\Delta t = .1(\Delta t \to 0)$	$\frac{1}{T}\int_0^T P_2(t)\,dt$, simulation	$\frac{1}{T}\int_0^T P_3(t)\,dt$, FD: $\Delta t = .1(\Delta t \to 0)$	$\frac{1}{T}\int_0^T P_3(t)\,dt$ simulation
one (1) year	.8042 (.8103)	.8101	.1477 (.1422)	.1428	.0481 (.0475)	.0471
two (2) years	.8585 (.8626)	.8620	.0600 (.0585)	.0583	.0815 (.0789)	.0797
three (3) years	.8689 (.8725)	.8719	.0259 (.0257)	.0255	.1052 (.1018)	.1026
five (5) years	.8691 (.8725)	.8722	.00346 (.00367)	.00361	.1274 (.1238)	.1242
ten (10) years	.8683 (.8715)	.8711	.54(-6) (.85(-6))	.30(-5)	.1317 (.1285)	.1289

A detailed comparison of the relative efficiency and accuracy of the finite-difference and simulation methods is beyond the intended scope of the present work, which is intended merely to verify feasibility of finite-difference methods in general, and to verify the specific finite-difference method of Chapter II. However, some preliminary comments on these important issues are appropriate. As coded to obtain the results presented here, the computational effort for the finite-difference method scales inversely as the cube of the time step. Thus a decrease of a factor of two in step size occasions eight times as much computational time. What is gained by that eightfold increased cost, at least for sufficiently small time steps, is an increase of a factor of two in time resolution (sampling frequency) and a reduction by a factor of two in the discretization error. If one wishes to obtain the same gains from the simulation, then there also will be

a factor of eight increase in the computational time, from a factor of two increase in the time for the "post-processing" sampling in time, and a factor of four increase in the required number of sample paths; the latter stems from the presumed inverse square root of number of sample paths dependence of error for the simulation.

Thus the computational requirements for the two approaches scale similarly, with time resolution and accuracy. For a time step of 0.2 years for the finite-difference method, and the same sampling period with 10,000 sample paths for the simulation, the two methods require roughly the same times (approximately 4 mins 15 secs and 3 mins 15 secs, respectively, on a Pentium 4 single processor PC). Exactly what one obtains in accuracy for these comparable efforts seems to depend sensitively on exactly what is computed. A detailed study of this important issue is not done here, but one can make some inference for differential quantities (e.g., the $P_i(t)$) from Figure 10. (especially the graph for the corrective maintenance state), and from Table 5 for integral quantities. The relative accuracy of the two approaches for rare events (e.g., occurrence of the preventive maintenance state, for a replacement period of ten years; cf. Table 5) is an especially intriguing issue that perhaps warrants subsequent detailed study. This is particularly important to considerations related to the relative merits of the two methodologies for application to the very difficult issue of prediction of low-probability high-consequence events.

3.3 An Example Application in RIAM

As discussed in Chapter I, as part of the RIAM process, PM Basis program gained its popularity in recent years because it is beneficial to the plant management to make maintenance decisions (for example, for people of risk averse, the lease risky policy might be taken), especially when the system or component is critical (risk related), either for safety or for generation. In this chapter, we in with the example of Section 3.2, but add hypothetical financial information, for purposes of illustrating how entry-time approaches can be applied to a LCM/PM based application.

In addition to the states and transition rates defined in the preceding section, the costs related to each state are defined as follows:

While the (generation-critical) component of interest is operating the plant net revenue at an annual rate of $50,000,000, conceived as revenue of $150M per year, less fixed expenses of $50M per year and variable operating expenses of $50M per year. Each planned outage costs $2,000,000 for repairs, or $10M per year, plus the fixed expenses, for a net annualized revenue of -$60M per year during planned outages for preventive maintenance. Each unplanned outage costs $10,000,000 ($25M per year), in addition to the $100M per year for fixed and variable expenses, for a revenue stream of -$125M per year during forced outages.

Hence the cost and revenue related to each state can be found in Table 6.

Table 6

Revenue and cost data related to each state

State No.	Net Revenue/Cost	Revenue/Cost Details	
1	$50M	Revenue	$150M
		Fixed Expense	$50M
		Operating Expense	$50M
2	-$60M	Repair Expense	$10M
		Fixed Expense	$50M
3	-$125M	Repair Expense	$25M
		Fixed Expense	$50M
		Operating Expense	$50M

In Figure 12 we plot, over an operating period of 20 years, the time-dependent state probabilities acquired by using the MatLab code for entry-time applications (see Appendix F for details), for replacement periods of $T_r = 0.8, 1.8$ and 3.8 years respectively with $\Delta t = 0.1$ years. The solid blue lines represent probabilities of states with a replacement period of $T_r = 0.8$ years, while the solid green line corresponds to $T_r = 1.8$ years, and the red solid line to $T_r = 3.8$ years.
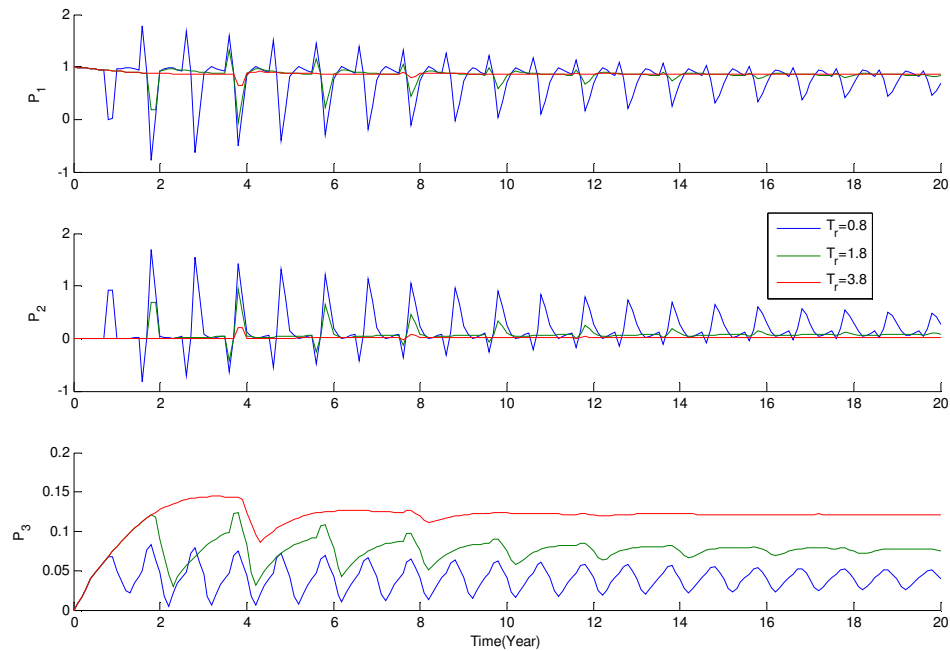
Figure 12. State probability plots, with replacement period as a parameter

The first overall observation is that the PM greatly improves the reliability of the system and hence decreases the risk of system failure (in state 3) over a 20 year time period comparing to the reliability performance with no maintenance. The probability plots for state in Figure 12 show that the probability that the system is in the failed state decreases as the corresponding replacement period T_r decreases, consequent to different PM policies.

Comparing the three different maintenance policies, there is not much improvement (numerically) when doing preventive maintenance more frequently. For example, with a more frequent preventive maintenance (e.g. $T_r = 0.8$), the averaged failure probability is

about 0.06 less than the averaged failure probability of a less frequent preventive maintenance (e.g. $T_r = 3.8$).

But from the viewpoint of a NPP life time, this can make a huge difference in reliability calculations. This is extremely important for current NPPs, which have been in operation for decades. It is also important for PRA/GRA models, as will be discussed in Chapter V.

Figure 13 consists of graphs of annual revenue, variance and skewness, for a plant lifetime of 20 years, and various representative values of T_r. Briefly, these were computed as follows:

When doing simulation, information from different sample paths is collected and used for final calculations. Here we use similar sample path idea that is used in simulation, the net revenue in year n, along a sample path ω, is

$$R^{(n)}(\omega) = \sum_{i=1}^{3} R_i \int_{n-1}^{n} I_i\left(S_\omega(t)\right) dt,$$

where:

R_i is the annualized net revenue in state i, as indicated in the system description of the preceding section (i.e., $R_1 = \$50M$ per year, $R_2 = -\$60M$ per year and $R_3 = -\$125M$ per year);

I_i is the indicator function for state i; and

$S_\omega(t)$ is the system state at time t, along sample path ω.

The expected value of that annualized net revenue is then

$$\overline{R}^{(n)} = \int R^{(n)}(\omega) \, d\omega = \sum_{i=1}^{3} R_i \int_{n-1}^{n} P_i(t) \, dt, \tag{18}$$

where

$$P_i(t) = \int I_i\left(S_\omega(t)\right) \, d\omega$$

is the probability the system is in state i at time t.

The Entry-time approach produces precisely discrete approximations to the probabilities $P_i(t)$. The expected net revenues in Figure 13 were produced by using the finite-difference methodology, with time step 0.1 years, and then evaluating the rightmost integrals in Equation (18) by means of the trapezoidal rule. Refinement to a step size of 0.05 years produced relatively minor changes in the computed values.

The annualized standard deviations and skewnesses were similarly computed, as respectively

$$\sigma^{(n)} = \sqrt{\sum_{i=1}^{3} \left[R_i - \overline{R}^{(n)} \right]^2 \int_{n-1}^{n} P_i(t) \, dt},$$

and

$$\gamma^{(n)} = \frac{\sum_{i=1}^{3} \left[R_i - \overline{R}^{(n)} \right]^3 \int_{n-1}^{n} P_i(t) \, dt}{\left[\sigma^{(n)} \right]^3}.$$
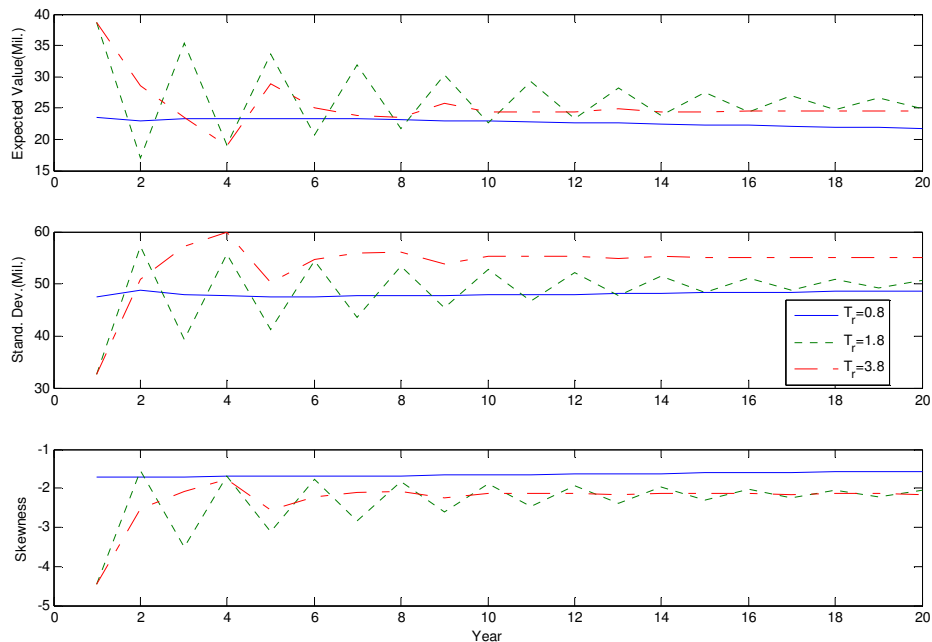
Figure 13. Annualized values of various measures of economic performance

The first overall observation is that the hypothetical plant under consideration has a high degree of inherent uncertainty in financial performance, as the standard deviation in annualized net revenue tends to be close to twice the expected net revenues. Further, the large negative values of skewness indicate that much of the variance is located along a long left tail of the underlying distribution; i.e., the business is subject to a substantial downside risk.

The most aggressive of the three preventive maintenance policies described, a replacement period of 0.8 years (PM cycle of 1 year), substantially reduces this downside risk, as indicated by:

i. a standard deviation that tends to be substantially smaller than that for the most passive PM policy (replacement period of 3.8 years), and slightly smaller than that for the intermediate policy (replacement period of 1.8 years);

ii. a variance that is substantially larger algebraically (i.e., less negative) than that of either of the two alternative policies.

This shortest of the three replacement periods considered is therefore likely to be adopted by concerns that are strongly risk averse. However, the graph of expected net revenue shows that this decrease in downside risk is purchased at a cost of some 10-15% reduction in expected net revenue, depending upon the year. Management more inclined to accept a higher degree of generation risk might be inclined to adopt the intermediate replacement period of 1.8 years.

As compared to this intermediate replacement period, the most passive replacement policy of a 3.8 year replacement period apparently provides no advantage in either expected net revenue or reduction in downside risk. For the assumed parameters the vast majority of instances will require corrective maintenance over a period of 3.8 years, so that this longest replacement period is essentially tantamount to a policy of running to failure.

As we can see from the above example that the comparison of PM policies is based on "maximize the revenue" strategy. However, its counterpart, "minimizing the cost" is often used in industry when doing such analysis. In Chapter V, such implementation (i.e. minimizing the cost) will be carried out in the analysis for PM policies of a main

generator system to accord with the way that is familiar to industry people who are doing similar analysis.

As demonstrated by the example above, the computational entry-time approach is capable of providing guidance as to PM policies that are most consistent with management objectives. Hence the entry-time approach can be applied to a LCM/PM based scenario in nuclear power plants where time-dependent feature is important. However, this methodology does require availability of suitable time-dependent failure rates. There are limited sources of such information that are available. Issues related to data and databases will be addressed in detail in the next chapter.

CHAPTER IV

DATA AND DATABASE FOR APPLICATIONS

We have demonstrated, in Chapter III, both the computational accuracy and the applicability of the entry-time processes. Also in Section 3.3, an example is given to show how the entry-time processes can be applied to a LCM/PM based scenario. Our next step is to focus on the application of this methodology to realistic NPP applications, especially in the arenas of LCM/PM based applications.

The first challenge to apply entry-time process to such applications is the availability of suitable time-dependent failure rates. As mentioned in the preceding chapters, that accurate values of the "transition rates" are crucial to the application of entry-time methodology. As we know, there are two types of transition rates: policy driven (e.g., PM policies) and stochastic (e.g., failures). The basic objective of this chapter is to ascertain the possibility of obtaining failure rates, for real-world SSCs in NPPs, via application of standard statistical techniques to existing databases for reliability of such SSCs. In this chapter, the issues of data and database for the application of entry-time processes to the application of NPP applications are discussed. The EPIX database is introduced in Section 4.1. In Section 4.2, the EPIX database is shown to be capable of providing time-dependent failure rates. Following that, the target system (main generator) for further analysis is selected in Section 4.2. Then different failure data for main generators was selected and tested using different data interpretation schemes in Section 4.4. In Section 4.5 the various results are compared,

and a "best data fit" distribution is selected as a basis for further work. Further detailed analysis is carried out in Section 4.6, to generate time-dependent failure rates and the corresponding distribution(s). These will then be employed in Chapter V, to generate various predictions via the entry-time model of the preceding chapters.

4.1 Introduction to the EPIX Database

The EPIX database [29] was employed as a source of the data used to obtain the transition rates used in this dissertation, in the context of the entry-time approach developed in Chapters II and III. The objective of this section is to review the history of this database, and its structure, especially as these are needed to justify its selection for use in this dissertation. These descriptions closely follow that in [29] and the USNRC websites [30].

The EPIX failure database for nuclear power plants components has experienced several stages from the early 1970s.

The first stage is set up of the initial data collection system. In the early 1970s, the industry and some research institutes recognized the need for failure data on nuclear plant components. As a result, a data collection system was developed whose objective was to make available reliability statistics (e.g., failure rates, mean-time-between-failures, mean-time-to-restore) for safety related systems and components. This system, the Nuclear Plant Reliability Data System (NPRDS), was developed by Southwest Research Institute (SwRI). Plants began reporting data on a voluntary basis in 1974, and continued reporting to SwRI until 1982.

In the second stage, failures of both safety and non-safety related components are reported. In January 1982, the Institute of Nuclear Power Operations (INPO) assumed management responsibility for the system. Originally the NPRDS only covered safety-related systems and components. However, later the scope was expanded to cover any system important to safety and any system for which a loss of function can initiate significant plant transients. By the end of 1984, 86 nuclear power plant units were supplying detailed design data and failure reports on some 4,000 to 5,000 plant components from 30 systems. Data reported to NPRDS consisted of two kinds of reports: engineering reports and failure reports. The engineering reports provided detailed design and operating characteristics for each reportable component. The failure reports provided information on each reportable component whenever the component was unable to perform its intended function.

In the third stage, EPIX replaces NPRDS. The NPRDS failure reports provided to INPO were generally generated by plant licensees utilizing maintenance records such as maintenance work orders. These reports utilized a standard set of component boundaries and failure mode definitions. The Equipment Performance and Information Exchange (EPIX) system replaced NPRDS since 1987.

EPIX consists of:

- a site-specific database controlled by each INPO member site with web-based data entry and retrieval,

- an industry database on the INPO web site where selected parts of the site-specific database are shared among plants,

- a retrieval tool that provides access to the vast historical equipment performance information available in the NPRDS.

Events reported to EPIX include both complete failures of components and degraded component operation. The number of demands and operating hours (i.e., reliability data) and the unavailability are required to be collected for components in safety-related systems, for each plant. In addition, contributors to EPIX are also to include one-time estimates of the number of demands and run hours for other risk-significant components.

In comparison to other database used in current nuclear industry, such as WASH-1400 [31] and the PLG[2] Database [32], the INPO-EPIX database is the best database available to us, for the following reasons:

- The EPIX database includes 400,000 failure reports on more than 900,000 components since 1973 while the WASH-1400 only contains data from early 1960 to 1973.

- The EPIX database includes both complete failures of components and degraded component operation, while the PLG Database focuses mainly on complete failure of components.

- It is feasible to generate time-dependent failure rate from the database due to the completeness of the data records.

---

[2] PLG was the former company name for current ABS Consulting Inc.

Information is extractable from the EPIX database by means of SQL[3] queries. In the following section, we will employ this capability to test the ability of the INPO-EPIX database to provide, in conjunction with standard statistical tools, adequate estimates of time-dependent failure rates to be used in the application of entry-time processes.

4.2 Applicability of the EPIX Database

As mentioned in Chapter I, aging is becoming more and more important in NPPs, many of which have been in operation for decades, some now longer than their originally planned lifetimes. A consistent treatment of the dynamics of the evolution of aging and maintenance is critical to the quantitative study of system reliability. In order to show the importance of aging and the applicability of entry-time approach, we reviewed the EPIX database to identify a system that has the following features:

- The system shows significant time-dependent (aging) features, i.e. it has time-dependent failure (transition) rates.

- The system is either safety related (for PRA model) or generation-risk related (for GRA model). That is, failure of the system will increase system risk or generation risk.

There are 21 tables in the INPO Database named "nrcRadsView" in which we can find almost all the failure records from different sources (NPPs) for different type of components. The database is in Microsoft Access format and it is feasible to acquire records from it by using SQL queries. Starting from the table "tblAlternateDevice,"

---

[3] Commonly expanded as Structured Query Language, is a computer language designed for the retrieval and management of data in relational database management systems.

where we see a list of all components, we can find the all types of components that have more than 1000 records in the database using an SQL query such as:

SELECT tblAlternateDevice.ComponentTypeCode,

Count(tblAlternateDevice.ComponentTypeCode) AS Number_of_Records

FROM tblAlternateDevice

GROUP BY tblAlternateDevice.ComponentTypeCode

HAVING ((((Count(tblAlternateDevice.ComponentTypeCode))>1000))

ORDER BY Count(tblAlternateDevice.ComponentTypeCode) DESC;

Please note that in the above SQL query, the condition is set as: "HAVING ((((Count(tblAlternateDevice.ComponentTypeCode))>1000)". The reason for that is a large number of failure records for a type of component is necessary in order to obtain good statistics.

As can be seen from Table 7 below, which was created using the above query, there are around 30 types of components that have more than 1000 records in this table. We are seeking types of components that have significant time-dependent features. Therefore, according to the Weibull parameters from Barringer (see footnote 4), we choose "CKRBRK" (Circuit Breaker) and "MOTOR" from the list. These have 103399 and 15723 records respectively. They will be used to test the ability of the INPO-EPIX database to provide, in conjunction with standard statistical tools, adequate estimates of time-dependent failure rates. The Weibull shape and scale parameters from the Barringer website are given in Table 8 and the parameters listed here will be compared to the parameters obtained from the data fit plots for Weibull distributions.

Table 7

List of components that have more than 1000 records in the EPIX database

ComponentTypeCode	Number_of_Records
VALVE	258183
CKTBRK	103399
RELAY	74095
IBISSW	72987
INTCPM	61439
IXMITR	56184
VALVOP	48475
INDREC	37013
IPWSUP	21363
ICNTRL	19023
ELECON	17837
MOTOR	15723
CRDRVE	14654
SUPORT	12818
ISODEV	11330
PIPE	10362
PUMP	10093
BLOWER	8799
ANNUNC	8616
HTEXCH	8434
TRANSF	8219
PANEL	7414
ACCUMU	7007
FILTER	6745
BATTRY	6398
LIGHT	4231
HEATER	4177
PENETR	3313
MECFUN	1773
GENERA	1682
WALL	1015

Table 8

Weibull parameters as suggested by the Barringer website[4]

Component Name	Weibull Shape			Weibull Scale (days)		
	Low	Typical	High	Low	Typical	High
Circuit Breakers	0.5	1.5	3.0	2792	4167	58333
Motors	0.5	1.2	3.0	46	6250	12500

Each general type of component tends to come in several different models. For example, Circuit Breaker Model DS 206 has two models: Model K and Model S. In order to determine the best estimate of failure rate for a certain component, we need to focus on components of the same model. The analysis done here is so focused.

For circuit breakers, we choose the models that have more than 100 records in the database, while for motors we choose the models that have more than 20 records. The difference is because there are substantially fewer records for motors than for circuit breakers.

After appropriate SQL queries, we find there are four models of circuit breakers (two different models, but each has type "K" and type "S") and 3 models for motors that meet the criteria of queries (i.e., have respectively more than 100 or 20 failure records in the database).

For circuit breakers the respective numbers of failure records (please refer to Appendix A for sample of the failure records) are as shown in Table 9. The corresponding results for motors are as in Table 10.

---

[4] http://www.barringer1.com/wdbase.htm

Table 9

Circuit breakers model and failure records in the EPIX database

Circuit Breaker Model Number	Type of the Model	Number of Failure Records
DS 206	K	30
	S	81
HFB3	K	17
	S	106

Table 10

Motors model and failure records in the EPIX database

Motor Model Number	Type of the Model	Number of Failure Records
CS VSS	S	23
TBDP	S	28
FTYPE AN	S	38

Once the components were identified, we employed the standard statistical software MiniTAB [33] to obtain the failure rate for each of the different types of components (model numbers), as will now be described. As a standard to judge which type of distribution we should choose, we use the A-D numbers (Anderson-Darling statistic[5]) as

---

[5] The Anderson-Darling statistic is a measure of how far the plot points fall from the fitted line in a probability plot. Minitab uses an adjusted AndersonDarling statistic, because the statistic changes when a different plot point method is used. A smaller AndersonDarling statistic indicates that the distribution fits the data better.

a measure of how well each of the three different distributions (Weibull, Exponential and Normal), as provided by MiniTAB, fits the observed distribution of failure times.

The results will be shown below, for the various model number and model types. Here we choose not to show all the plots for each model type; rather, we plot here only the Weibull, Exponential and Normal distribution fits for circuit breakers with model number DS 206 and type K. For the remaining plots, please refer to Appendix B.
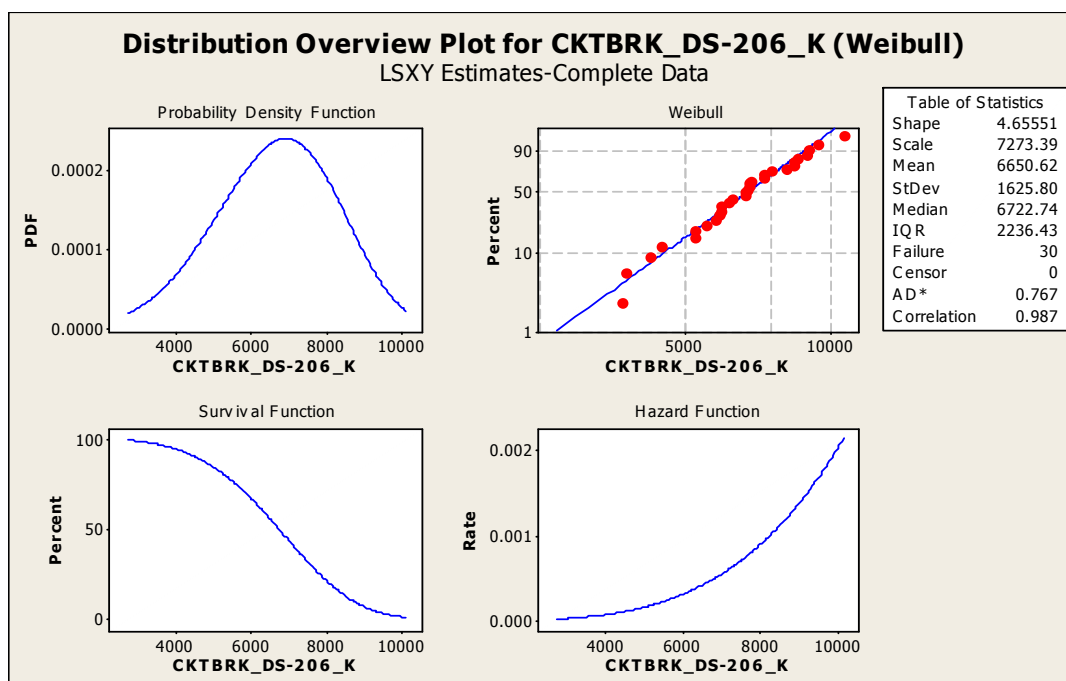
Figure 14. Weibull distribution plots for circuit breakers (DS 206 and type K) [6]

---

[6] Throughout the dissertation, the units for all X axels in the MiniTab plots are days, if not specified otherwise.

A typical Weibull distribution can be found in the example given in Section 3.1. From the plotted MiniTAB results in the upper right of Figure 14 we can see that the Weibull distribution fits circuit breakers with model number DS 206 and type K failure records very well. This "percent plot [7]" shows that almost all the failure "points" fall closely around the percentage plot line, which means that the distribution plot agrees with the failure record data very well. Also the "Rate plot"[8] (lower right of Figure 14) shows that there are significant aging effects for this type of circuit breakers, as the hazard rate (failure rate) increases significantly as the system ages.

A typical form of the exponential distribution pdf function is:

$$f(x, \lambda) = \begin{cases} \lambda e^{-\lambda x}, x \geq 0 \\ 0 \quad , x < 0 \end{cases}$$

where λ is a constant failure rate for the distribution.

From the exponential distribution plots (Figure 15), we can see that the constant failure rate does not apply for the failure distribution of this particular type of circuit breakers. The "percent plot" (upper right plot) shows that almost all the failure "points" fall far away from the percentage plot (see also footnote 7) line, which means that the distribution plot does not agree with the failure record data at all. These graphically intuitive observations correspond more quantitatively to a much larger value of the A-D

---

[7] Fitted line of percent plot, which is a graphical representation of the percentiles. To make the fitted line, Minitab first calculates the percentiles for the various percents, based on the chosen distribution. The associated probabilities are then transformed and used as the y-variables. The percentiles may be transformed, depending on the distribution, and are used as the x-variables. The transformed scales, chosen to linearize the fitted line, differ depending on the distribution used.

[8] Also known as hazard rate, or failure rate, which is identical to the failure rate that was used in the entry-time models.

statistic for the exponential distribution than was observed previously for the best-fit Weibull distribution. The inability of a constant failure rate to fit the data presumably is a consequence of aging effects in the DS 206 Type K circuit breakers.
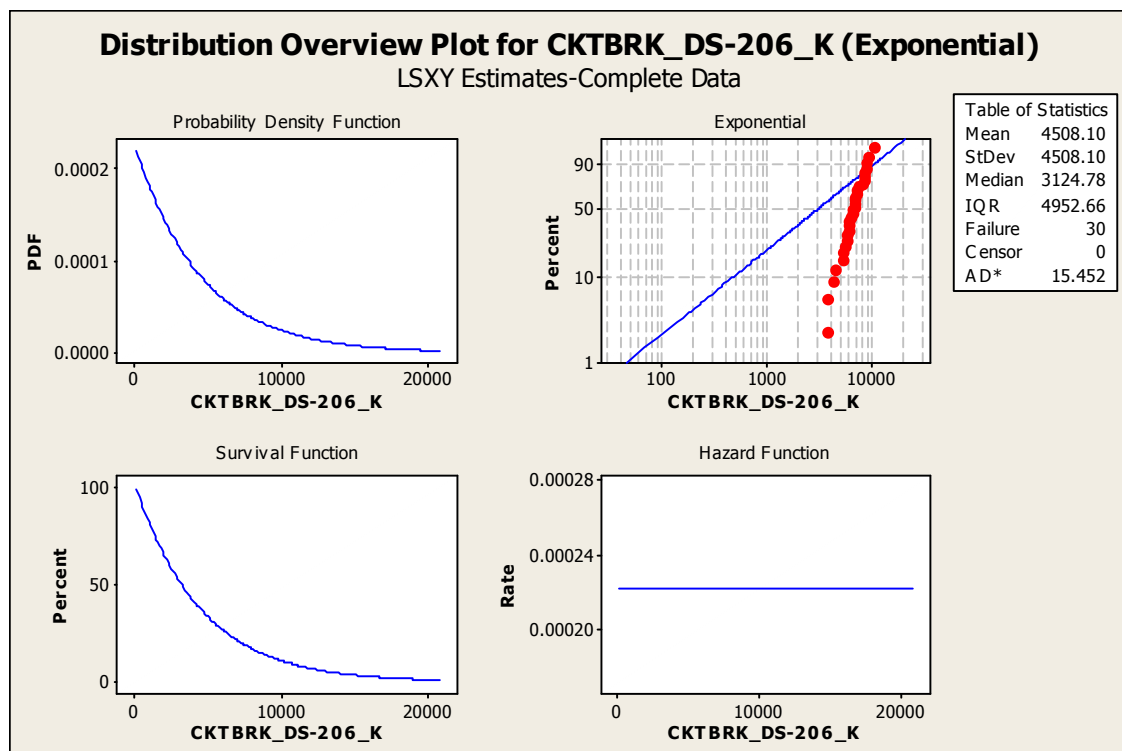
Figure 15. Exponential distribution plots for circuit breakers (DS 206 and type K). (The horizontal axes are time, in days)

The typical form of the probability density function for a normal distribution is:

$$f(x) = \frac{1}{\sigma\sqrt{2\pi}} \exp(-\frac{(x-\mu)^2}{2\sigma^2})$$

where μ is the mean and σ is the standard deviation of the distribution.
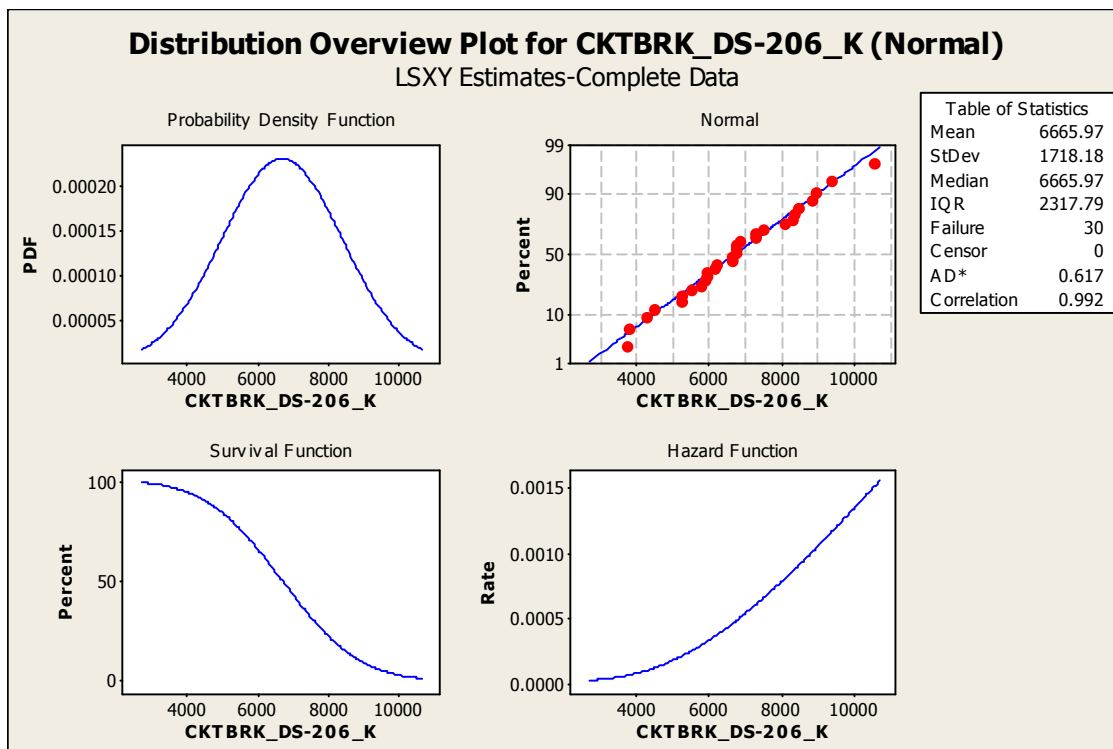
Figure 16. Normal distribution plots for circuit breakers (DS 206 and type K)

As clearly shown from the plots in Figure 16, same as the Weibull distribution plots in Figure 14, the normal distribution fits the failure records very well and the A-D statistic number is very small (the A-D number for normal distribution is 0.617, as compared to 0.767 for the Weibull distribution). The "percent plot" (upper right) shows that almost all the failure "points" fall closely around the percentage plot (see also footnote 7) line, which means that the distribution plot agrees with the failure record data very well. Also the "Rate plot" shows that there are significant aging effects for this type of circuit breakers; that is, the hazard rate (failure rate) increases significantly as the system ages. The differences between the two distributions (Weibull and normal) lie not

only in the way the failure rates increase, but also in the shape of the associated pdf (probability density function) plots.

One thing in common between the two acceptable "best fits" (Weibull distribution and normal distribution) is that, no matter how the failure rate is distributed, the failure rates increase as the component ages. This is exactly one of the important features that we are seeking, for an application of the entry-time approach in a RIAM based scenario for NPPs.

Table 11

A detailed comparison of A-D numbers and Weibull parameters

Component	Model	Type	A-D-Weibull	A-D-Exponential	A-D-Normal	Weibull Shape	Weibull Scale(Days)
CKTBRK	DS 206	K	0.767	16.452	0.617	4.6	7273
		S	2.789	8.659	0.969	0.99	5536
	HFB3	K	1.421	5.033	1.293	2.6	5848
		S	3.467	43.466	0.74	2.3	7151
MOTOR	CS VSS	S	1.515	3.75	0.872	1.18	6078
	TBDP	S	0.749	4.448	0.674	1.56	6238
	FTYPE AN	S	3.099	11.722	0.835	1.42	8051

Without considering other factors (as will be discussed in detail in Sections 4.3 and 4.4 below, using the A-D numbers and plot observations), we can see clearly that the

failure rate is not constant for DS 206 Type K circuit breakers . On the contrary, the component failure shows some considerable time-dependent features. Similar results hold for the other components (cf. Appendix B). The A-D-statistics for the fits to the various distributions are shown in Table 11.

As we can see from Table 11 that the A-D number using exponential distribution is the largest for each type of model; this means that none of the failure distribution for any of the models follow an the exponential distribution. However, both the Weibull and normal distributions give a good fit, with the normal distribution seeming slightly preferable. Also, a comparison of the Weibull parameters given in Table 11 with those in Table 8 shows that the parameters acquired by fitting the failure with Weibull distributions agree with the "typical" Weibull parameters as suggested by the Barringer website (see also footnote 4) for both circuit breaker and motor.

Therefore, we can draw the conclusion that the INPO-EPIX database is capable of providing appropriate failure rates for use within the entry-time model developed in the preceding Chapters II and III, and that circuit breakers and motors provide instances of the behavior of interest (time-dependent failure rates). In the following sections we therefore pursue more detailed parameter measures and comparisons, to choose both which distribution to use in the entry-time applications, and an appropriate "target system" for application of the entry-time methodology.

4.3 Selection of Target System (Main Generator)

The applicability of the EPIX database has been demonstrated in the preceding section. The next step is to identify a system suitable for entry-time applications, and for

which adequate data exist. Identification of such a "target system" is the objective of this section.

As stated in Chapter I, one of the requirements of the RIAM application is that the failure of the system will increase system risk or generation risk, which means that the system is either safety related or generation-risk related. We choose the main generators as an application in this dissertation to demonstrate the applicability of the entry-time approach to any RIAM based applications in NPPs. Their failure constitutes a generation risk. An introduction to the main generator and its auxiliary systems is found in Section 5.1 below.

This choice is partially motivated by availability of detailed information about main generators from STP (South Texas Project Nuclear Power Plant), where there have been some recent issues with the main generators. A further reason is existence, in the EPIX database, of extensive failure data for main generators, including those at STP.

As mentioned in the preceding section the hazard rate extracted from the failure data is identical to the failure rate needed for use in the entry-time model. Further study of the failure data from the EPIX database for the main generator shows that the hazard function obtained from the data analysis do display aging (time-dependent, cf. Sections 4.4, 4.5 and 4.6), which is an important factor for a demonstration of the utility of the entry-time model.

Because of the generation-risk related property of the main generators, it is almost certain that any failure will be discovered immediately by plant personnel, once it occurs. Therefore, the failure data queried from the EPIX database (e.g. Failure discovery data,

estimated age at failure etc.) is expected to very closely reflect the actual time when a failure occurred.

In the following sections, the failure data for main generators acquired from the EPIX database is analyzed using Minitab software to extract failure distribution and further failure rates to be used in the entry-time application. Due to the generation risk related properties of generator failures, in the analysis, only the failures that resulted in significant power generation loss are queried from the EPIX database. Because those failures can, and in fact normally do, lead to 100% power loss, which is equivalent to reactor trip, we name those failures as "trip-equivalent failures". Just as in the preceding section, we use the MiniTab software to fit the failure data into different distributions to see which best fits the failure data; this "best fit" distribution will be subsequently used in the entry-time model.

This analysis is performed in the following way: First, we choose three different datasets of main generator failure records (all Westinghouse-manufactured, all Westinghouse-manufactured serial numbers similar to STP, STP only). Then for each dataset, we use two different data interpretation methods to fit the failure dataset to each of the Weibull and lognormal distributions. The methodological issues for extraction of failure rates from EPIX database using MiniTab software will be discussed in the following Section 4.4 and the results will be presented in the subsequent Section 4.5.

4.4 Techniques for Extraction of Failure Rates: Methodological Issues

In this section the hazard function from a "best fit" distribution will be used to extract failure rates needed for application of the entry-time methodology. Those are the

primary results needed from empirical data for application of entry-time technique. When we fit the different datasets extracted from the EPIX database with different distributions, to find the best fit for the failure data, the following assumptions are applied: a) All subsequent failures are independent of the prior failures; b) When a system is repaired (not a full system replacement) from a failure, the system is "as-good-as-old" so that any aging effects persist and the failure rates are still dominated by aging effects, if any.

In this section, three different datasets of main generator failure records (all Westinghouse-manufactured, all Westinghouse-manufactured serial numbers similar to STP, STP only) are extracted from the EPIX database; the corresponding query criteria are discussed in Subsection 4.4.1. In Subsection 4.4.2, the data acquired from the database are interpreted according with different plant procedures. Also the different "censoring schemes" used in MiniTab are discussed in Subsection 4.4.2.

4.4.1 Data Selection

As discussed in Section 4.3, the choice of main generator is partially motivated by availability of detailed information about main generators from STP (South Texas Project Nuclear Power Plant), where there have been some recent issues with the main generators. We therefore wish, in the application of entry-time model, to include the failure data for STP main generators. When extracting data from the database, analyzing the fit of the data to different distributions, we have presumed that the failure of components/systems with same or similar model numbers tend to follow same type of distributions. The STP main generators are manufactured by Westinghouse, whose main

generators are also used in some other utilities; however, the specific model used at STP is rarely used elsewhere. In an effort to obtain good statistical results, we therefore have three options in terms of the nature of the failure data to e extracted from the EPIX database. We describe the options in order of largest amount of data (least restrictive) to smallest amount of data (most restrictive) in the following paragraphs.

The first option is to query all the failure records from the EPIX database for main generators manufactured by Westinghouse (including STP main generators), and we name this dataset as "Westinghouse Dataset" (Dataset 1). Among the three options or search criteria, this option is the least restrictive and hence gives the largest amount of data. However, due to the "mixture" of data (different model numbers) from different sources (different nuclear power plants and different units), the failure data may not fit any type of distribution well; this effect will be seen in the results presented in Section 4.5.

The second option is to query all the failure records for main generators manufactured by Westinghouse that have model numbers similar to those of the STP main generators (i.e. only the last few digits of the model numbers are different, which implies similar design with only slightly differences), and we name this dataset as "Model Specified Dataset" (Dataset 2). As mentioned earlier in this section, we presume that the failures of components/systems with same or similar model numbers tend to follow the same distribution. Therefore, "Model Specified Dataset" is able to give adequate amount of "samples" (failure records) and it is feasible to generate a failure distribution that all the failure data tend to follow using the data in this dataset. The

advantage of using "Model Specified Dataset" is that selecting more data has the advantage of giving better statistics by including systems that are dissimilar, in some respect, to those at STP. However, the disadvantage of it is that the distribution acquired from the dataset might tend to deviate from the distribution for the failure of STP main generators.

Comparing to the two options above, the last option is to query the failure records for main generator with STP model number without considering failures at other plants, and we name this dataset as "STP-only Dataset" (Dataset 3) Apparently the failure records from a single nuclear power plant (2 individual units) may not provide sufficient sample size to show good statistical results, and hence give a failure distribution that fits well the failure data in this dataset, as shown in the following section of this chapter. However, this is only a hypothesis not a demonstration and there is future work that ultimately is needed in this regard, but that is outside the scope of this dissertation.

In the following Subsection 4.4.2, the datasets specified in this section will be interpreted in accord with different assumed operational procedures, e.g. discovery by inspection and discovery by alarm. The corresponding MiniTab treatment of each of these interpretations is also given in the following subsection.

4.4.2 Data Interpretation

In this subsection, the data from the acquired from the EPIX database using SQL queries are interpreted in two different ways in accordance with two different operational procedures at nuclear power plants and the way the failures were discovered.

Data in "Model Specified Dataset" as queried from the EPIX database can be found in Table 12 and the data in the "Westinghouse Dataset" can be found in Appendix C. Table 12 gives the estimated age at failure for all main generators that have similar model number to those at STP.

When querying the EPIX database to obtain the data in Table 12, first the main generator model number for STP main generators was acquired by querying the "Device Table", and then the main generators with same or similar model numbers as that at STP were queried from the same table. After that, the detailed failure information including "estimated age at failure", "failure discovery data" and other information were extracted from the database through a series of queries involving several tables and using the inner-join technique for SQL.

In general, and absent further detailed information, there are two possible interpretations of an observation of a single failure event (e.g. the failure event corresponding to any single datum in Table 12). Such an event can be discovered some time after the failure, or it can be discovered immediately after the incident. Those two types of observation correspond to two different operational procedures, which we indicate respectively as "discovery by inspection" and "discovery by alarm." More generally, the failures from any dataset discussed in the previous subsection are a mixture of the two different types of observations, i.e., they can be discovered by inspection (only know the failure occurred before this inspection and after the previous one) or they can be discovered by alarm (exact failure time). However, from the information in the EPIX database *per se*, it is not feasible to ascertain which type of

observation a single failure corresponds to. In order to better understand a particular failure, individuals, documents or reports associated with that failure must be consulted. This is not feasible for the current research.

Therefore, we choose to assume each of the two types of observations for each dataset. That is, the failure data from each dataset are treated by each of the "discovered by inspection" procedure or the "discovered by alarm" procedures. The way in which each of these procedures is embodied in the MiniTab software will now be discussed.

In MiniTab software, there are three different types of censoring schemes. (For a detailed explanation of "censoring," and examples of these censoring schemes, please see Appendix D.). These three schemes are "Right Censored", "Left Censored" and "Interval Censored". Those three types of censoring schemes correspond to three different types of observations: When we only know that the failure occurred *after* a particular time, the "Right Censored" scheme is applied; when it is only known that the failure occurred *before* a particular time, the datum is identified as "Left Censored" scheme is used; when we know that the failure occurred *between* two particular times, the "Interval Censored" scheme is applied. And when the failures are exact, no censoring scheme is needed in the analysis.

Table 12

Failure date for main generators of similar models as STP

EstAgeAtFailure
2715
3367
3385
3494
3940
3975
4006
4011
4030
4372
4377
4453
4465
4619
4725
4742
4762
5051
5157
5200
5781
5883
5986
5996

Corresponding to the interpretation of plant procedure, "Interval Censored" data will be used in the MiniTab when the failure is assumed to be discovered by inspection because we know the failure occurred between two individual inspections; "noncensored" data (exact failure data) will be used when the failure is assumed to be discovered by alarm.

As mentioned in the preceding subsection, because of the generation-risk related property of the main generators, it is almost certain that any failure will be discovered immediately by plant personnel, once it occurs. This presumably is why, as shown in the Section 4.5, the "exact failure data" consistently provides the best fit for the failure data. Thus we will ultimately choose to use failure data represented as noncensored.

To summarize: We have three different datasets (Westinghouse, Model Specified and STP-only), two interpretations (discovery by inspection and discovery by alarm) and three different parametric distributions (exponential, lognormal and Weibull). Collectively this corresponds to 3×2×3=18 different combinations of choices. From the analysis in Section 4.2, we have drawn the conclusion that failure rate for components are not ell represented by constant failure rates, which correspond to exponential distributions. A detailed analysis (not shown here) of the main generator failure data confirms that conclusion for our target system (main generators). Therefore, in the following section only distribution plots using the Weibull and lognormal distributions are displayed, which reduces the number of combinations to 12. Further, in the analysis of the following section, lognormal instead of normal distributions are used, because sometimes the normal distribution can predict failures at negative times, which are not possible in practice.

4.5 Techniques for Extraction of Failure Rates: Comparison of Results

In the preceding section, the methodological issues of extracting failure rates from EPIX for the application of entry-time model were discussed. In this section we will compare results for the three datasets acquired from the database using different query

criteria, with censored or non-censored data as needed for different observations. The results are presented in the order of dataset; for each dataset, it is ordered by type of observation; and for each observation we present and discuss the fit to first the Weibull, then the lognormal distribution.

4.5.1 Results for Westinghouse-manufactured Main Generators

The data in this dataset were queried from the EPIX database using the following search criteria: *Search the failure records for Main Generators manufactured by Westinghouse*. A report consisting of 100 records in total is generated by this query (see Appendix C for the complete report).

In the following, we first (subsubsection 1) treat the data by "discovery by inspection" scheme, defined as follows: Within the MiniTab formatting, the first failure is labeled "Left censored," and the last failure is labeled "Right censored." These choices are based on the assumption that the first failure happened before the first inspection and the failures following the last one will occur some time after it. All others failures are labeled as, "Interval censored" which corresponds to the assumption that failure occurred some time before discovery and after the preceding discovery of a failure at the same plant. Second (subsubsection 2), the data will be treated as "discovery by alarm" observations, where all failures are recorded as exact within their MiniTab representation, so that no censored data are used.

4.5.1.1 Results for Westinghouse-manufactured Main Generators Using "Discovery by Inspection" Scheme

In Figure 17, a two-parameter Weibull distribution is used to fit the failure data in the Westinghouse dataset, assuming discovery by inspection, with left censoring prior to first discovery, right censoring subsequent to last and all others interval censored. The plot at upper right shows that, although most of the data points fall around the percentage plot (see also footnote 7) line, there are some points, especially at earlier times and at later times, that depart significantly from the percentage plot. This is presumably reflected in the relatively large A-D number (4.269).
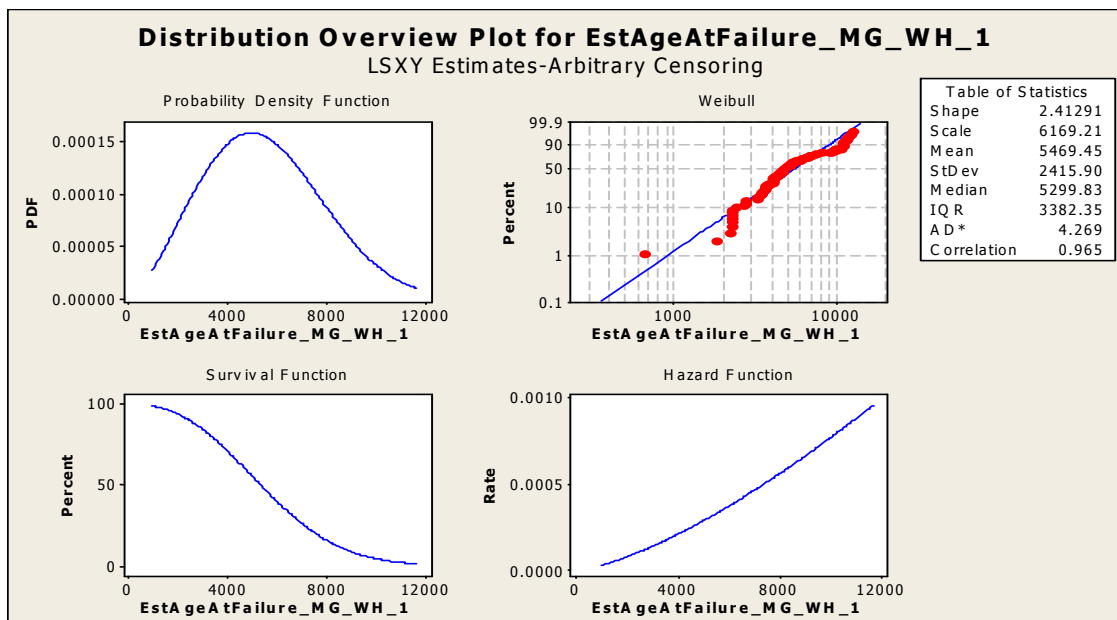
Figure 17. Two-parameter Weibull distribution overview plot using "discovery by inspection" scheme for Dataset 1

The corresponding results for the lognormal fit to the failure data in this group, using "discovery by inspection" is shown in Figure 18. As in the Weibull distribution plot in Figure 17, we can see that although most of the data points fall around the percentage plot (see also footnote 7) line, there are some points, especially at early time and later time, that depart from the percentage plot; however, now the A-D number is much smaller (1.262) than that for the Weibull distribution.
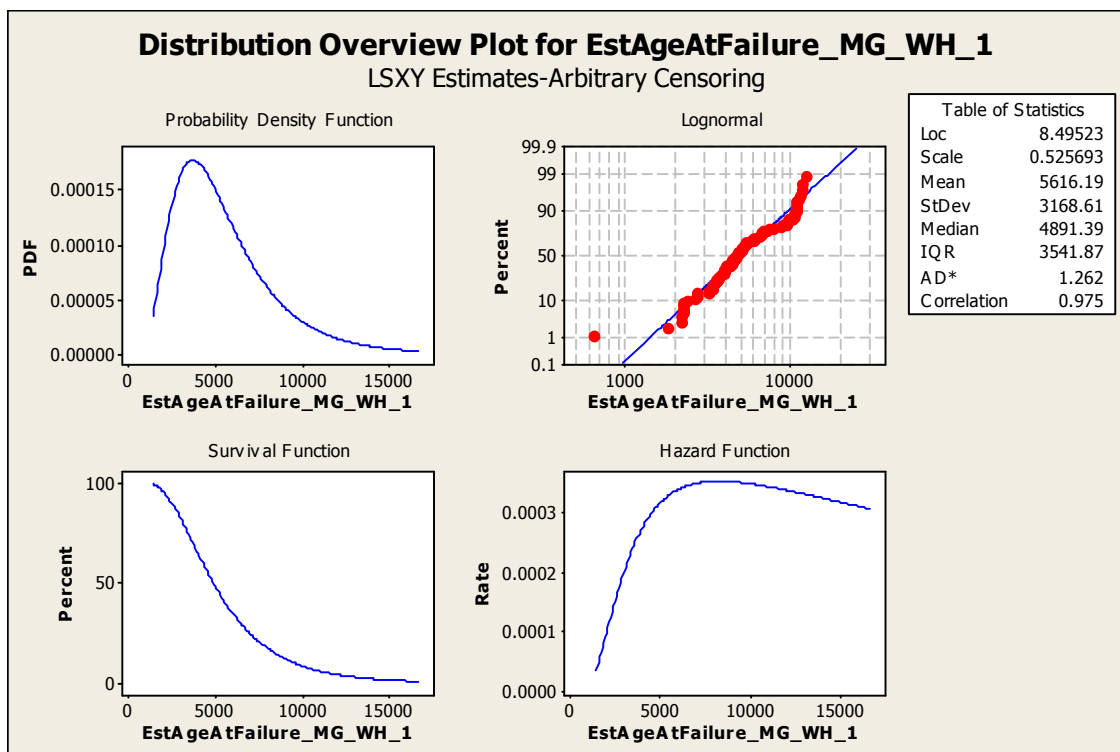
Figure 18. Two-parameter lognormal distribution overview plot using "discovery by inspection" scheme for Dataset 1

It can be seen from the lower right plot hazard plot in Figure 18 that the failure rate increases first and then decrease eventually after some peak point, which rarely happens for component degradation. This phenomenon is known as the "Fountain of Youth" (or "Ponce de Leon") effect, which is a well-know deficiency of lognormal distributions. However, the discussion in Section 5.3 shows that the choice of lognormal or Weibull distribution does not change the results much. The explanation of this phenomenon should be further explored in future research, but here the discussion of the reason is out of the scope of the topic in this section.

4.5.1.2 Results for Westinghouse-manufactured Main Generators Using "Discovery by Alarm, with No Censoring" Scheme

In this section, instead of using the "discovery by inspection" scheme, the same failure data from "Westinghouse Dataset" are tested using the "discovery by alarm, no censoring" scheme, which assumes all failures were discovered by alarm and hence the plant personnel were notified immediately.
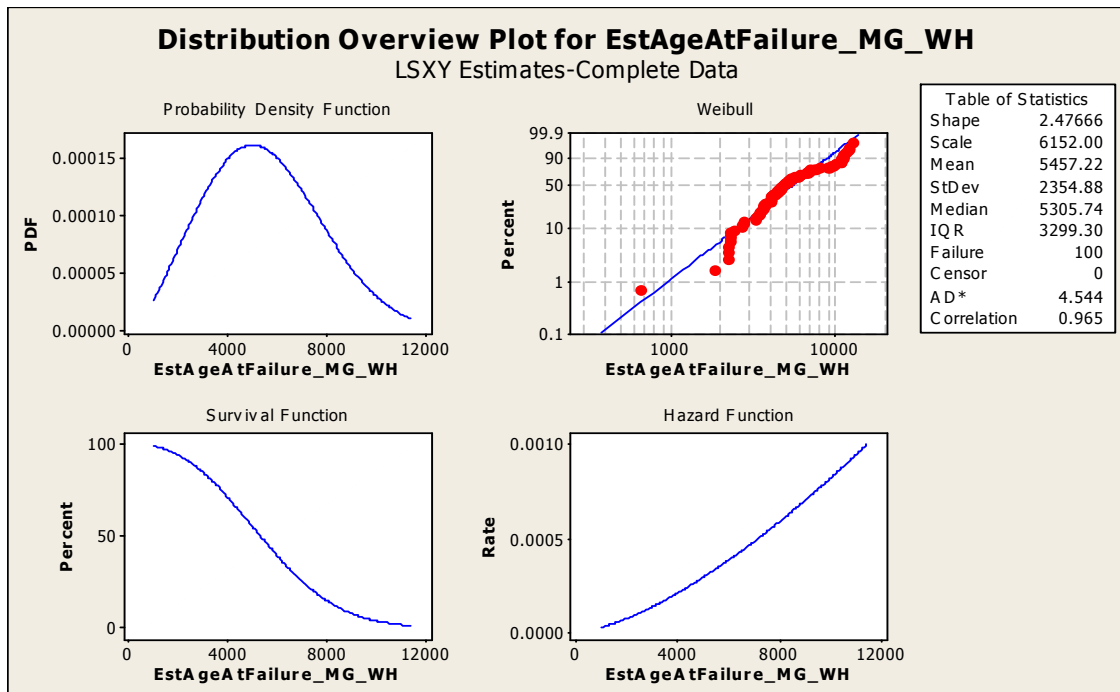
Figure 19. Two-parameter Weibull distribution overview plot using "discovery by alarm, with no censoring" scheme for Dataset 1

The results for the Weibull distribution are shown in Figure 19. The A-D number greater than 4.5 suggests the Weibull distribution does not provide a good fit. As compared to the Weibull distribution with "discovery by inspection" scheme in Figure 17, the A-D number is even larger using the discovery by alarm scheme than under the discovery by inspection approach.

Distribution Overview Plot for EstAgeAtFailure_MG_WH
LSXY Estimates-Complete Data

Table of Statistics	
Loc	8.49523
Scale	0.516051
Mean	5588.05
StDev	3086.80
Median	4891.39
IQR	3474.27
Failure	100
Censor	0
AD*	1.173
Correlation	0.975
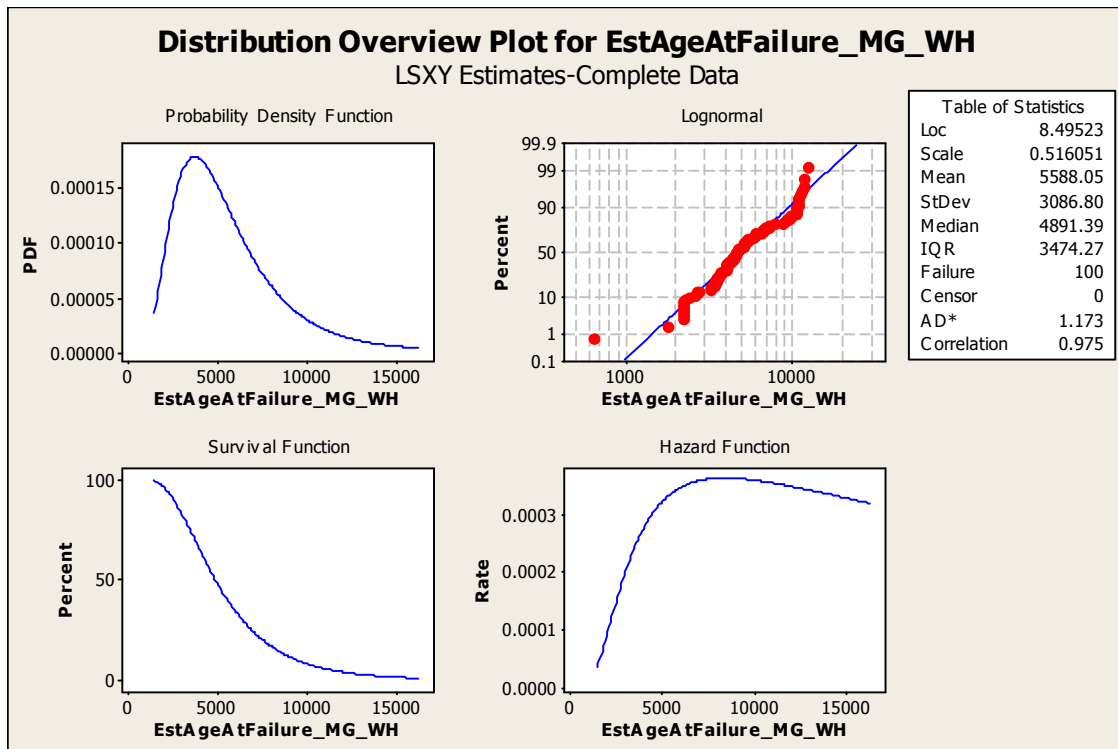
Figure 20. Two-parameter lognormal distribution overview plot using "discovery by alarm, with no censoring" scheme for Dataset 1

The lognormal distribution plot using "discovery by alarm, with no censoring" scheme is shown in Figure 20. As for the discovery by inspection scheme, the lognormal distribution fits the failure data better than the Weibull distribution; as judged by A-D numbers and probability plots. Also as for the discovery by inspection scheme, the lognormal failure rate ultimately decreases. As previously mentioned, explanation of this phenomenon should be further explored in future research, but here the discussion of the reason is out of the scope of the topic in this section.

In Figures 21 and 22 the 95% probability plots with discovery by alarm are given in both Weibull and lognormal distributions, to give an alternative view of the failure data.
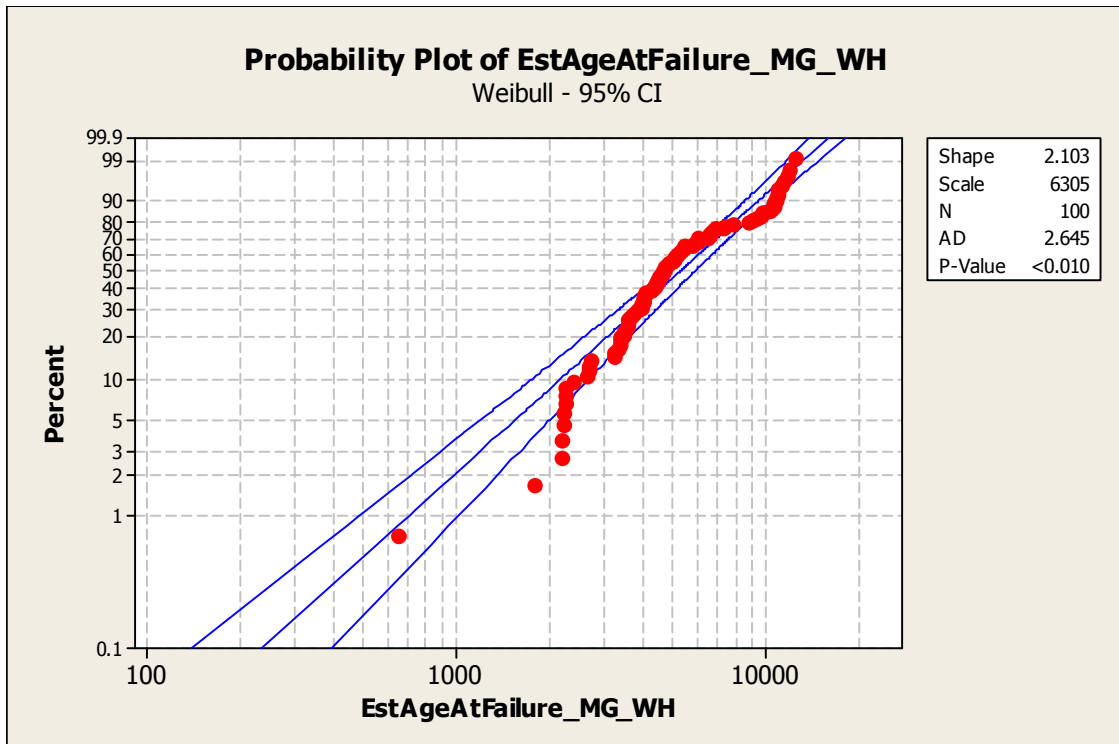
Figure 21. 95% probability plot using Weibull distribution with exact failures for

Dataset 1

Comparing the probability plot using Weibull distribution (Figure 21) and the one using lognormal distribution (Figure 22), it is easy to see the obvious difference, by inspection. More points fall outside the 95% region in the Weibull distribution then in the lognormal distribution. Also, a comparison of A-D numbers for 95% probability

plots confirms that the lognormal distribution is a better fit than the Weibull distribution

(1.057 vs. 2.645).
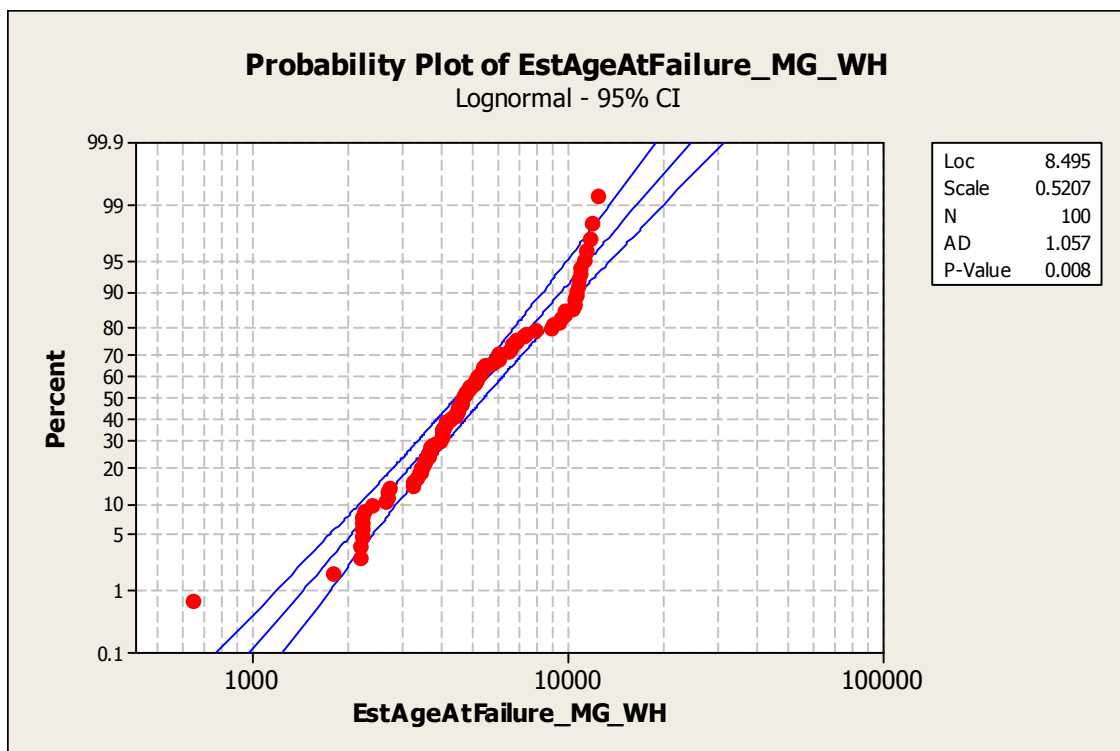
Figure 22. 95% probability plot using lognormal distribution with exact failures for

Dataset 1

4.5.2 Results for Westinghouse-manufactured Main Generators Similar to Those

Models Used at STP

Similarly, we can plot different distributions using the two data interpretation

schemes for data in "Model Specified Dataset". In this data-selection method only

failure records for main generators manufactured by Westinghouse and with similar model number as those for STP were extracted from the database. The hope is that this will yield a tighter and more coherent distribution of the failure data than was found in the preceding data-selection approach.

The search criterion for this dataset is: Search the failure records for main generators manufactured by Westinghouse and with similar model number as that of STP. The 24 resulting records are shown in Table 12.

As for the data in "Westinghouse Dataset", in the following section we first (subsubsection 1) treat these data by "discovery by inspection" observation, and then (subsubsection 2) following the "discovery by alarm" assumption, wherein all failures are exact and no censored data is used.

4.5.2.1 Results for Westinghouse-manufactured Main Generators Similar to Those at STP Using "Discovery by Inspection" Scheme

Similarly, the failure data is first fit to a (two-parameter) Weibull distribution (Figure 23). The first overall observation of the plots is that with fewer data points and similar model numbers, the data fit into Weibull distribution very well comparing to those in the "Westinghouse Dataset" (mixed data from the same manufacturer). Also a smaller A-D number (1.429, vs. 4.269) suggests that the failure data agree fit a Weibull distribution well.
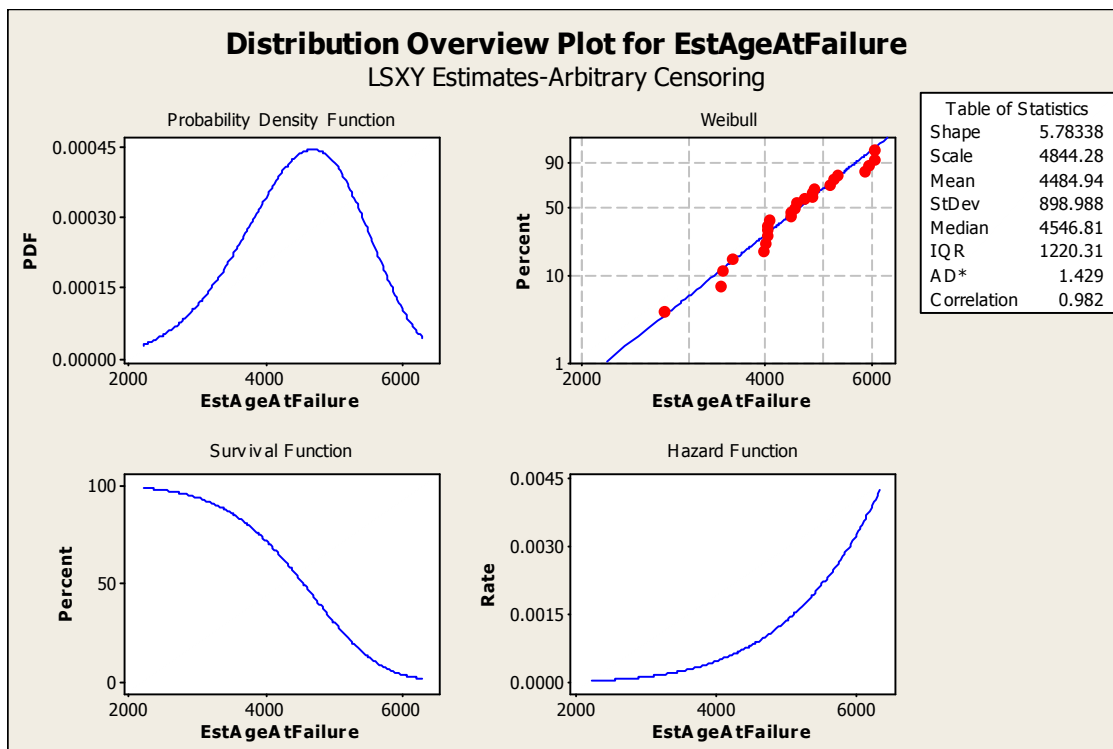
Figure 23. Two-parameter Weibull distribution overview plot using "discovery by inspection" scheme for Dataset 2

Figure 24 is the lognormal distribution using the data in this group. Just as the Weibull distribution above (Figure 23), almost all the points fall near the probability plot line, which means that the (best-fit) distribution agrees with the actual failure data distribution. A comparison of A-D numbers shows that the lognormal distribution is a better fit than Weibull because the A-D number is smaller (1.179, vs. 1.429).
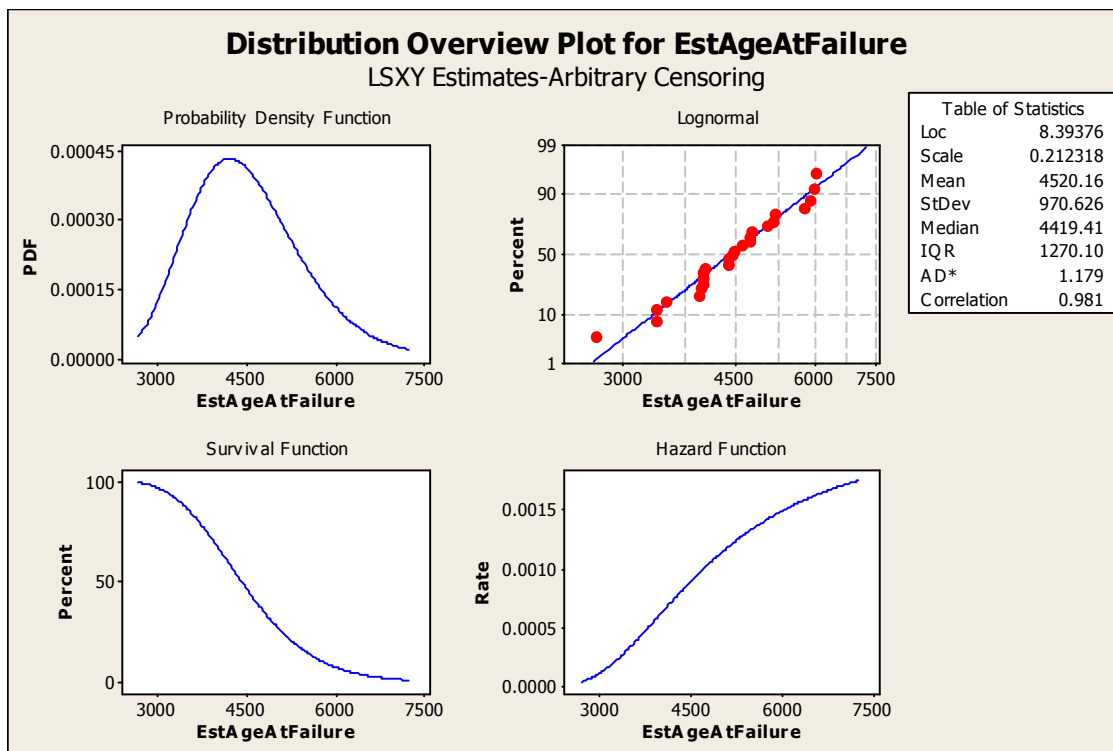
Figure 24. Two-parameter lognormal distribution overview plot using "discovery by inspection" scheme for Dataset 2

A small A-D number (1.179) in the lognormal distribution plot (Figure 24) shows the accuracy of the data fit to this distribution. The Pearson Correlation Coefficient[9] of 0.981, which is close to one (1), tends to confirm this conclusion.

---

[9] The Pearson correlation measures the strength of the linear relationship between the X and Y variables on a probability plot. The correlation will range between 0 and 1, with higher values indicating a better fitting distribution.

4.5.2.2 Results for Westinghouse-manufactured Main Generators Similar to Those at STP Using "Discovery by Alarm, with No Censoring" Scheme

In this section, instead of using the "discovery by inspection" scheme, the same failure data from "Model Specified Dataset" are tested using the "discovery by alarm" scheme, which assumes plant personnel were notified immediately upon failure.
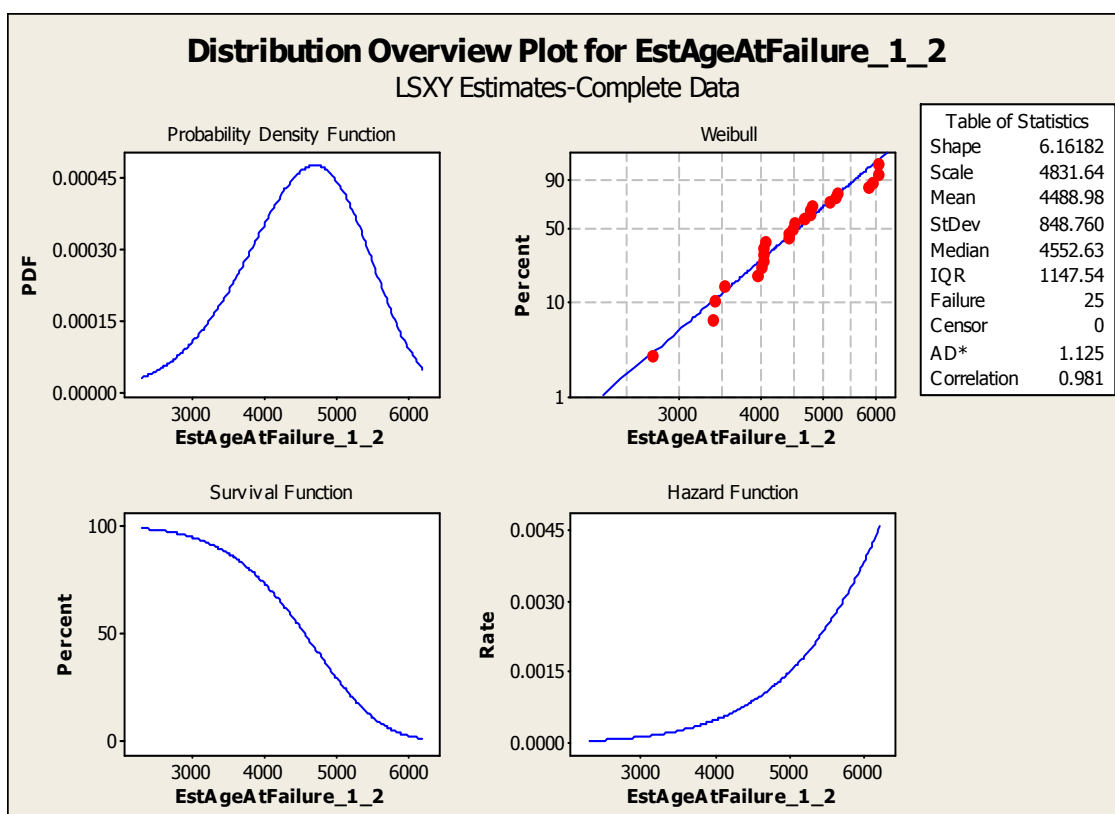
Figure 25. Two-parameter Weibull distribution overview plot using "discovery by alarm, with no censoring" scheme for Dataset 2

Figure 25 and Figure 26 are plots using the two-parameter Weibull distribution and the lognormal distribution, respectively. The Pearson Correlation Coefficients for the two distributions are both 0.981. The A-D number of the latter (0.784) is smaller than that of the former (1.125), which means that the lognormal distribution is a better fit than the Weibull distribution.
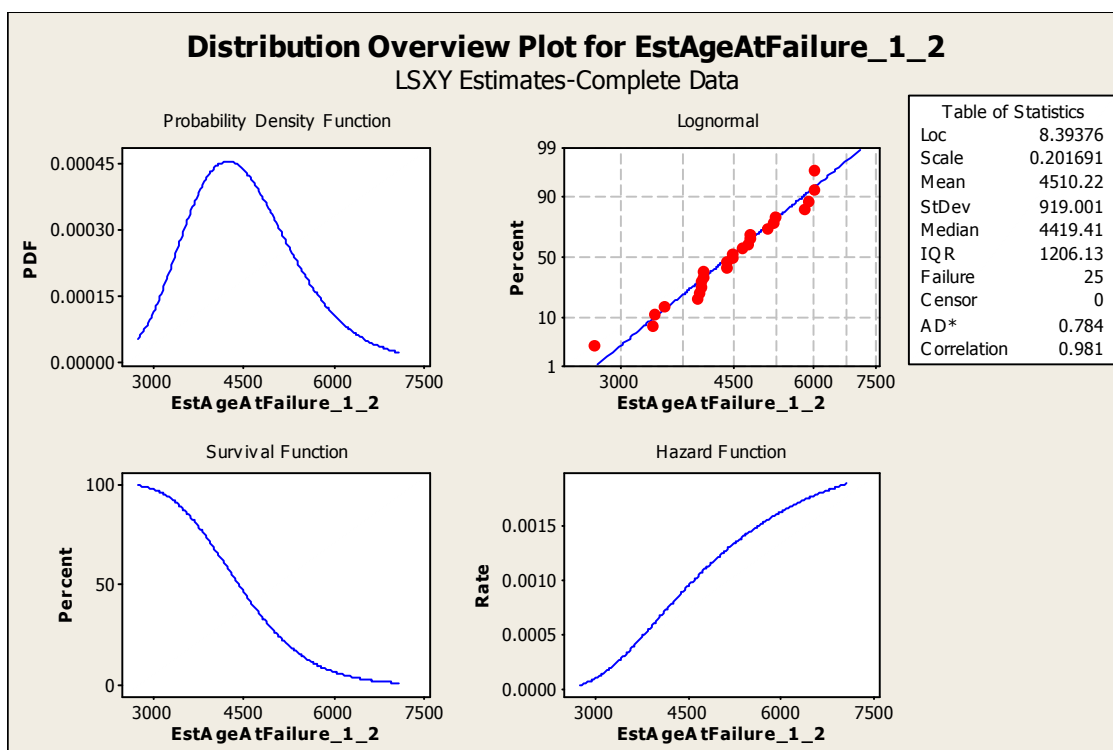
Figure 26. Two-parameter lognormal distribution overview plot using "discovery by alarm, with no censoring" scheme for Dataset 2

In Figures 27 and Figure 28, the 95% probability plots with exact failure data are given respectively for the Weibull and lognormal distributions, to give an alternative view of the failure data in "Model Specified Dataset".
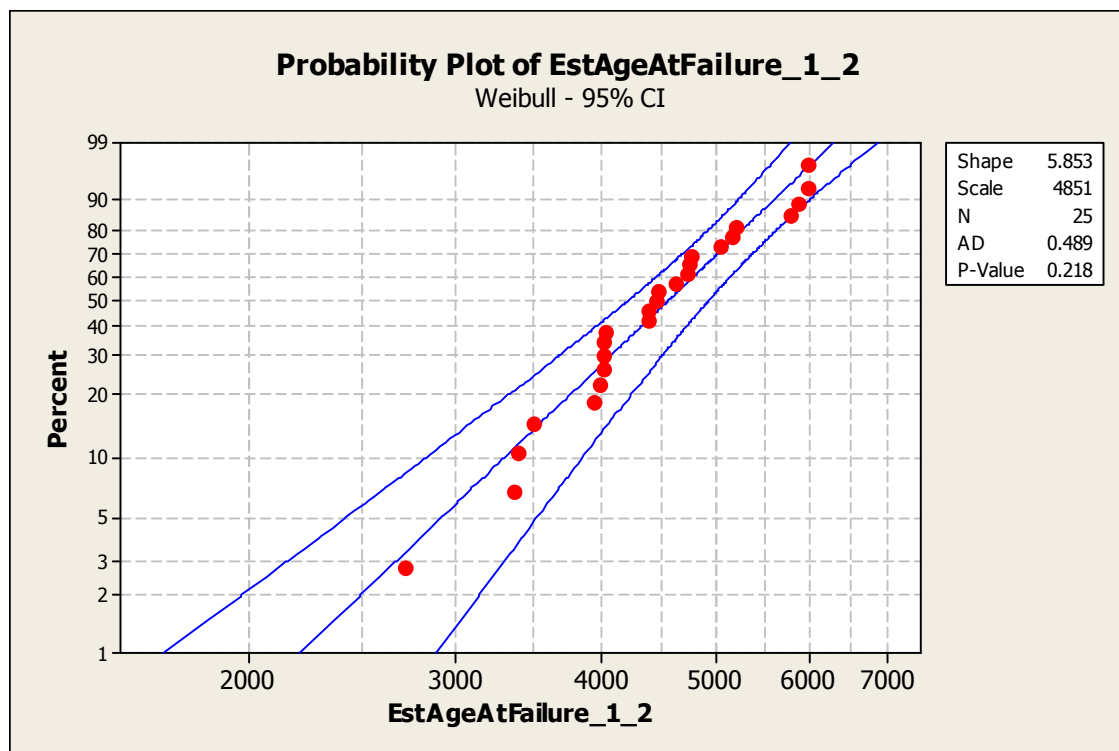
Figure 27. 95% probability plot using Weibull distribution with exact failures for

Dataset 2

Similarly to the probability plot in the "overview" plots, the 95% probability plot gives the 95% confidence region and the corresponding A-D number is a measure of how closely the data points fall into this region rather than on a single line as the probability plot in the "overview" plots. Hence by inspection of Figure 27 and Figure 28,

one can easily find that all the points fall into this 95% probability region for both of the plots. Meanwhile, the A-D numbers in both distributions are much smaller than all others in the plots for the all-Westinghouse dataset, which suggests that the failure data in "Model Specified Dataset" can fit into both Weibull and lognormal distributions very well and hence can be used for the entry-time applications.
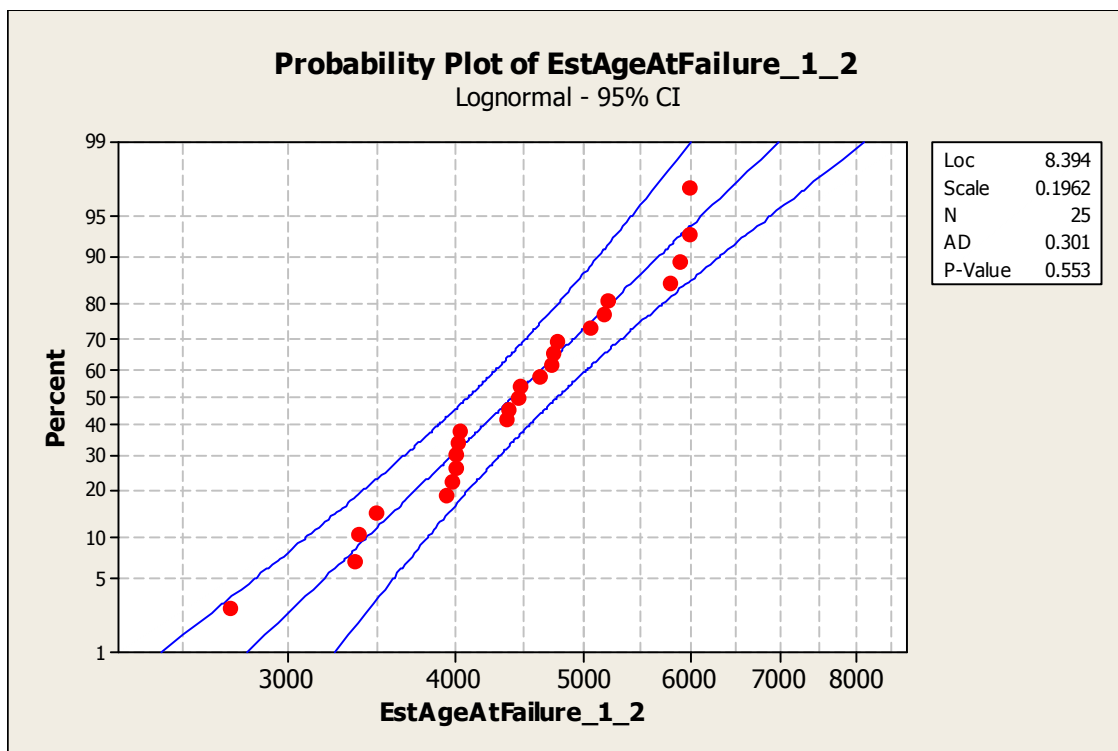
Figure 28. 95% probability plot using lognormal distribution with exact failures for

Dataset 2

4.5.3 Results for STP Main Generators

In the following, we plot different distributions using the two data interpretation schemes for data in "STP-only Dataset". In this data-selection method only failure records for main generators at STP were extracted from the database.

As for the other two datasets, in this subsection, we first (Subsubsection 4.5.3.1) treat the data as representing "discovery by inspection" observations. Following that, the data will be treated following the "discovery by alarm" scheme, in which all failures are exact and no censored data is used.

The results for this dataset "STP-only Dataset" are given in Table 13.

Table 13

Failure date for main generators with STP model numbers

Age
3494
3975
4006
4011
4244
4372
4377
4453
4520
5051
5883

Table 13 shows the estimated age at failure for main generator failures at STP. A close look at the data highlighted in the table (also in red color) reveals that there were some failures occurred in a very short time period. A detailed study of the STP documents for those failures shows that the third failure (day 4011) in the highlighted region results from incorrect maintenance of the previous failure (day 4006). Therefore the two failures are not independent, so that the "bad as old" assumption is invalid. The "good as new" assumption might be true, but would need to allow for infant mortality in the failure mode that was attempted to repair. An entry time model could accommodate that, but would need to allow for multiple entry times, for each failure mode. This possibility will be further discussed in the concluding Chapter VI.

4.5.3.1 Results for STP Main Generators Using "Discovery by Inspection" Scheme

Using the failure with STP main generator model, the Weibull distribution plots, with "discovery by inspection" scheme, are given in Figure 29.
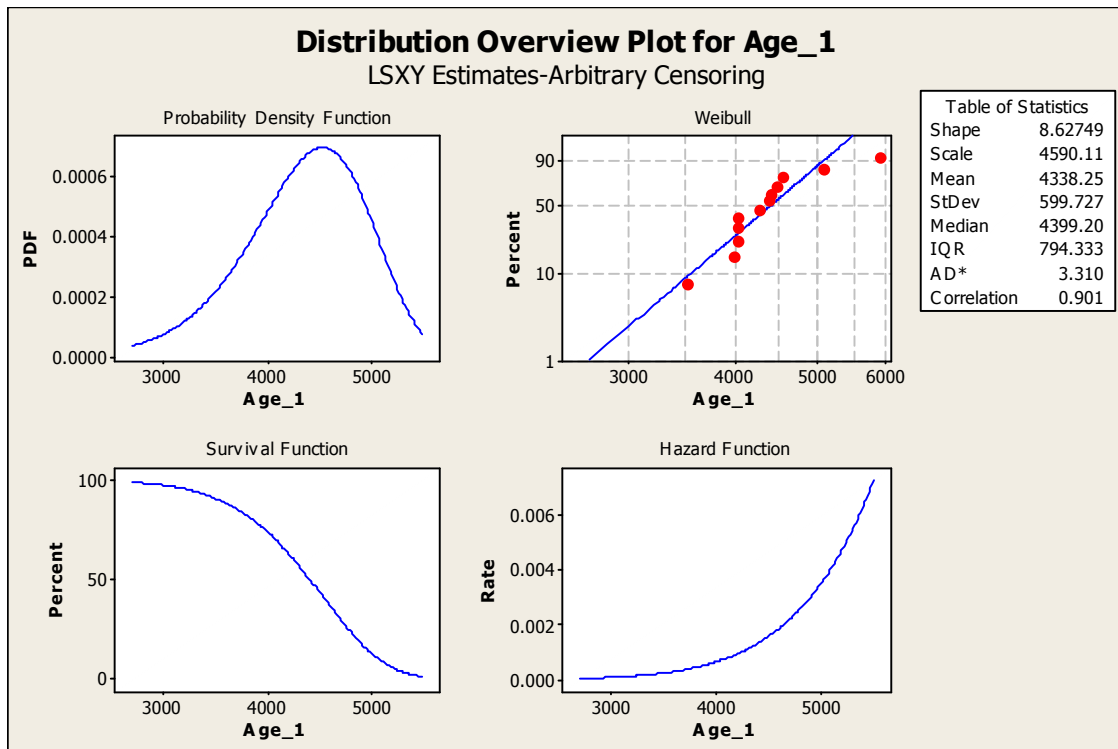
Figure 29. Two-parameter Weibull distribution overview plot using "discovery by

inspection" scheme for Dataset 3

Comparing to its "counterpart" plot in Figure 23 which plots all the failure data with similar model number, the A-D number in this plot is much larger (3.310 vs. 1.429). The reason for that probably lies in the fact the limited sample space (amount of failure data) is not sufficient to provide good statistics.
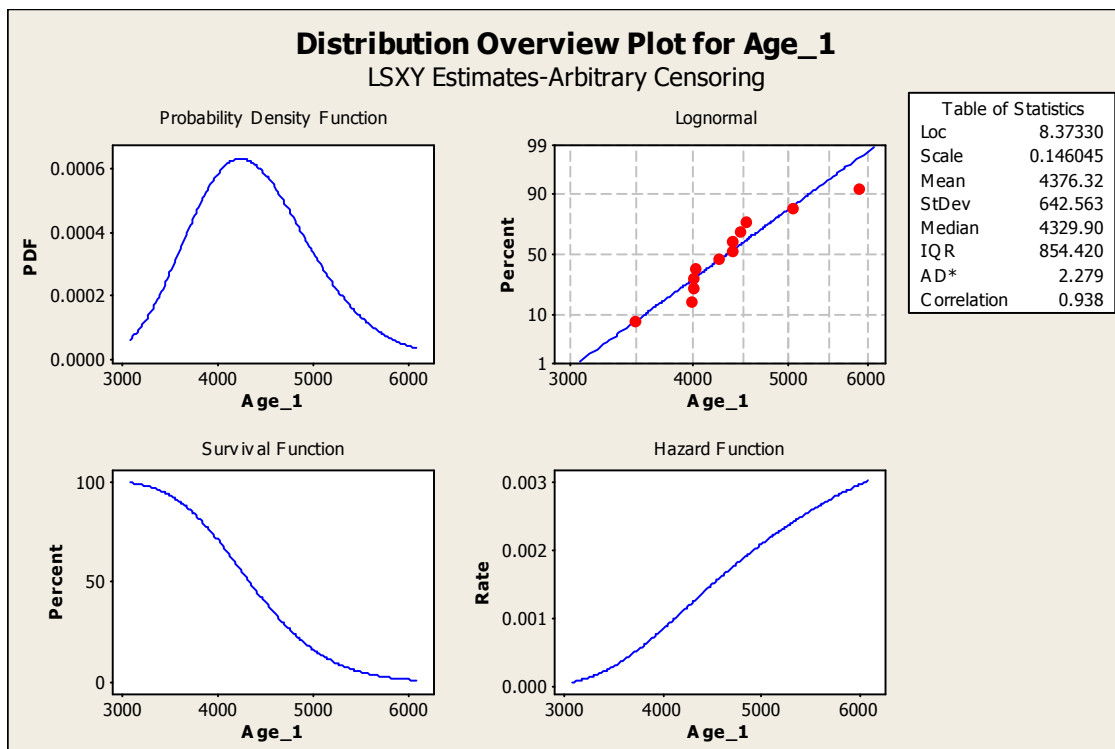
Figure 30. Two-parameter lognormal distribution overview plot using "discovery by inspection" scheme for Dataset 3

With comparison to Figure 29, the lognormal distribution plots in Figure 30 shows a slight decrease in A-D numbers (2.279 vs. 3.310) and increase in Pearson Correlation number (0.938 vs. 0.901). However, the distribution fit is not as good as in "Model Specified Dataset" (i.e., all Westinghouse-manufactured generators with similar or same model number to those at STP; cf. Figure 24).

4.5.3.2 Results for STP Main Generators Using "Discovery by Alarm, with No Censoring" Scheme

In this subsubsection, instead of using the "discovery by inspection" scheme, the same failure data from "STP-only Dataset" are tested using the "discovery by alarm, no censoring" scheme.
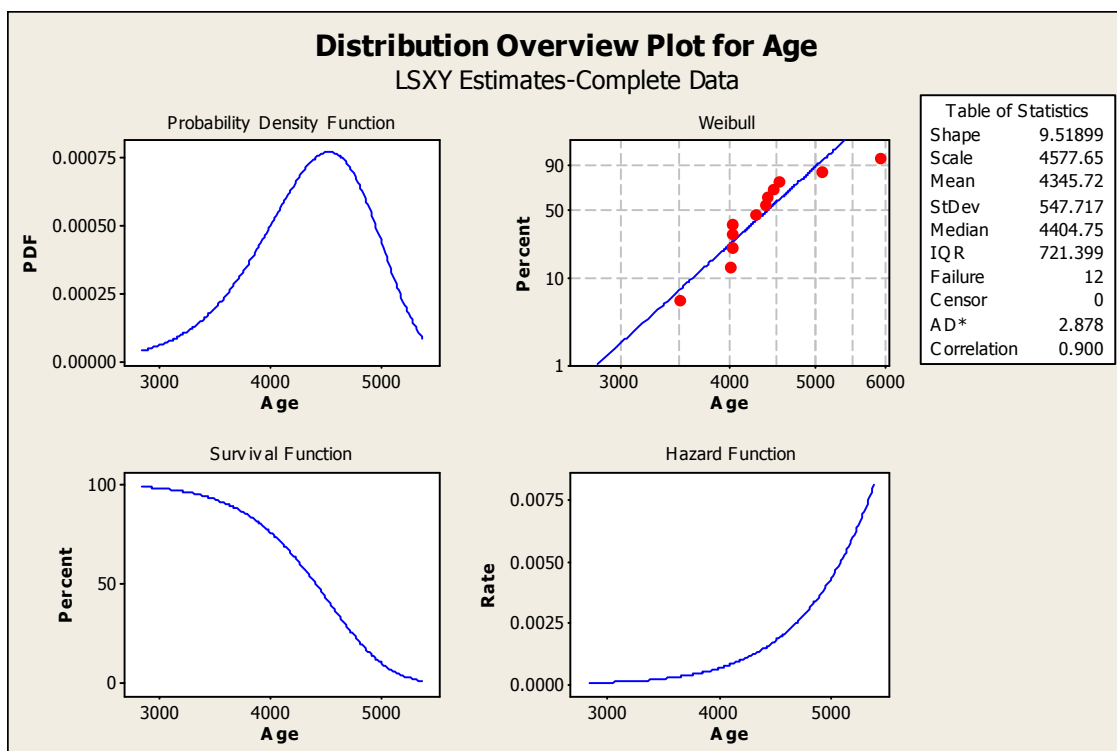
Figure 31. Two-parameter Weibull distribution overview plot using "discovery by alarm, with no censoring" scheme for Dataset 3

With comparison to Figure 29, where the "discovery by inspection" scheme is applied, the Weibull distribution plot in Figure 31 which uses "discovery by alarm, with no censoring" scheme has a larger A-D number and a smaller Pearson Correlation Coefficient, and this means that the "discovery by inspection" scheme provides a better fit for data in "STP-only Dataset". Further comparison of the data is given in Subsection 4.5.4.
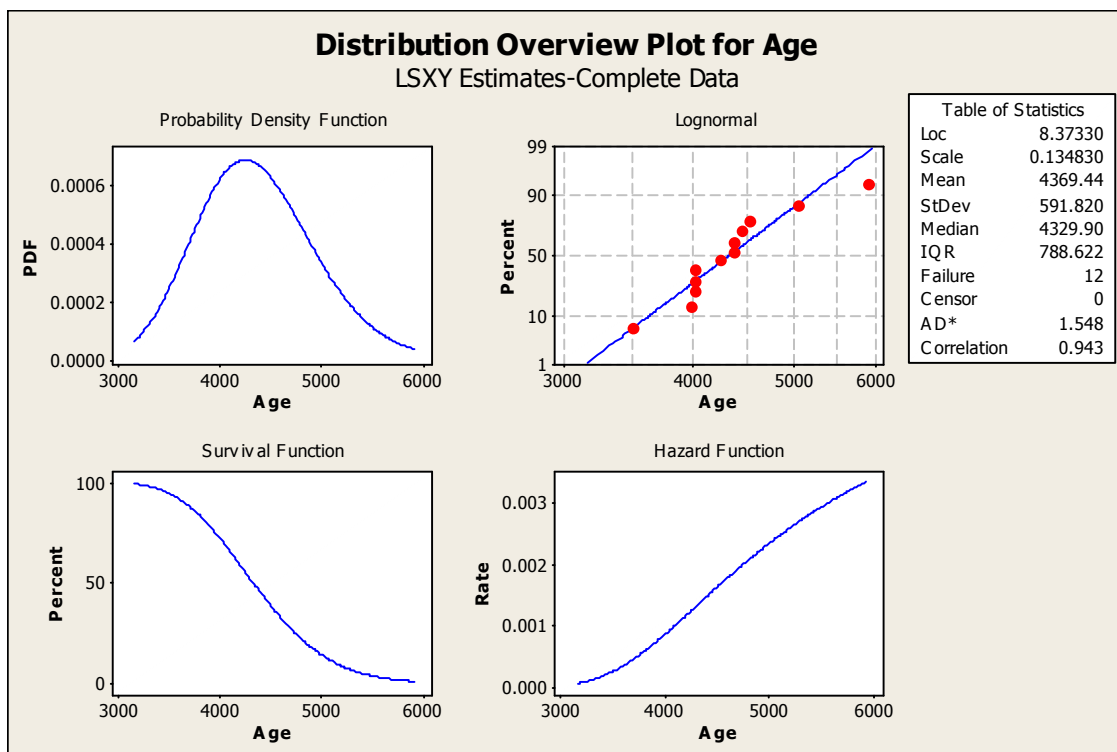
Figure 32. Two-parameter lognormal distribution overview plot using "discovery by alarm, with no censoring" scheme for Dataset 3

Just as the Weibull distribution plot in Figure 31, with comparison to Figure 30 where the "discovery by inspection" scheme is applied, the lognormal distribution plot in Figure 32, which uses "discovery by alarm, with no censoring" scheme has a smaller A-D number and a larger Pearson correlation coefficient.

In the following, the 95% probability plots with exact failure data are given in both Weibull and lognormal distributions to give an alternative view of the failure data.
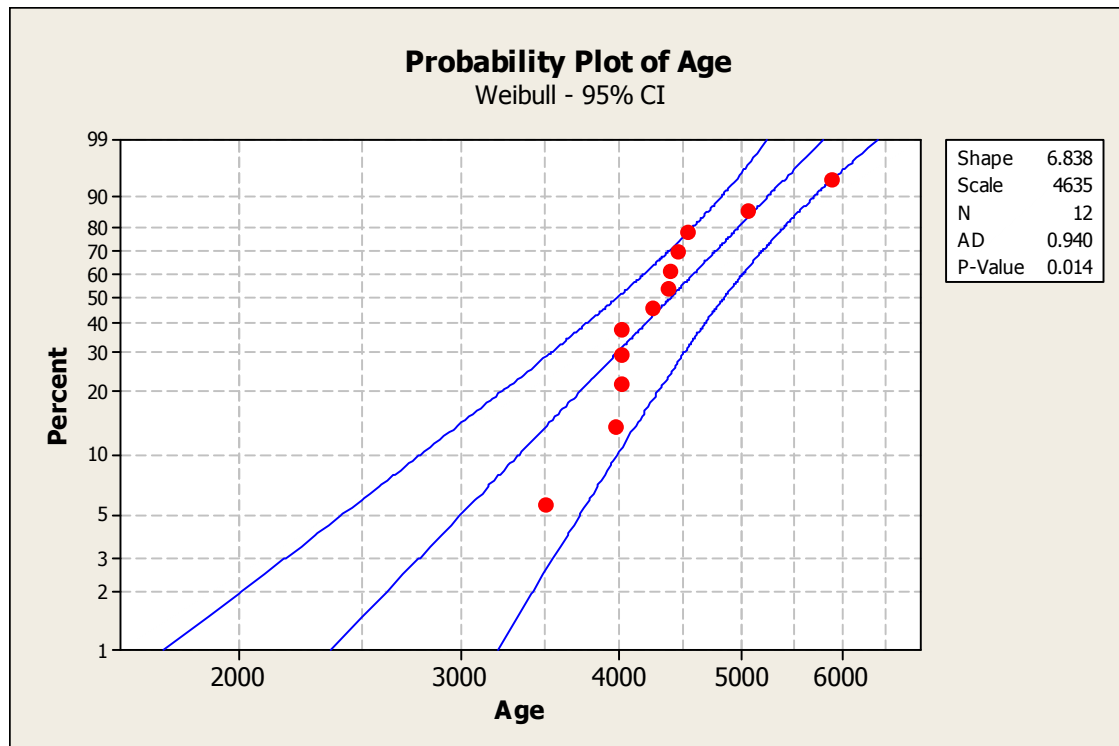
Figure 33. 95% probability plot using Weibull distribution with exact failures for Dataset 3

As can be seen from the two 95% probability plots, using Weibull (Figure 33) and lognormal (Figure 34) distributions, almost all the data points fall into the 95% plot region. However, there are only a few data that fall around the center line; most of the data fall close to the boundary. A detailed comparison of A-D numbers of censoring schemes will be discussed Subsection 4.5.4.
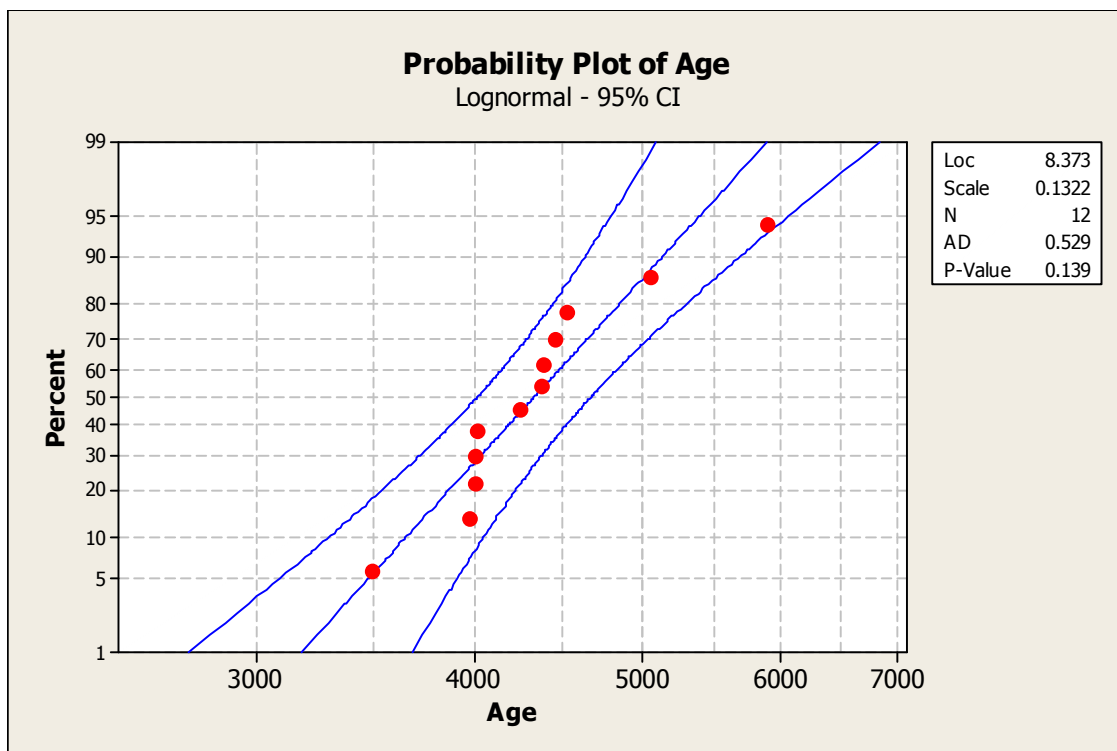
Figure 34. 95% probability plot using lognormal distribution with exact failures for

Dataset 3

4.5.4 Summary of Results

We have, in the preceding sections, tested the three datasets using two different data interpretation schemes with two different distributions, for a total of 12 cases. In this section, the results from those analyses are presented and compared to find the "best" distribution and the best data interpretation scheme.

Using both A-D number and Pearson correlation coefficient as standards in selecting the distribution for the main generator failure data, one can summarize the preceding results in this section as follows:

1) Presumably because of the "mixture feature" of failure data for different model numbers, even though they are from the same manufacturer, the data in the first Dataset (all main generators that are manufactured by Westinghouse) do not fit into any distribution as well as the other two groups. The reason for that presumably is that different models have different failure distribution (e.g. mixture of normal distributions and Weibull distributions), so that the mixture of different distributions does not fit well (large A-D number) to any single simple parametric statistical distribution.

2) For failure records that contain only STP model number (there are no other NPPs using main generators of the exact model number as STP), due to the limited data points (fewer than 20 failure points), the sample space is insufficient to provide good statistics. Also because of the connections between some failures as discussed in the preceding section, the data in this dataset is not good enough for prediction purposes.

3) However, the failure data from model numbers that are similar to STP model show some strong statistical features to predict the time-dependent failure rate for main generator and do future performance analysis for the following reasons:

    a. The sample space is sufficiently large to permit meaningful statistical analysis

    b. Because the search criterion is set by "similar models" and "same manufacturer", the components/systems in this dataset tend to have similar failure distributions. Hence when they are put together, they fit into some distributions very well.

From this summary, we therefore draw the tentative conclusion that the data in "Model Specified Dataset" (i.e. the data searched by the criteria: "Similar model number" and "same manufacturer") is preferable for extracting the failure rates needed for application of the entry-time model to main generators.

More detailed comparison of the A-D numbers and Pearson correlation coefficient s can be found in the following Table 14. (The results for the exponential distribution are also summarized in this table, although not shown above in detail):

Table 14

A complete comparison of A-D numbers and Pearson correlations

Dataset NO.	Records Num.	Data Censoring Type[10]	Distribution Type	A-D Number	Pearson Corr.
1	100	discovery by inspection	Weibull	4.269	0.965
			Exponential	21.247	N/A
			lognormal	1.262	0.975
		discovery by alarm, with no censoring	Weibull	4.544	0.965
			Exponential	22.844	N/A
			lognormal	1.173	0.975
2	25	discovery by inspection	Weibull	1.429	0.982
			Exponential	13.812	N/A
			lognormal	1.179	0.981
		discovery by alarm, with no censoring	Weibull	1.125	0.981
			Exponential	15.151	N/A
			lognormal	0.784	0.981
3	12	discovery by inspection	Weibull	3.310	0.901
			Exponential	7.885	N/A
			lognormal	2.279	0.938
		discovery by alarm, with no censoring	Weibull	2.278	0.900
			Exponential	8.216	N/A
			lognormal	1.548	0.943

As conclusion, data in "Model Specified Dataset" (All Westinghouse-manufactured main generators similar to those at STP generators) will be used for further analysis and the "discovery by alarm, with no censoring" scheme will be applied to the analysis. Further detailed analysis will be carried out in the following section, to generate time-

---

[10] See examples in appendix D for details of the different data censoring procedures.

dependent failure rates and the corresponding distribution(s). These will then be employed in Chapter V, to generate various predictions via the entry-time model of the preceding chapters.

4.6 Further Main Generator Failure Data Analysis

Based on the analysis done in the preceding section, data from failure of similar model numbers ("Model Specified Dataset") will be used in this section. Further, the detailed analysis of this section will be based on the assumption these data represent using "discovery by alarm, with no censoring" scheme based on the comparison of A-D numbers and Pearson correlation numbers.

In this section, rather than two-parameter Weibull and two-parameter lognormal distributions, we use the three-parameter versions of these two distributions to fit the indicated data. The hope is that this will provide further precision for the data fitting. Comparing to the two-parameter Weibull and two-parameter lognormal distributions, the three-parameter versions of these two distributions have a location parameter (also known as "threshold"). The threshold is a shift of the distribution away from 0. A negative threshold shifts the distribution to the left of 0, and a positive threshold shifts the distribution to the right of 0. All failure data points must correspond to a time greater than the threshold. The probability density functions of three-parameter lognormal distribution and three-parameter Weibull distribution can be seen in the following equations respectively (The corresponding two-parameter distributions are similar to the three-parameter ones, but the threshold λ is zero):

$$f(x) = \frac{1}{\sqrt{2\pi}\sigma(x-\lambda)} \exp\left\{-\frac{[\ln(x-\lambda)-\mu]^2}{2\sigma^2}\right\}$$

where μ is the location parameter, σ is the scale parameter and λ is the threshold parameter for the (three-parameter) lognormal distribution.

$$f(x) = \frac{\beta}{\alpha}(x-\lambda)^{\beta-1} \exp\left[-\left(\frac{(x-\lambda)}{\alpha}\right)^{\beta}\right]$$

where α is the scale parameter, β is the shape parameter and λ is the threshold parameter for the (three-parameter) Weibull distribution.
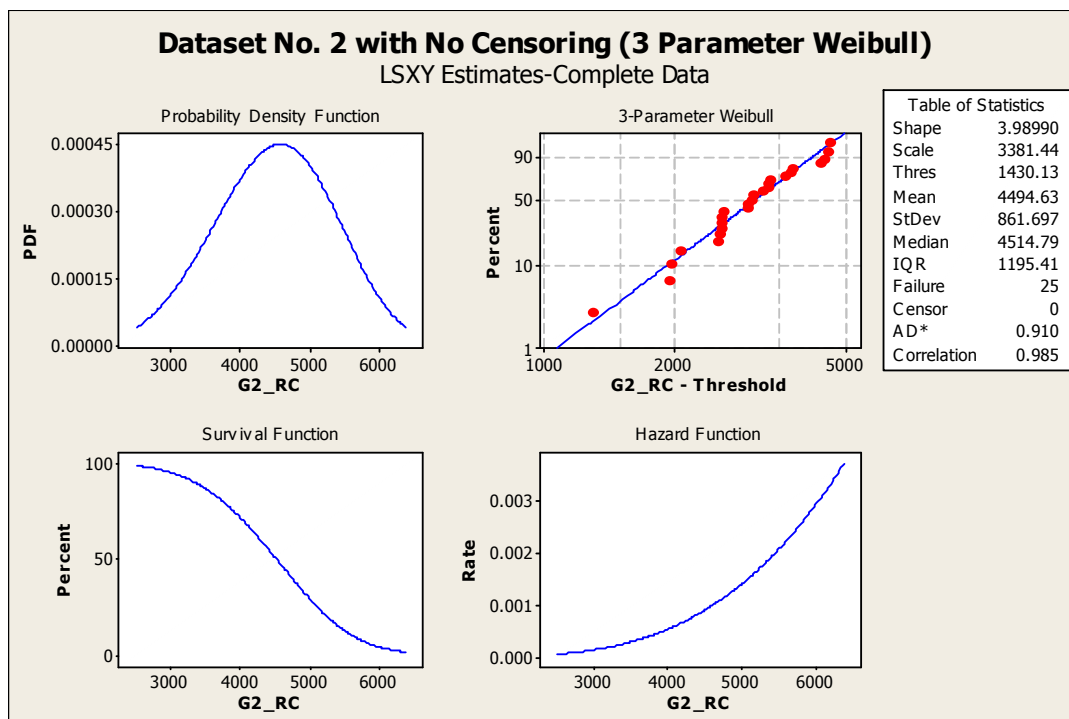
Figure 35. Three-parameter Weibull distribution plot using "discovery by alarm, with no censoring" scheme

Figure 35 is a distribution overview plot of the data in "Model Specified Dataset" using "discovery by alarm, with no censoring" scheme for three-parameter Weibull distribution. With a small A-D number (0.910) and the Pearson correlation coefficient (0.985) close to one, the distribution plot agrees well with the actual failure data. A comparison with the corresponding two-parameter Weibull distribution (cf. Figure 25) shows that the three-parameter Weibull gives a better fit (A-D number 0.789, Pearson correlation 0.986) than the two-parameter Weibull distribution, which has a A-D number of 1.125 and a Pearson correlation coefficient of 0.982 (cf. Figure 23).
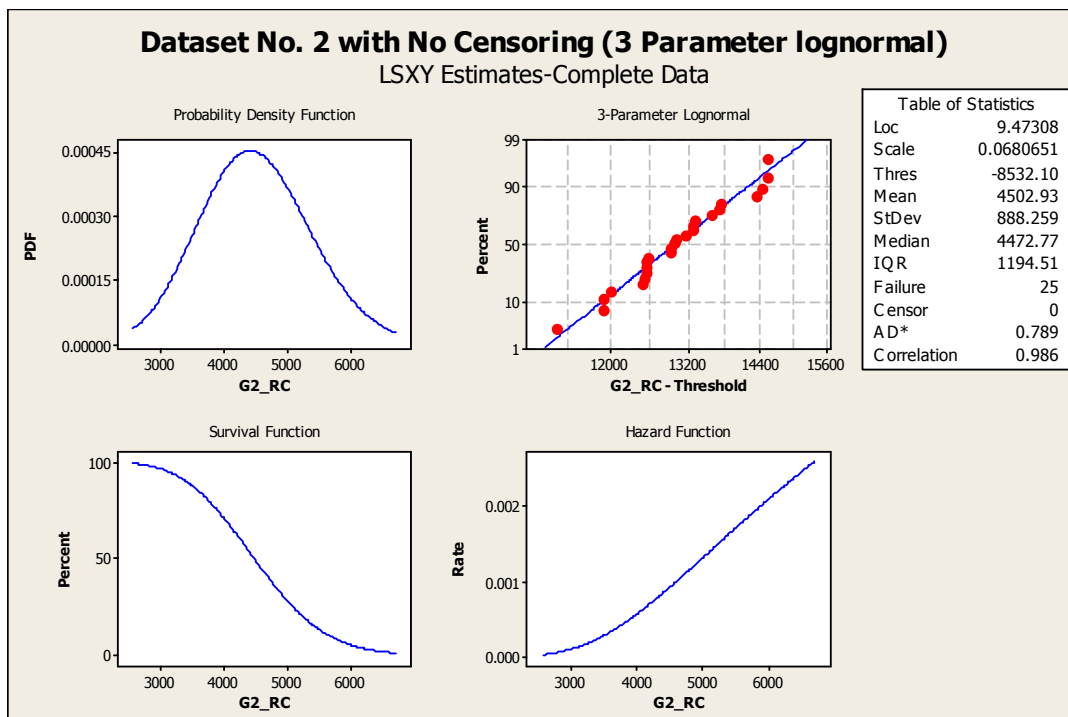
Figure 36. Three-parameter lognormal distribution plot using "discovery by alarm, with no censoring" scheme

Figure 36 shows the three-parameter lognormal distribution plot. As we can see from the parameter table that the A-D number is small and the Pearson correlation coefficient is close to one, which means that this distribution can be a good fit of the dataset. However, the threshold value in the table is negative. A negative threshold shifts the distribution to the left of 0, and all data must be greater than the threshold. Therefore the negative threshold suggests that there are some negative values in the data distribution, which is not practical for our application because the age at failure must be non-negative value.
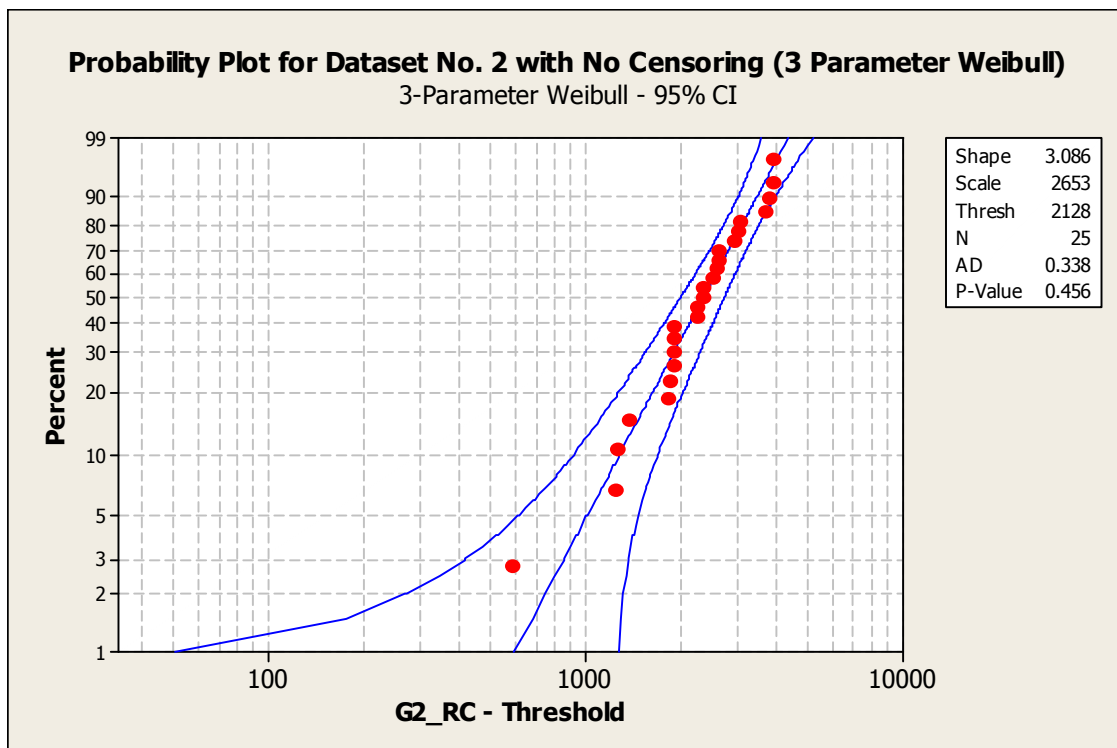
Figure 37. 95% probability plot with three-parameter Weibull distribution

The 95% probability plots are given for both the three-parameter Weibull (Figure 37) and three-parameter lognormal distributions (Figure 38). From the plots we can see that all the data points fall into the 95% probability region.

Same as the three-parameter lognormal distribution overview plot give in Figure 36, the 95% probability plot using three-parameter lognormal distribution in Figure 38 also presents negative threshold. Since the negative threshold number has some disadvantage for this particular application, the two-parameter three-parameter lognormal distribution is preferred when comparing to the three-parameter one.
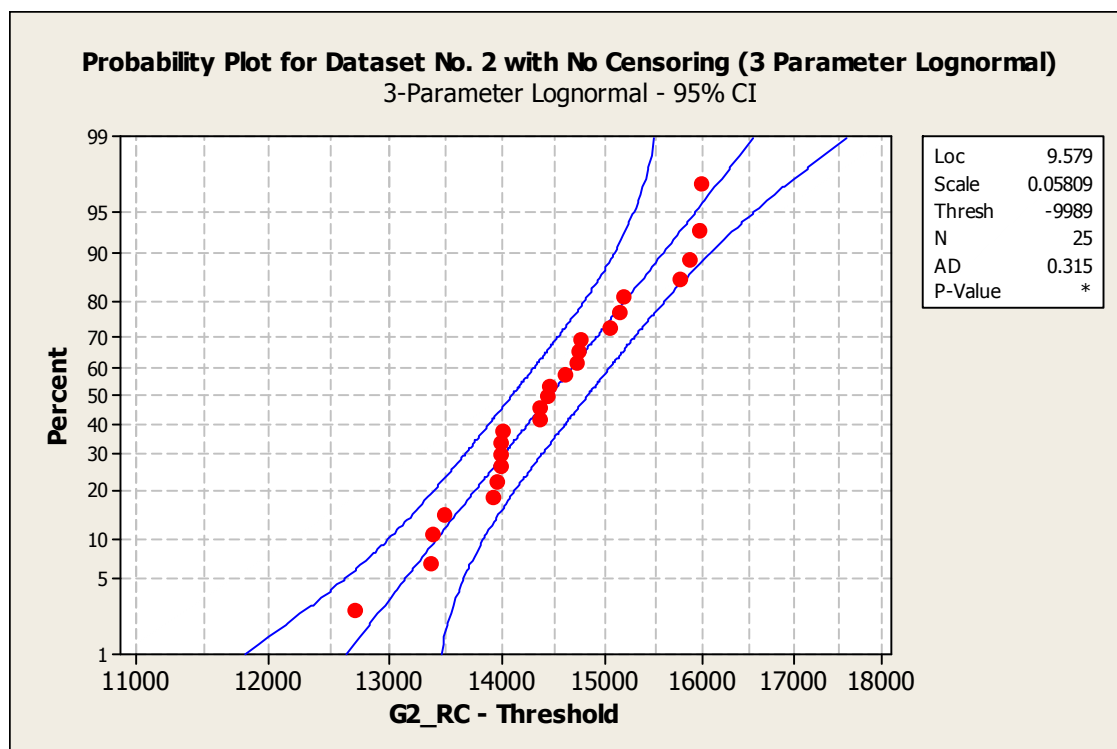
Figure 38. 95% probability plot with three-parameter lognormal distribution

The comparison of all the parameters using the four different distributions is listed in Table 15 below.

Table 15

Comparison of different parameters for Weibull and lognormal distributions, with two and three parameters

Data Distribution	A-D* Number	Pearson Corr.	95% Prob. Plot (A-D Number)	95% Prob. Plot (P-value[11])
Weibull	1.125	0.981	0.489	0.218
lognormal	0.784	0.981	0.301	0.553
3-Parameter Weibull	0.910	0.985	0.338	0.456
3-Parameter lognormal	0.789	0.986	0.315	N/A

Please note here that the P-value for 3-parameter lognormal distribution is represented by an asterisk as seen in Figure 38. According to the manual for Minitab software, "An asterisk appears in place of a p-value for the 3-parameter lognormal, 3-parameter gamma, and 3-parameter loglogistic distributions. The asterisk indicates that MiniTab cannot calculate a p-value for that distribution."

The OSL (observed significance level) probability [34] therefore is now used for testing the distributions listed above. If $OSL < 0.05$ then the distribution assumption is

---

[11] Used in hypothesis tests to help decide whether to reject or fail to reject a null hypothesis. The p-value is the probability of obtaining a test statistic that is at least as extreme as the actual calculated value, if the null hypothesis is true. A commonly used cut-off value for the p-value is 0.05. For example, if the calculated p-value of a test statistic is less than 0.05, you reject the null hypothesis.

rejected and the error committed in so doing is less than 5%.The OSL formula is given

by:

$$OSL = 1/\{1 + \exp[-0.1 + 1.24\ln(AD^*) + 4.48(AD^*)]\}$$

where

$$AD^* = (1 + 0.2/\sqrt{n})AD$$

and n is the sample number.

Table 16

Comparison of A-D numbers and OSL numbers

Data Distribution	A-D* Number	A-D Number	OSL	A-D* Number (95% Prob. Plot)	OSL (95% Prob. Plot)
Weibull	1.125	1.0817	0.0078	0.5086	0.2075
lognormal	0.784	0.7538	0.0509	0.3130	0.5345
3-Parameter Weibull	0.910	0.8750	0.0252	0.3515	0.4556
3-Parameter lognormal	0.789	0.7587	0.0494	0.3276	0.5040

From Table 16, we can see that only the OSL for two-parameter lognormal

distribution is greater than 0.05. According to the rule quoted above, "If $OSL < 0.05$

then the distribution assumption is rejected and the error committed is less than 5%", the

lognormal distribution is selected as the best fit for data in group 2. Also the

corresponding OSL number for 95% probability plot is the largest comparing to other

values. Therefore, the best fit for the data in group 2 with right censoring is two-

parameter lognormal distribution. A further discussion of how the choice of distributions can affect the results is given in Subsection 5.3.

In the application of the following Chapter V, the unit of time will be years instead of days. We therefore plot the corresponding data in group two with year as unit in Figure 39, and provide the corresponding distribution parameters (Table 17):
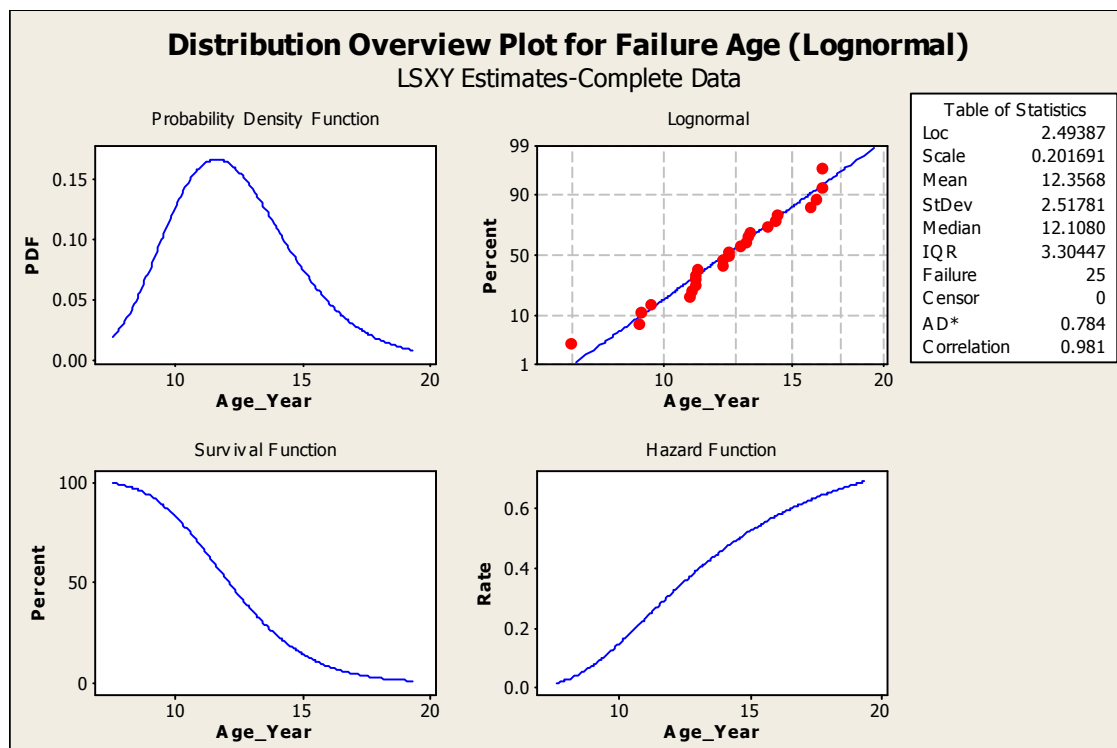
Figure 39. Distribution plot using lognormal distribution

Table 17

Parameters that will be used for further analysis

Parameter Name	Shape	Scale
Parameter Value	2.49387	0.201691

In the following Chapter V, the failure distribution data (Table 17) extracted from the analysis of this chapter will be applied to the entry-time model, to provide a generation-risk assessment for main generators.

CHAPTER V

APPLICATION OF ENTRY-TIME MODEL TO NPP APPLICATIONS

In Chapter III the entry-time approach is verified by comparison to semi-analytical results and simulations. In Chapter IV the time-dependent data failure-rate data necessary to application of the entry-time methodology are extracted, for certain classes of main generators, from the corresponding failure data found in the INPO-EPIX database. In this chapter, the potential real-world application of the entry-time approach is illustrated by way of realistic questions related to the maintenance of main generators in nuclear power plants.

In Section 5.1, the main functions and structures of the main generator system are introduced, followed by the state definitions and assumptions underlying the subsequent entry-time analysis of main generators in Section 5.2. In Sections 5.3 and 5.4, the entry-time approach is applied to the issue of optimizing maintenance policies for main generators. This is done in two separate parts: reliability performance analysis (Section 5.3) and financial analysis (Section 5.4). In the reliability analysis, the time-varying system-state probabilities are determined under different preventive maintenance policies; in the financial analysis, the net present value (NPV) of cost and other financial data are calculated from the entry-time probability analysis, for the various maintenance policies, and the cost-optimal maintenance policy is determined. In Section 5.5, possible application of the entry-time model to PRA/GRA analysis is outlined as a potential direction for future research in this field.

5.1 Introduction to the Main Generator System

The introduction of the main generator is mainly sourced from NPP system notebooks. The function of main generators is to produce electrical power, at rated voltage and frequency, to be delivered to the electrical power grid and consumers. This is accomplished by using electromagnetic induction to convert mechanical energy, as delivered to the generator rotor from the system turbine, into electrical energy. This energy is delivered in MWe (megawatts electric), at the appropriate power rotor, as measured at the main generator terminals and allowing for the power requirements of the plant. The generator voltage is normally 20-22 kilovolts. The frequency is either 50 or 60 cycles per second, depending on the needs of the power grid and consumers. This frequency is determined by the rotating speed of the generator which is between 1500 and 3600 revolutions per second.

The generator consists of an exciter, a stator and rotor. The exciter keeps a low current going through the wires of the rotor. When this rotor turns, the magnetic field associated with this rotor current induces a voltage in the stator. The generator also has a voltage-regulator that maintains the voltage within acceptable limits.

For the generators to work properly, the following auxiliary equipment is required: excitation system, hydrogen gas control system, seal oil system and stator cooling-water system.

The function of the excitation system is to control the magnetizing current to the rotor winding. This control is obtained by fast-acting automatic voltage regulators, which serves to maintain the generator output voltage.

The main generator components (stator winding, stator core and rotor winding) require enhanced cooling in order to maintain the temperature rise of electrical insulation within acceptable thermal limits and prevent excessive thermal aging. The cooling is provided by hydrogen gas control system, seal oil system and stator cooling-water system.

Hydrogen gas is used for cooling of stator core and rotor winding. In order to contain the hydrogen within the generator, hydrogen seals are required to prevent leakage along the rotating shaft. The hydrogen seals require continuous supply of clean degassed oil. This oil is supplied to the seals by a separate seal-oil auxiliary system, which includes oil pumps, filters, coolers, along with associated pressure and flow controllers. An oil system is used for lubricating the bearings on the generator.

The main generators may fail due to various component failures. In summary, the main generator can fail because of stator, rotator or exciter failures, or it can fail because of the failure of one of its many supporting systems, some of which are described above. In our analysis, we will focus on failures that lead directly to loss of power generation. From perusal of the EPIX database records, we find almost all power generation loss (Mwh Loss in the database) comes from failure of rotors. The reason for that is it normally takes a longer time for the system to recover once a rotor failure occurs, while exciter failure is easier to fix and does not lead to extended power generation loss. Comparing to rotor and exciter, the stator has much lower failure rate and hence we can ignore the failure of stator. In fact, no stator failure events are found in the database.

As for supporting system failures, sometimes they can lead to power loss due to downgraded power generation. For example, problems with hydrogen cooling will lead to loss of power generation, because the generator can not run at full power without adequate cooling. However, such problems or supporting system failures do not result in full loss of power generation, which means that they do not lead to "reactor trip equivalent" type of failures.

Given this introduction of the main generator system and its possible failures, the main objectives of generator maintenance and aging management are respectively:

- Maintain generator reliability and availability for power generation

- Ensure generator life expectancy to be comparable to other main unit components, such as turbine, steam generators and the reactor.

In this dissertation, we are mainly focused on the generator maintenance, in order to maintain generator reliability and availability for power generation. To reach this objective, preventive maintenance is done to the main generator system in NPPs to increase the likelihood of reliable performance. Because the cost associated with maintenance varies according to different policies, a financial analysis has to be done when making maintenance decisions; one industry standard for this purpose is the EPRI PMBasis program [28]; however, that program is somewhat qualitative in nature, and here we are exploring a prototypical more quantitative approach.

In the following sections of this chapter, the entry-time model is used to analyze the reliability of a main generator system, under different maintenance policies. Definitions and the corresponding assumptions are given in Section 5.2, the reliability performance

analyses and financial analyses are carried out in Section 5.3 and Section 5.4 respectively.

5.2 Definition of States and Assumptions

The components of main generator system and the objective of generator maintenance are outlined in the preceding section. To apply the entry-time approach to the maintenance of the system, a definition of states appropriate to the objectives of the particular analysis is required. (It was already mentioned in Chapter II that the definition of states for entry-time model is sufficiently flexible so as to allow for the needs of a particular application.) In this section, a definition of states appropriate to analysis of the maintenance issues for main generators is given, and the assumptions associated with those states are discussed.

The most important part of the revenue loss is main generator failure, which leads directly to reactor trip and hence 100% power generation loss and corresponding losses such as repair and O&M costs. Hence in our analysis, we consider the failures that lead to 100% power generation losses. For example, a catastrophic failure of the main generator leads to a reactor trip; also, once such an unplanned failure happens, it takes longer time for the system to be restored (to go back to 100% power generation). For example, an unplanned rotor failure may take up to 10 months outage time, given there are no spare rotors. Comparing to the catastrophic failures, a noncatastrophic failure may also lead to reactor trip and hence 100% power generation loss, however, it does not take much time (sometimes around 10 days or even shorter) for the system to restore power generation.

When the main generator is in a reduced power state, it does not necessarily trip the reactor, hence the corresponding loss is negligible if the down power rate is low comparing to the loss due to catastrophic and noncatastrophic failures that will result in trip of the reactor.

With this larger picture in mind, we make the following assumptions for the analysis of this chapter:

1) When considering main generator failures, only "trip-equivalent" (i.e. those failures that lead to 100% power generation loss or trip of the reactor) catastrophic and noncatastrophic failures will be counted

2) Even when the system is running in degraded state, i.e. operating with some deficiencies, it still generates 100% power

3) 95% and 5% split in failure rate between noncatastrophic and catastrophic failure modes. This assumption is based on the similar analysis done at STP.

4) When doing preventive maintenance, we consider only the rotor/stator rewind which normally takes places every 15 years (for rotor rewind) or 20 years (for stator).

5) After rewinding or replacement, the system is as good as new.

Hence we define the following system states for the main generator:

1) State 1: Normal running state with 100% power generation

2) State 2: Out of service due to preventive maintenance

3) State 3: Out of service due to noncatastrophic failures

4) State 4: Out of service due to catastrophic failures

The transition relationship among the states is defined as follows:

- Rewind or replace the system after a fixed replacement period T_r

- After the replacement time t_r, the system goes back to state 1

- The transition rates from state 1 to state 3 and 4 are defined by the failure

  distribution from the previous analysis, according the failure data from

  the INPO-EPIX database, and further there is a 95%/5% split in failure

  rate between noncatastrophic and catastrophic failure modes

- When the system is repaired after t_{nc}, it returns from state 3 to state 1

- When the system is repaired after t_c, it returns from state 4 to state 1

- There are no transitions among any other states

The transition relationship can be seen in the following figure (Figure 40)
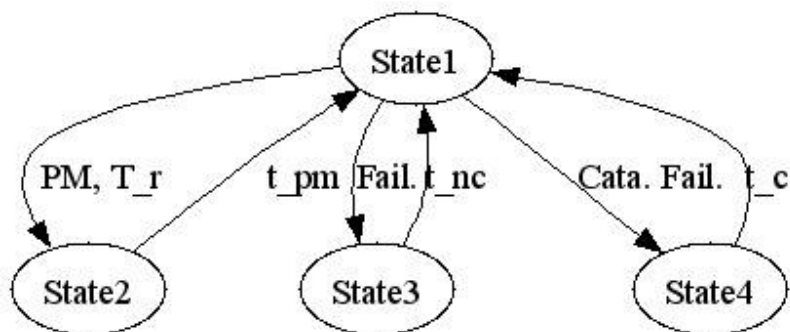
Figure 40. Transition relationships between states

As we can see from the lognormal distribution overview plots in Figure 41 using the

data acquired from the analysis in Subsection 4.5.4, because aging does not have a

strong effects to the system at a early stage (see the discussion in Section 4.4), the probability density function and cumulative distribution function for failures are relatively small when age is less than 10 years, but the cdf for failures increase rapidly (pdf becomes significantly positive) between 10 and 15 years. Hence it is reasonable to draw a tentative conclusion that there is no need to do a routine preventive maintenance at earlier stage (for example, 5 or 6 years of the age), as the aging effects have not become a big concern (failures are highly unlikely). However, if the infant-mortality is considered in the analysis, then preventive maintenance may become important. This will be further studied when doing the detailed analysis to the system in the following sections (cf. Section 5.3).

Also according to judgment from engineers at nuclear power plant, the main parts of the main generators (for example, rotors) are replaced around every 10 to 15 years. We therefore choose to use replacement period T_r as a parameter to do the following analysis; i.e. we choose representative values of T_r as 6, 10, 12, 16 and 20, to assess how the failure probability differs as the replacement period T_r changes. In NPPs, when doing preventive maintenance, the PM periods likely would be subordinated to refueling outages. Here for $T_r = 12$, other than the lognormal distribution as chosen from the preceding chapter, Weibull distribution is also applied to the analysis to see the effects of choice of different distribution. Additionally, the policy of run-to-failure ($T_r = \infty$) is analyzed, and compared to the other policies, for both distribution types.
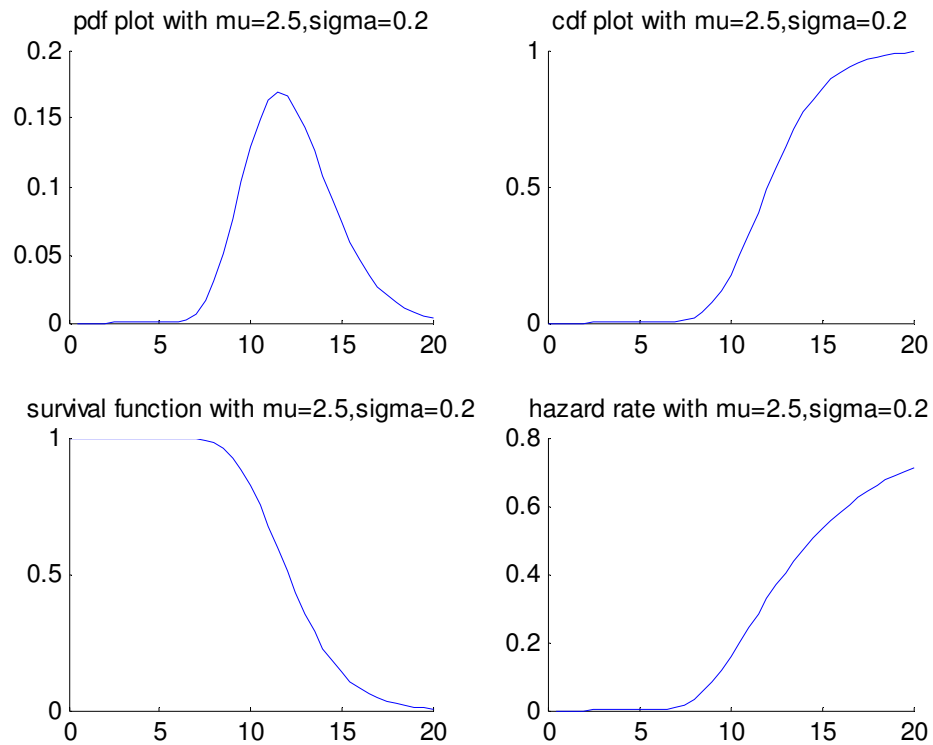
Figure 41. lognormal distribution overview plots

Current NPPs have been running for decades (for STP, both units have been running for almost 20 years). Most of them have a design life of 40 years and the license may be extended to another 20 years. Therefore, most commercial NPPs have a plant life at around 50 years. Hence it is reasonable to do a 50-year analysis when doing life-cycle management calculations. In the analysis below, a terminal time of 50 years is therefore employed.

Based on the above, we have the following defined states and parameters for the analysis to the main generator system:

States defined for the main generator system:

- State 1: Normal running state with 100% power generation

- State 2: Out of service due to preventive maintenance (100% power loss)

- State 3: Out of service due to noncatastrophic failures (100% power loss)

- State 4: Out of service due to catastrophic failures (100% power loss)

Corresponding cost and revenue information associated with each state will be given in Section 5.4, which treats a related financial analysis. When carrying out preventive maintenance, the activity typically has been planned in advance, with all parts and materials pre-ordered. Therefore it tends to take a much shorter time than when the system needs to be repaired or replaced after an unplanned catastrophic failure. Normally preventive maintenance, whether replacement or repair, can be done within 3 to 4 months, with all parts and components preordered and ready. Therefore, $t_r = 0.3$ years is used as a typical time in the preventive maintenance state (state 2). In the analysis done to the main generator system. However, when a catastrophic failure occurs, given there are no spare components to be installed immediately and some big components have to be ordered from the manufacturer, it could take up to 1 year to replace the failed component/system before the main generator system and the nuclear unit are back to service. The system restore time needed for a catastrophic failure varies according to the particular failed components of the system, and can be 6 to 12 months. Hence it is reasonable to assume the time needed to recover from a catastrophic failure is

around t_c = 0.8 years. For a noncatastrophic failure, no special components orders are required and it takes a relatively shorter time for the system to return to normal running state, compared to the time needed for a catastrophic failure. Again, the system restore time needed for a noncatastrophic failure also varies according to the failed components of the system, and can be 1 to 3 months. A system restore time of $t_{nc} = 0.2$ years is applied in the analysis.

Therefore, we have the following parameters used in the calculation and analysis:

- Replacement time: $t_r = 0.3$ years

- Noncatastrophic failure repair time: $t_{nc} = 0.2$ years

- Catastrophic failure repair time: $t_c = 0.8$ years

- Terminal Calendar time: 50 years

In the next section, using the lognormal failure (hazard) rate (see also Figure 41 above), probability plots using different preventive maintenance periods as parameter are plotted and compared against each other. Also probability plots using Weibull distribution are compared to those from the lognormal distribution, with the same preventive maintenance periods applied.

In the section following that, a financial analysis is described, for different scenarios. This includes the net revenue for each state, expected yearly net revenue, standard deviation and skewness. Specifically, the NPV (Net Present Value) cost is calculated for each case, and the results are applied for decision-making purposes.

5.3 System Reliability Analysis

In this section, system state probabilities are computed, using the entry-time methodology previously developed and different preventive maintenance periods as parameters. Based on these results, the corresponding system reliability analysis is then carried out.

As can be seen from Figure 41, the probability density function for failure is relatively small when time is less than 6 years, but becomes significantly larger between 10 and 15 years. It reaches a maximum at around the 12th year. In the following analysis, we will select some maintenance policies that collectively capture all significant changes in this probability density. First, we choose $T_r = 12$, when the probability density reaches its maximum. Then $T_r = 10,16$ are applied to catch the beginning and end, respectively, of the significantly large range of values in the probability density. Also $T_r = 6$, is tested to study the effect of sufficiently frequent to prevent even the beginning of aging effects. $T_r = 20$ is applied to show the impacts of longer maintenance period to the system reliability performances. Additionally, $T_r = \infty$ (not shown in the plots below) is applied to the entry-time model to demonstrate the run-to-failure policy, which sometimes is adopted by plant maintenance personnel for the maintenance of components or systems.

To start the discussion, we choose $T_r = 12$ (i.e. to replace the system every 12 years).
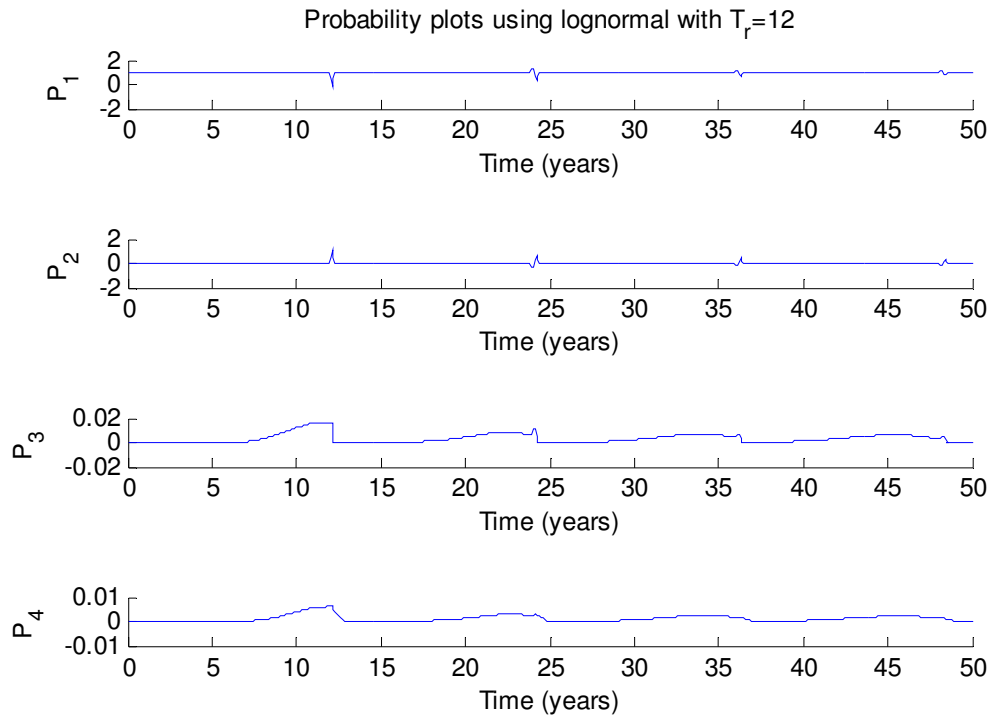
Figure 42. States probability plots using lognormal distribution, with T_r=12

As can be seen from Figure 42, with a preventive maintenance policy of replacement every 12 years the probability of failure (either noncatastrophic or catastrophic, i.e. P_3 or P_4) is always small, but becomes noticeably nonzero around year 6, and increases out to year 12. At that point the replacement causes the probability of (either type of) failure to decrease sharply. Further, the probability that the system is in preventive maintenance state (P_2) increases correspondingly. Note the occasional appearance of computed state probabilities greater than one (1) or less than zero (0); these phenomena were previously discussed in Subsection 3.2.2.
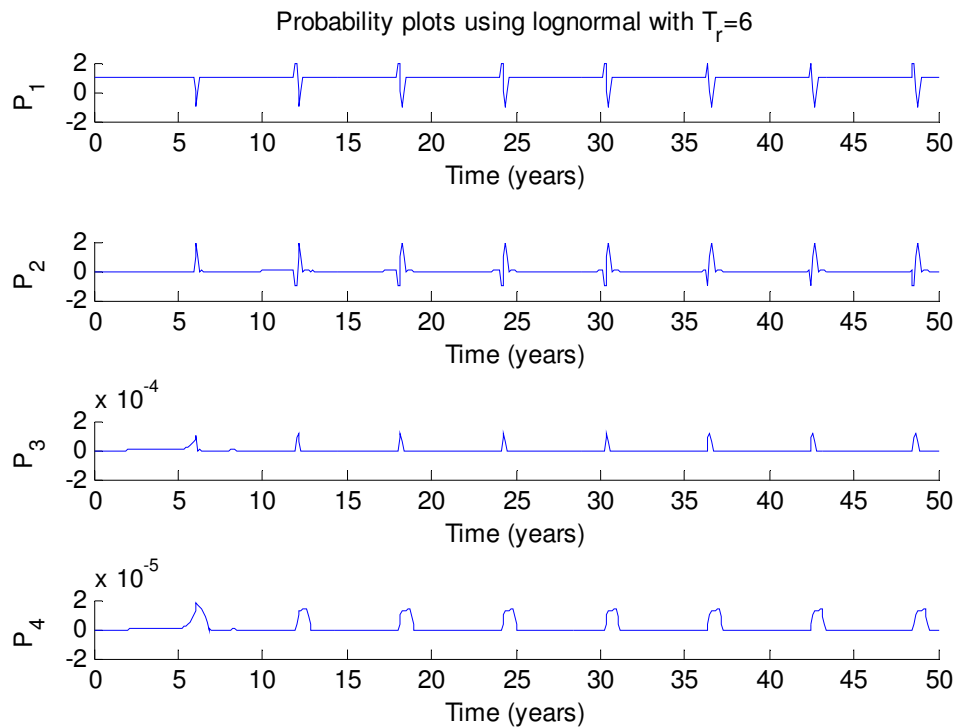
Figure 43. States probability plots using lognormal with T_r=6

Similar to the plots given in Figure 42, state probability plots using the lognormal distribution with $T_r = 6$ (replace the system every 6 years) are shown in Figure 43. It shows in the figure that the preventive maintenance of the system decreases the probability that the system is in failure state (both catastrophic and noncatastrophic failures, i.e. P_3 and P_4) every 6 years. And the probability that the system is in preventive maintenance state (P_2) increases correspondingly. Before the maintenance, the

probability the system is in failure states (P_3 and P_4) increases as the system ages. Comparing to the policy to replace the system every 12 years, the much shorter maintenance period (6 years) has greatly decreased the risk of failure and hence increased the system reliability performance. That is, from Figure 43 we can see that both P_3 and P_4 are around the magnitude of 10^{-4}, while P_3 and P_4 from Figure 42 show a magnitude of 10^{-2}. It is clear that the system failure probability with 6-year-period maintenance policy is roughly around 1% of the system failure probability with 12-year-period one. The reason for that is, with a shorter maintenance period, the system was replaced before it ages, which thus prevents the aging effects from ever occurring. However, when comparing system reliability performance for different maintenance policies, we can not judge only based on the failure state probabilities; other factors, such as system availability and economic issues, should be taken into account when making decisions regarding maintenance and repair policies. The system availability performance will be discussed later in this section for different maintenance policies and the financial analysis (NPV etc.) will be given in the following section.
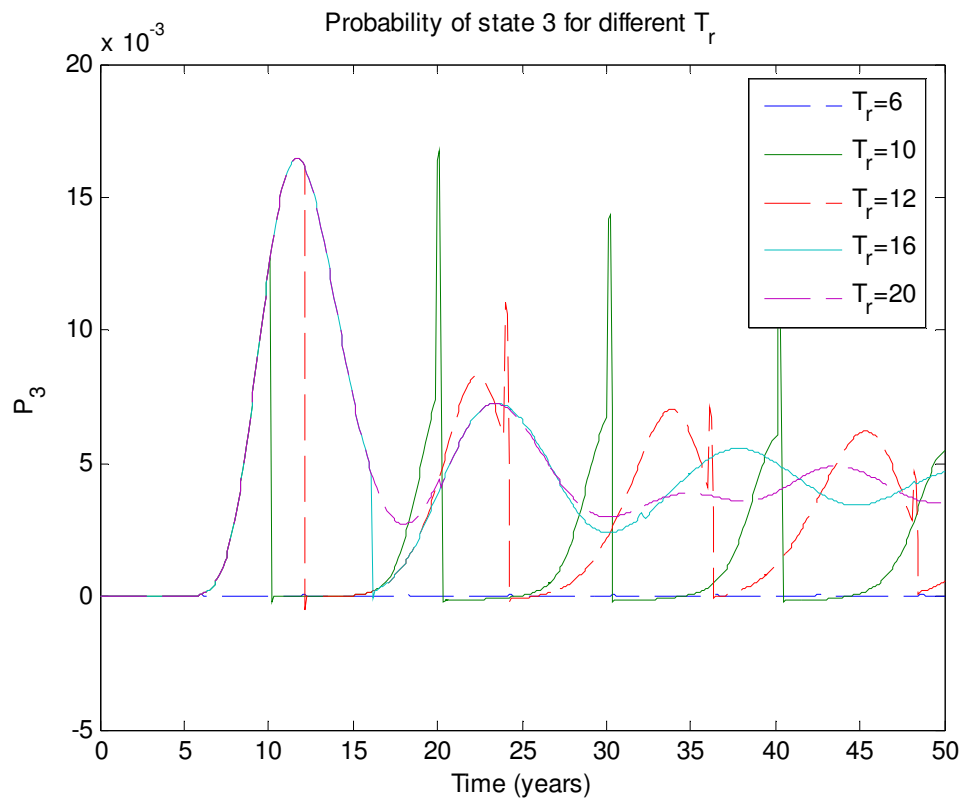
Figure 44. Probability plots of noncatastrophic failures using lognormal distribution

Figure 44 shows the probability plots for noncatastrophic failure, using preventive maintenance time as a parameter. It can be seen from the figure that some of the plots overlap with each other and the plot for $T_r = 20$ overlaps with all other lines for time before 15 years. The reason for that is obvious: Before the preventive maintenance is done, the system tends to have the same reliability performance. While after the preventive maintenance, the system reliability performance changes accordingly and the probability plot lines separate afterwards. From the plots we can see that the shortest maintenance period ($T_r = 6$, the blue dash line)) has the smallest probability of failure.

With longer and longer maintenance period, as the system ages, the probability that system is in the noncatastrophic failure state becomes larger. Normally, when the system was replaced, the preventive maintenance action would prevent the aging effects, for example, the 10-year-period maintenance policy decreases the failure probability around every 10 years. However, when the system was replaced using a 20-year-period maintenance policy, the preventive maintenance action did not help a lot in enhancing the system reliability performance. As we look back to the lognormal distribution plots in Figure 41, it is easy to find out the reason: after 20 years of operation, it is almost certain that the system eventually will be in failure state due to the aging effects, hence there will not be too much help to do a preventive maintenance at that time.

Comparing to Figure 44, Figure 45 shows the probability plots for catastrophic failures using preventive maintenance time as a parameter. Similarly to the noncatastrophic failure plots, we can see from Figure 45 that the shortest maintenance period ($T_r = 6$, the blue dash line)) has the smallest probability of failure. However, due to the same reason as stated above, when the system was replaced according to the 20-year-period maintenance policy, the preventive maintenance action did not help a lot in enhancing the system reliability performance.
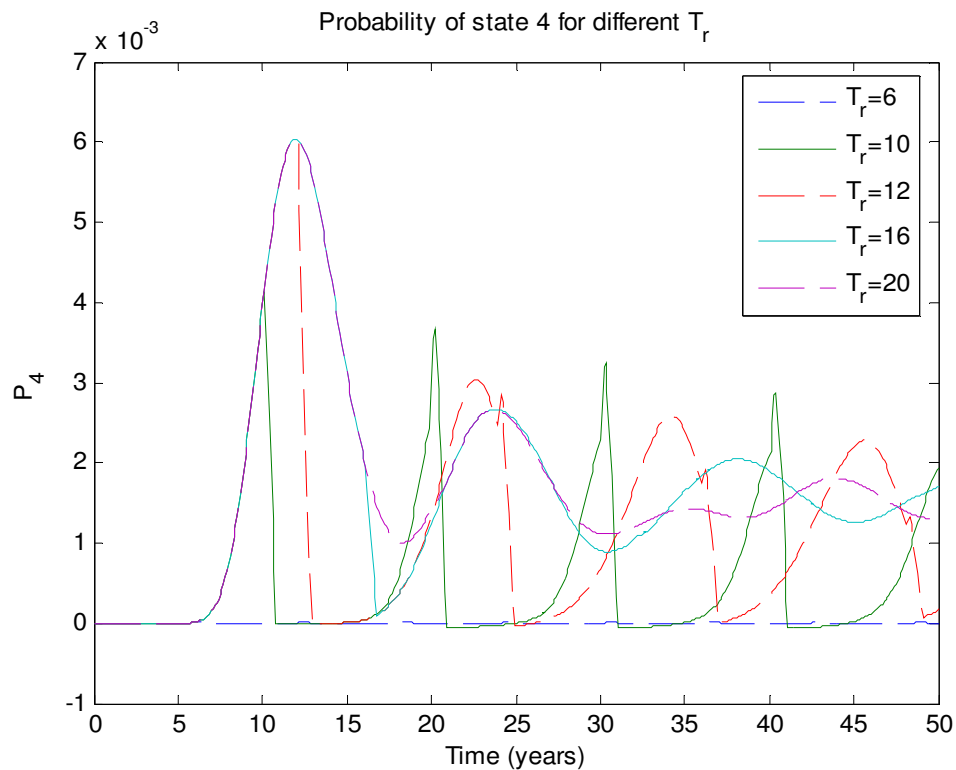
Figure 45. Probability plots of catastrophic failures using lognormal distribution

Based on the analysis of Chapter IV, the lognormal distribution was chosen as the primary distribution for the reliability performance analysis in the present chapter, with different preventive maintenance periods as parameter. However, the probability density functions (pdf) and the cumulative distribution functions (cdf) plots using the parameters acquired from the failure data in Chapter IV with lognormal distribution and Weibull distribution are very identical, as seen in Figure 46. The only significant difference between the two distributions is the hazard rate (failure rate) plot as shown in the lower right of Figure 46. As discussed in Subsection 4.5.1, due to the differences in the failure rates, Weibull distribution is preferred in some studies because the failure rate for this

distribution follows natural observations better than that for lognormal distribution. However, the study in this section shows that there is no significant difference in the results when using Weibull or lognormal distributions given that they both fit the failure data well.
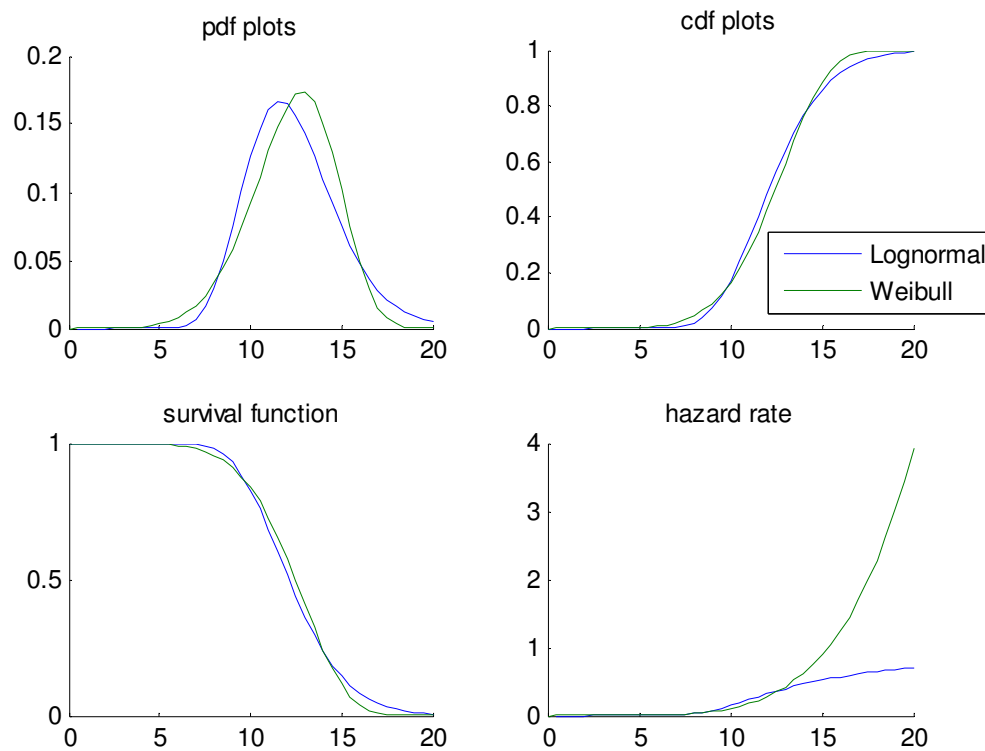
Figure 46. Comparison of reliability performance of lognormal and Weibull distributions

It is easy to see from the plot that the hazard rates of the two are quantitatively comparable roughly before 13 years but the difference between the two increases dramatically after that point. For Weibull distribution, the hazard rate increases faster

than that of the lognormal distribution. Some may argue that the Weibull distribution is a more "reasonable choice" for reliability analysis because it tends to be consistent with what is observed from aging effects, but others may prefer using lognormal distribution because it takes into account the "infant mortality" feature (the failure rates tends to increase first and then decrease. cf. Figure 18) which can be often found in system and component failure.

Then it comes to the following question: When doing system reliability performance analysis, which distribution is preferable, lognormal distribution or Weibull distribution, or does perhaps the choice of distributions does not make any difference on the performance analysis?

To explore these issues, in the following, Weibull distribution will be applied to the analysis using a 12-year-period preventive maintenance policy. The corresponding reliability plots acquired using Weibull distribution will be compared to those acquired using lognormal distribution with the same preventive maintenance policies to see the effects of different choices of distributions.

As can be seen from the figure below (Figure 47) that the policy to replace the system every 12 years decreases the probability that the system is in failure state (both catastrophic and noncatastrophic failures, i.e. P_3 and P_4) every 12 years. And the probability that the system is in preventive maintenance state (P_2) increases correspondingly. Before the preventive maintenance occurs, the probability that the system is in failure state increase as the system ages. Hence the maintenance policy enhanced the system reliability performance.
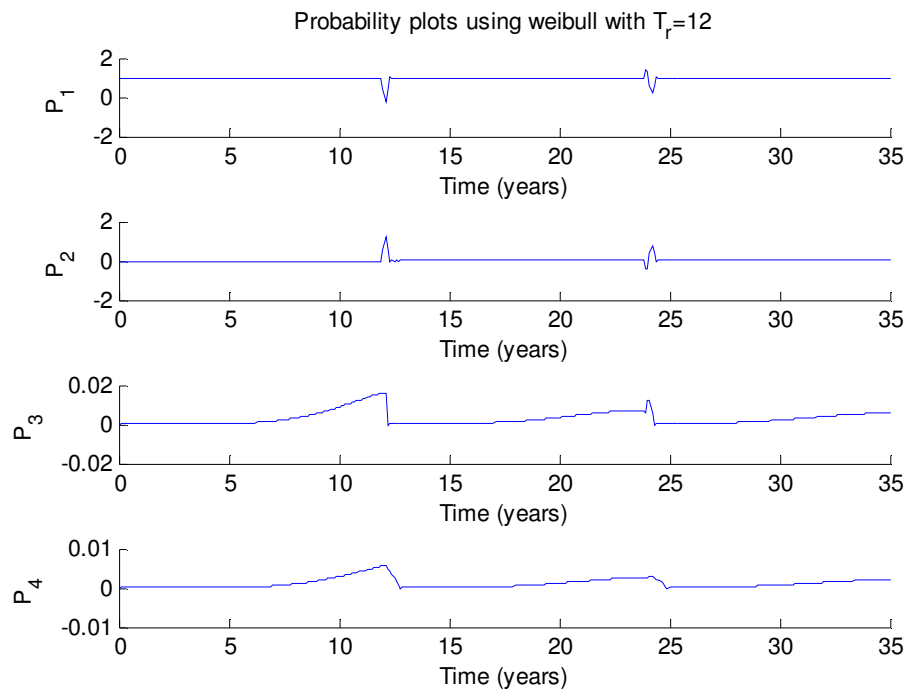
Figure 47. States probability plots using Weibull distribution with T_r=12

The reliability plots acquired using Weibull distribution are compared to those acquired using lognormal distribution with the same preventive maintenance policy ($T_r = 12$) in Figure 48. A rough look at the figures gives the impression that there is no prominent differences for state probability plots, between using the Weibull and the lognormal distributions, especially in probability plots for state 1 (running state) and state 2 (preventive maintenance state). This is understandable from the plots of Figure 46 because the probability density functions (pdf) and the cumulative distribution functions (cdf) plots using the parameters acquired from the failure data with lognormal distribution and Weibull distribution are almost identical. Therefore it can be foreseen

that the state probability plots overlap a lot with, only negligible differences. However, there are notable differences between the two plots for both state 3 (noncatastrophic failure state) and state 4 (catastrophic failure state); more details of these are shown in the plots of Figure 49 and Figure 50.
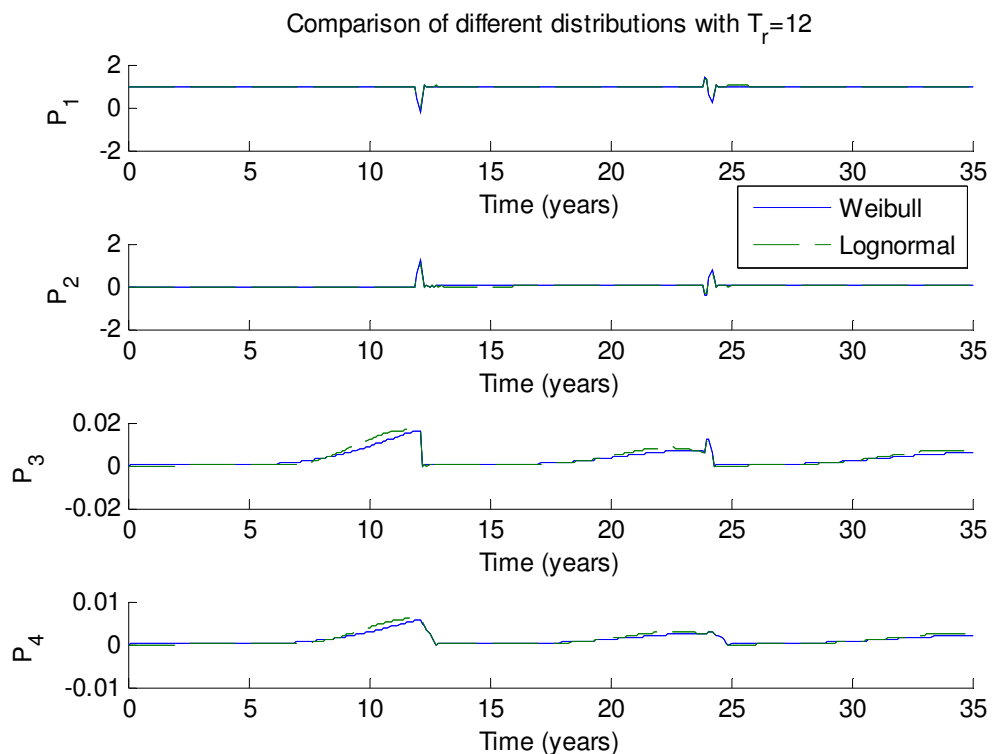
Figure 48. States probability plots comparison with T_r=12

Figure 49 shows the state probability plot for P_3 (noncatastrophic failure) which is an enlarged version of the plot for P_3 in Figure 48. From this plot we can see that although the noncatastrophic failure plots using the two different distributions are almost the same, there are some notable differences. The difference in the plots is because of the

different probability density values and different failure rates (hazard rates) for the two distributions at the same given time. However, as we compared the difference between the two, it is easy to see that the difference is so small (around 10^{-3}) that we sometimes can ignore it when doing reliability analysis such as PRA and GRA.
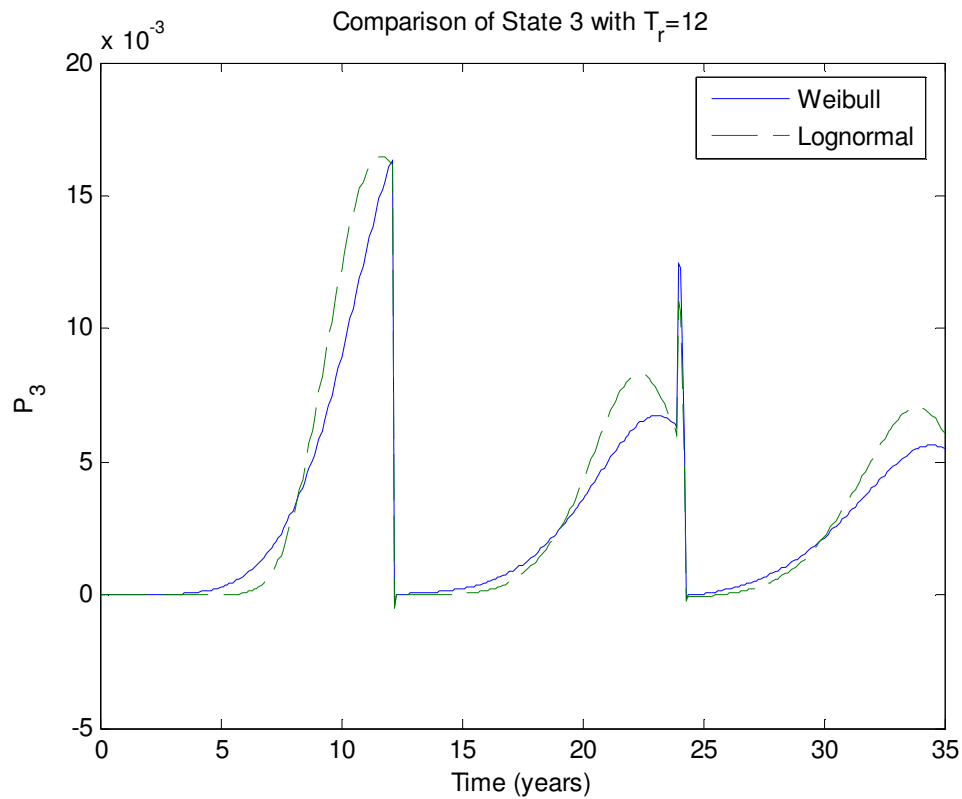
Figure 49. Probability plots of noncatastrophic failures

Similarly, Figure 50 shows the state probability plot for P_4 (catastrophic failure) which is an enlarged figure for P_4 in Figure 48. Again, here we see a lot of similarities, and some differences. The shape of the catastrophic failure curve is almost the same as

that for the noncatastrophic failures, because of the assumed constant (95-5 percent) split between the two.
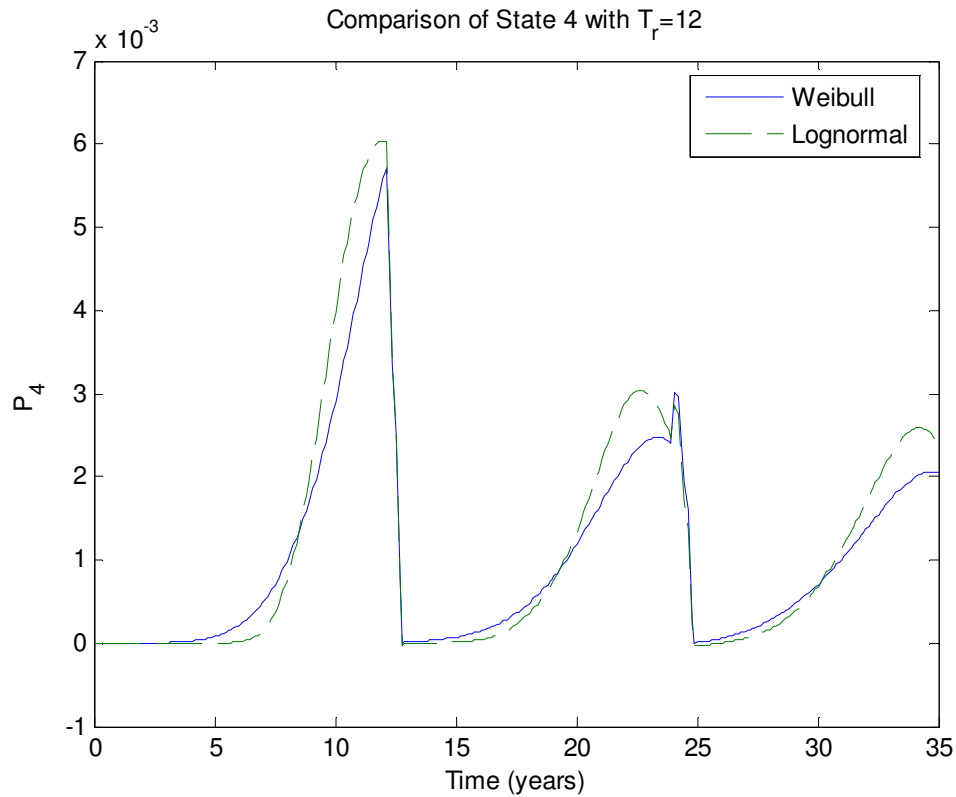
Figure 50. Probability plots of catastrophic failures

From the preceding analysis, we can see that a proper preventive maintenance can enhance the system reliability performance and hence decrease the probability that the system is in failure state (noncatastrophic and catastrophic failure). However, as the system ages, doing preventive maintenance at a very long period (for example, 20 years

for this problem) does not help a lot in enhancing the reliability performance, as it is almost surely certain the system will fail before maintenance is performed..

As far as the choice of parametric form for the underlying failure distribution is concerned, even the analysis done in Chapter IV suggests that lognormal distribution is preferred to Weibull distribution, however, no matter whether Weibull or lognormal distribution is applied in the reliability analysis, no major differences are found for the reliability plots (state probability plots) for the preventive maintenance polices tested ($T_r = 12, 15, 20$ and ∞, only $T_r = 12$ is shown in the plots, others give similar results). Therefore, we can use both distributions in the analysis to this system.

Considering only reliability performance, one may prefer the shortest preventive maintenance period because of the low failure probabilities. However, cost/revenue is affected by maintenance policies and hence connected to the reliability performance corresponding to those policies. For example, comparing to the 6-year-period maintenance policy (as shown in Figure 43) to the 12-year-maintenance policy (as shown in Figure 42), the former has a better reliability performance because the preventive maintenance successfully prevents the aging effects before they take effect, but the related maintenance cost would be more than that of the latter.

Therefore, when making decisions regarding maintenance and repair policies, multiple factors such as reliability, availability, risk/safety, cost and revenue should all be taken into account. In the following section, an economic-related cost-benefit analysis will be done for different maintenance policies, and the related reliability/availability performance, as regards the main generator system in nuclear power plants.

5.4 Financial Related Analysis of the System

System reliability performance, such as failure probabilities and system availabilities, can sometimes be used as important input for decision-making processes, especially for PRA and GRA analysis. However, when it comes to the plant management level, not only the reliability performance, but also the financial performance is used as merit-of-comparison. In the present section, a financial analysis is carried out, as an adjunct to maintenance decisions for plant management. The expected (mean) net present value (NPV) cost is used as the figure of merit in comparing different preventive maintenance policies. Also the variance and skewness related to each policy are given as supplemental information for the decision making process.

To begin with, financial parameters related to each state (operation, preventive maintenance and failures) must be determined, based on some assumptions for NPP operation.

Consider a NPP with designed power generation capacity of 1200MW per unit. The expected market electricity price is around \$40/MW, and we will consider the net present values (NPV) cost for the NPP with fifty years of operation.

When the system is in the operating state, the NPP generates electricity at full capacity and the utility sells the electricity at market price to make profit. The cost associated with the normally operating state can be divided into two major parts: fuel cost and O&M (Operation and Maintenance) cost. Hence the net profit for the operation state (state 1) can be expressed as:

$$Net\ \mathrm{Re}venue = Power\ Generation\ \mathrm{Re}venue - (O\&M\ Cost + Fuel\ Cost)$$

For states other than the operating state, when the main generator is offline due to maintenance or failure, there is no electricity generation and therefore no profit from the power generation. However, the utility needs to purchase electricity from other sources, such as a coal-fired power plant, to ensure normal electricity supply to its customers. Here we make an assumption that when the nuclear utility purchases electricity from elsewhere, the utility sells it at the same price and hence does not make any profit out of it. Therefore, when the system is offline, there is only cost related to that state. In general, there is no fuel cost when the system is offline, hence we have the cost in the following three parts: O&M (Operation and Maintenance) cost, cost of extra engineers and craftsmen cost for repair and maintenance, and the corresponding components and materials cost. Since the extra crafts and engineers cost can be grouped in the O&M cost, we have only two sources of cost when the system is in a non-operational state (PM state, noncatastrophic state and catastrophic state): O&M cost (including the extra engineers and crafts cost, varies for different states) related to that state and the corresponding components and materials cost.

To take into account the needs of extra personnel, when the system is in each non-operational state, other than the basic O&M cost, an adjustment factor (α_i for state i) is applied to each state to accommodate the actual cost associated with that state. Here we use the O&M cost for operational state (State 1) as the base cost. When the system is in preventive maintenance state (State 2), because the maintenance is planned and the components can be pre-ordered, the extra O&M cost will be less than the cost when the system is in a catastrophic failure state (State 4), but the O&M cost must be higher than

a noncatastrophic failure (State 3) due to the urgent needs of system recovery. Hence the adjustment factor assumed here for state 2 is $\alpha_2 = 1/5$. The adjustment factors for state 3 and state 4 are taken as $\alpha_3 = 1/6, \alpha_4 = 1/4$ respectively.

For components and materials cost associated with each non-operational state, the following assumptions are made: When the system is in preventive maintenance state (state 2), the cost of purchasing components and materials is $10,000,000. When the system is in a noncatastrophic failure, the cost related to that is $5,000,000 because it is relatively easy to recover from that state. For recovery from catastrophic failure, due to the necessity for rush orders to avoid long waiting time for components and materials, the cost is more significant; it is taken here as $20,000,000 for the duration of recovery. From the assumptions in the previous sections, we have different maintenance/repair duration for each of the non-operational state, hence the corresponding yearly components and material cost for each non-operational state can be calculated by:

$$(C \& M \ Cost)_i = (Cost \ per \ duration)_i /(Duration \ Time)_i$$

Hence the yearly components and materials cost for the three non-operational states are as in the following table (Table 18):

Table 18

Components and materials cost for the three non-operational states

State No.	2	3	4
Recovery time (year)	0.3	0.2	0.8
Cost per duration (Mil. $)	10	5	20
Annual cost	33.33	25	25

Therefore, the total cost for the three non-operational states can be expressed using the following equation:

$$(Total\ Cost)_i = (C\ \&\ M\ Cost)_i + (O\ \&\ M\ Cost)_i$$
$$= (C\ \&\ M\ Cost)_i + (Base\ O\ \&\ M\ Cost) \times (1 + \alpha_i)$$

Hence, we have the general equation for the calculation of net profit/cost for each state as follows:

$$(Net\ \mathrm{Re}venue)_i = (Generation\ \mathrm{Re}venue)_i - (Fuel\ Cost)_i$$
$$-(C\ \&\ M\ Cost)_i - (Base\ O\ \&\ M\ Cost) \times (1 + \alpha_i)$$

Based on the above analysis, we can calculate the net revenue/cost for each of the four states. Detailed revenue/cost balance table can be found in Appendix E. The numbers used in the calculations are based on discussion with NPP personnel. Table 19 below shows the total annual net revenue/cost for all states:

Table 19

Annual net revenue/cost for all states

State No.	1	2	3	4
Duration Time (year)	N/A	0.3	0.2	0.8
O&M Cost adjustment	0	1/5	1/6	1/4
Generation Revenue (Mil. $)	420.48	0	0	0
Fuel Cost (Mil. $)	36.50	0	0	0
O&M Cost (Mil. $)	146.00	175.20	170.33	182.5
C&M Cost (Mil. $)	N/A	33.33	25.00	25.00
Net Profit/Cost (Mil. $)	237.98	-208.53	-195.33	-207.50

As mentioned in Chapter III, "minimizing the cost" is often the stated objective of analyses in industry. In this chapter, the application of entry-time analysis to support such an objective (i.e. minimizing the cost) will be illustrated, for PM policies relative to the main generator system. Although the focus here will be on minimizing cost, in accord with the industry norm, we still begin with a revenue calculation, to indicate how the two formulations are related.

From the results of the reliability analysis of the preceding section, we already know the state probabilities for the system, at any given time t, within the initial 50 years of operation. Therefore, the annual state probabilities can be calculated by integrating the state probabilities over each year. Once we have the state probabilities $P_i(t)$ for all four states over 50 years, using the net profit/cost data (R_i) given in the table above (Table 19), the expected value of the annualized net revenue, the annualized standard deviations and skewnesses are calculated using the formulas for same that are given in Section 3.3.

The Entry-time approach produces precisely discrete approximations to the probabilities $P_i(t)$. The time stream of expected net revenues plotted in Figure 51 were produced by using the finite-difference methodology and the failure rates acquired from the analysis in Section 4.3, with time step 0.1 years, and then evaluating the rightmost integrals by means of the trapezoidal rule. Refinement to a step size of 0.05 years in the entry-time calculation produced relatively minor changes in the computed values.
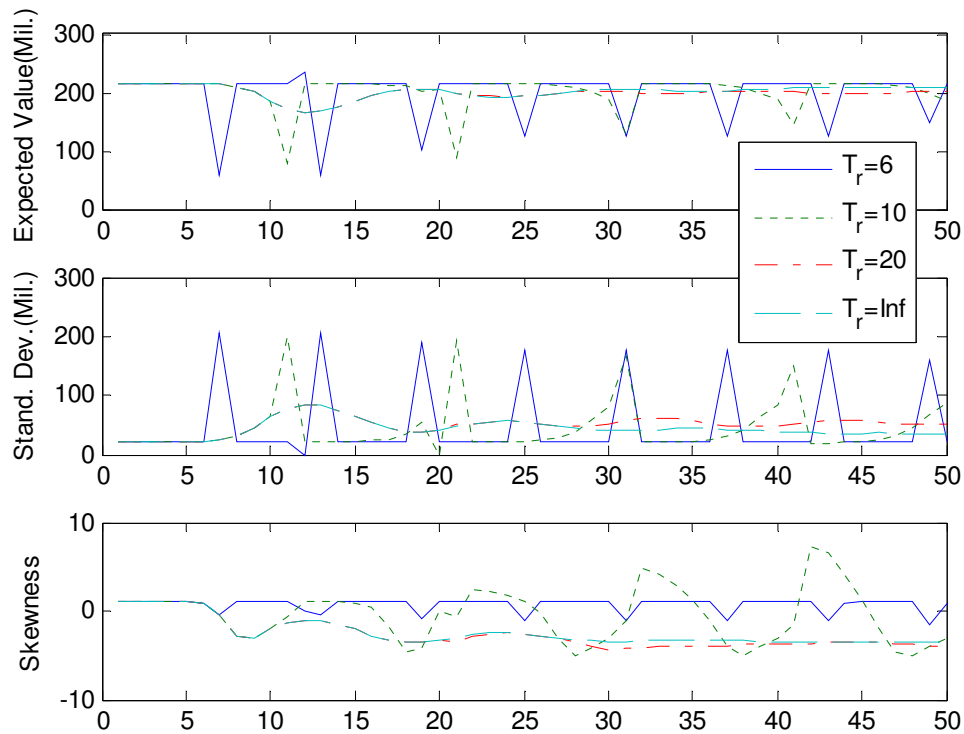
Figure 51. Comparison of financial parameters for different PM policies

The first overall observation is that expected net revenues for this system are typically rather large and that the system has some degree of uncertainty in financial performance, as there are periods during which the standard deviation (variance) in annualized net revenue tends to have values of the same order as the expected net revenues, especially when maintenance is done to the system more frequently (for examples, $T_r = 6$ years). Further, the large negative values of skewness indicate that much of the variance is located along a long left tail of the underlying distribution; i.e., the business is subject to a substantial downside risk.

The most aggressive of the three preventive maintenance policies described, a replacement period of 6 years (PM cycle of 6 years), substantially reduces this downside risk as can be seen from the "skewness" plot in Figure 51.

This shortest of the three replacement periods considered is therefore perhaps most likely to be adopted by concerns that are strongly risk averse. However, the graph of expected net revenue shows that this decrease in downside risk is purchased at a cost of some 10-15% reduction in expected net revenue, depending upon the year. Management more inclined toward (financial, not safety) risk might be inclined to adopt other maintenance policies expected to provide more revenue, while still maintaining the safety goal.

As compared to this other replacement periods, the most passive replacement policy of "run-to-failure" (i.e. never do preventive maintenance to the system) provides no advantage in either expected net revenue or reduction in downside risk. In fact, the run-to-failure policy has the "most negative" skewness comparing to other policies and hence has the most significant downside risk. Taking into account both financial and reliability considerations, the run-to-failure policy seems unlikely to be adopted by informed plant management teams.

More detailed analysis is done to the system based on cost associated with each state. From the way the profit is defined (*Profit = Generation Revenue - Cost*), it is clear that any loss of production should be considered as part of the loss in cost calculation. This can be seen from the basic algebra shown below:

$$\text{Profit} = (G_1 - C_1) + (0 - C_2) + (0 - C_3) + (0 - C_4) = G_1 - C_1 - C_2 - C_3 - C_4$$

where G_1 is the generation risk cost from when the system is in state 1 (normal operation state) and C_i is the expected value of the *actual cost* associated to state i.

Here we define the effective cost for any non-operational state to include the power generation loss in the following way: $(Effective\ Cost)_i = C_i + G_i, \quad i = 2, 3, 4$, hence the total annual cost is:

$$\begin{aligned}
\text{Cost} &= C_1 + (C_2 + G_2) + (C_3 + G_3) + (C_4 + G_4) \\
&= G_2 + G_3 + G_4 + C_1 + C_2 + C_3 + C_4 \\
&= G - (G_1 - C_1 - C_2 - C_3 - C_4)
\end{aligned}$$

where $G = G_1 + G_2 + G_3 + G_4$ is the total annual revenue without any cost which is a constant value.

From the above equation, we can see that when the cost is defined in the way such that any production loss is also counted as part of the lost, then the maximizing profit strategy is equivalent to the minimizing cost strategy. And such calculations can also be carried by using the entry-time approach. The corresponding effective cost rates of the various states are given in Table 20. (In comparing these rates for States 3 and 4, note that while the cost *rates* are similar, the cost of a catastrophic failure is larger because the time spent in that state is larger.)

Table 20

Annual effective costs associated with each state

State No.	1	2	3	4
Generation Loss (Mil. $)	0	420.48	420.48	420.48
Fuel Cost (Mil. $)	36.50	0	0	0
O&M Cost (Mil. $)	146.00	175.20	170.33	182.5
C&M Cost (Mil. $)	N/A	33.33	25.00	25.00
Cost (Mil. $)	182.50	629.01	615.81	627.98

Similar to the revenue calculations, using the effective cost data given in the table above (Table 20), the expected value of the effective costs, and the annualized standard deviations and skewnesses are calculated. Also the expected values of the net present values (NPV) of effective costs were calculated for each preventive maintenance policy, as an adjunct in making maintenance decisions. Here the NPV was calculated using the equation,

$$P^{(n)} = \frac{F^{(n)}}{(1+i_f)^n}$$

where $F^{(n)}$ is the revenue at n^{th} year, and $P^{(n)}$ is the present value corresponded to the revenue at the nth year ($F^{(n)}$). Further, i_f is the inflation-adjusted interest rate which has included the effects of real interest rate (i) and the inflation rate (f). The relationship of the three is defined as

$$i_f = i + f + if \quad [35].$$

Hence the net present value (NPV) over N years can be expressed as:

$$NPV = \sum_{n=1}^{N} P^{(n)} = \sum_{n=1}^{N} \frac{F^{(n)}}{(1+i_f)^n}$$

Please note there that constant interest rate and constant inflation rate are applied to the calculation. The values for the rates were taken as $i = 5\%$ and $f = 2.5\%$ respectively by referring the most recent government data [36]. Therefore the inflation-adjusted interest rate is $i_f = 7.63\%$.

Using the parameters defined and the equations given above, the expected NPV cost can be calculated for the 50 year plant life. The corresponding results are given in Table 21. From the expected NPV cost values in this table, one can see that the maintenance policy of replacing the system every 10 years ($T_r = 10$ years) brings the minimum expected net present value effective cost to the NPP. The more aggressive maintenance and dense preventive maintenance cost of replacing the system every 6 years ($T_r = 6$ years) brings the largest expected net present value cost to the NPP. Some risk-adverse people in the management may prefer a shorter maintenance policy to get the best system reliability performance; however, in reality they have to take into account the financial performance in order to minimize the net cost while still meeting the safety/reliability requirements, which is especially true for the current commercial nuclear power plants in operation. Therefore, a balance of reliability/risk and net cost is often needed when making maintenance decisions in commercial nuclear power plants.

Table 21

NPV cost for all the PM policies over 50 years

PM (Years)	6	10	12	16	20	Never
NPV (Mil.)	2306.4	2243.1	2258.9	2277.8	2277.6	2271.6

Figure 52 shows the plot of NPV cost over 50 years, for different maintenance policies. It is easy to see from the figure that the minimum value of the expected NPV effective cost would be acquired when T_r is close to $T_r = 10$ years. i.e., with a preventive maintenance policy to replace the system every N years where $6 < N < 12$, we should expect to see the minimum NPV cost for 50 years.

Detailed analysis was done using preventive maintenance policy of replacing the system every N years where $6 < N < 12$. Table 22 shows the expected value of NPV effective cost results corresponding to all the preventive maintenance policies. Also the cumulative distribution function (cdf), survival functions at the time of preventive maintenance are given to demonstrate the reliability performance for that particular maintenance policy. The average skewness is also given to help understand the financial performance of each maintenance policy and help make maintenance decisions as regard to when the best period is to replace the system.
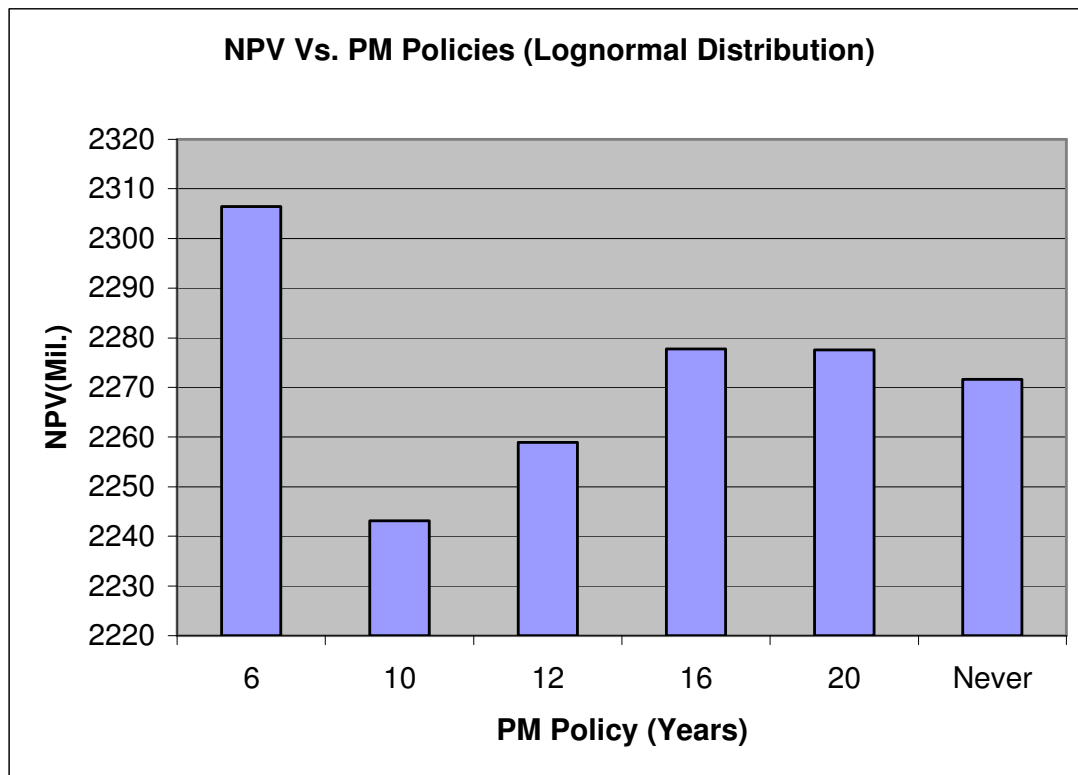
Figure 52. Comparison of expected value of NPV cost over 50 years plant life, for

different maintenance policies

Table 22

NPV for all the PM policies over 50 years using lognormal distribution

PM (Years)	6	7	8	9	10	11	12	16	20	Never
NPV (Mil.)	2306.4	2276.3	2255.2	2244.0	2243.1	2249.2	2258.9	2277.8	2277.6	2271.6
cdf	2.5e-4	0.0033	0.0200	0.0707	0.1715	0.3171	0.4823	0.9165	0.9936	1.0000
Survival function	0.9998	0.9967	0.9800	0.9293	0.8285	0.6829	0.5177	0.0835	0.0064	0.0000
Average Skewness	2.2271	2.3750	2.6159	2.9064	3.0312	2.5763	1.7460	1.0821	1.3210	1.6200

From Table 22, we can see that the survival function at the time of preventive maintenance decreases as the maintenance period increases. The average skewness value increases first as the time for preventive maintenance increases from T_r=6 years to T_r=10 years and then decreases as the maintenance period increases, and there is a slightly change after T_r=16 years. A detailed analysis of the variation in skewness and survival function will be given later in this section.
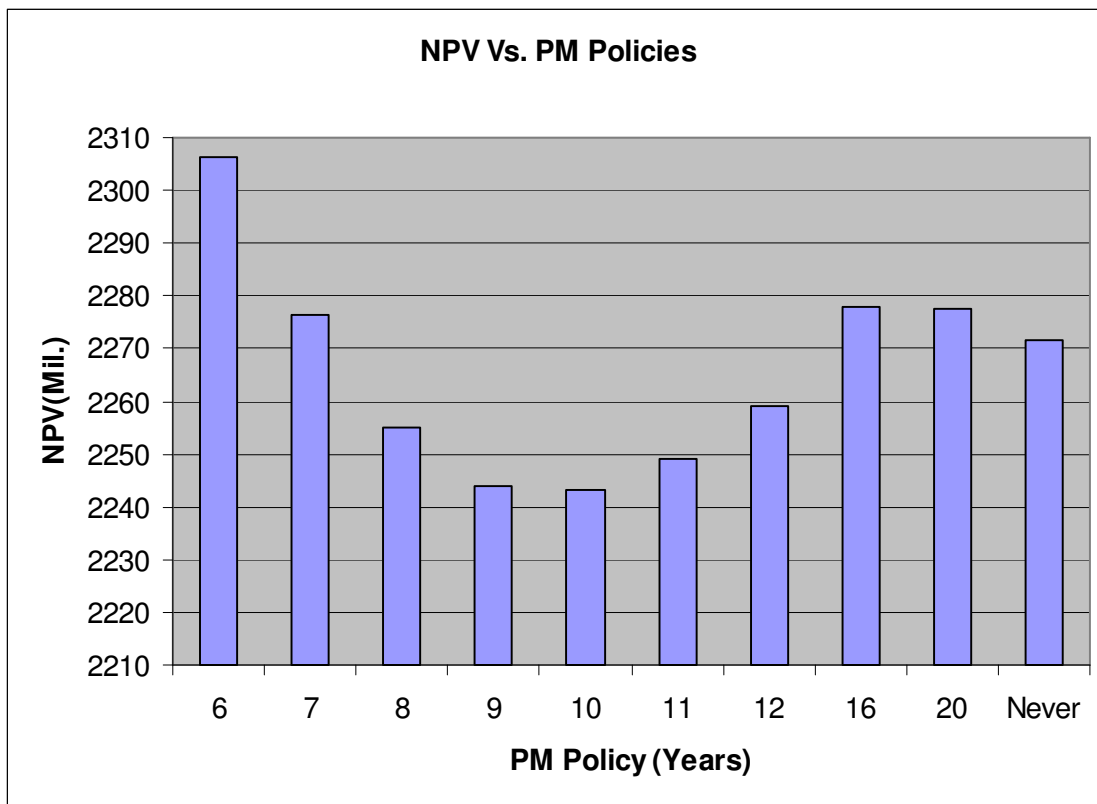
Figure 53. Detailed comparison of NPV of 50 years for different maintenance policies

Figure 53 shows the expected net present values of the effective costs, from using different maintenance policies over a 50-years lifetime. As mentioned before, the minimum expected net present value effective cost ocurs for maintenance periods somewhere between 6 years and 12 years. The plot above shows that the minimum net present value cost comes with the maintenance policy to replace the system every 10 years (T_r=10 years). However, the difference in NPVs for T_r=10 years and T_r=9 years is not significant, as seen from Table 22 and Figure 53. Based only on NPV effective cost, one may prefer to choose the maintenance policy to replace the system every 10 years (T_r=10 years) which minimize the NPV cost for a 50 year lifetime. Again, back to the original goal of the maintenance of a commercial nuclear power plant, we want to minimize the cost (represented by expected NPV effective cost in this example) while still having acceptable reliability performance. Hence more analysis needs to be done and more performance needs to be compared in order to make final maintenance decisions. In the following, the NPV cost and the survival function as well as the average skewness will be plotted together to give us a better understanding of both the financial performance and the risk/reliability performance for each preventive maintenance policy.
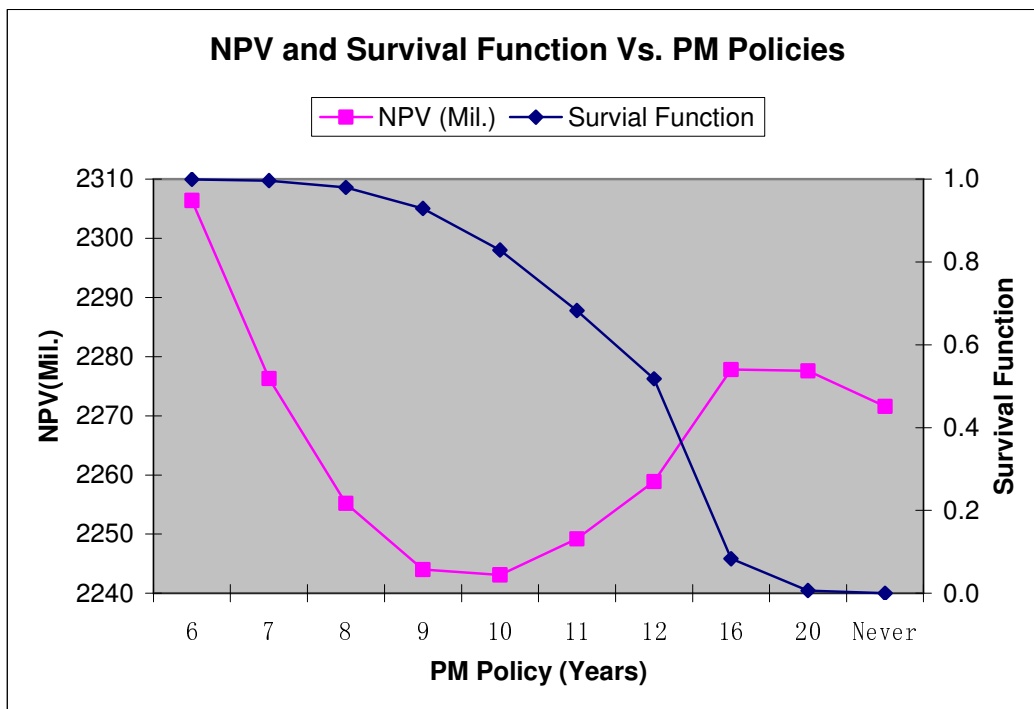
Figure 54. NPV and survival function of 50 years for different maintenance policies

From the plot above (Figure 54), we can see that the survival function decreases as the maintenance period increases. When the NPV cost reaches its minimum at $T_r = 10$, the survival function takes the value of 0.8285 and hence the corresponding cdf value for failure is 0.1715, which means that the cumulative failure probability at the time when preventive maintenance is done is slightly more than 17% and therefore the cumulative survival probability is somewhat less than 83%. For risk-averse management, that might be a very high detriment to choosing such a large replacement period. For maintenance policies $T_r = 9$, $T_r = 10$ and $T_r = 11$, the NPV cost for these three maintenance policies are $2244.0M, $2243.1M and $2249.2 respectively, hence there are only small

differences among the three NPV values; however, the cumulative survival probability values for the three policies are 0.9293, 0.8285 and 0.6829 and the difference between the former two values is 0.1008. That means the cumulative probability of failure increases about 10% if we choose the maintenance policy of replacing the system every 10 years ($T_r = 10$) instead of replacing it every 9 years ($T_r = 9$). This 10% increase is generally regarded as very large number in reliability analysis, especially for generation/risk related systems such as the main generators.

Since there is no significant difference between the NPV cost acquired using the two different maintenance policies ($T_r = 9$ and $T_r = 10$), while there is big difference in the reliability performance, the one with better reliability performance will tend to be preferred. Hence, if we want to choose between the two maintenance policies, $T_r = 9$ is probably preferable to $T_r = 10$ because of its high reliability performance and low NPV cost value, provided the a cumulative failure value of 7% (the cdf for $T_r = 9$ is 0.0707)is acceptable.
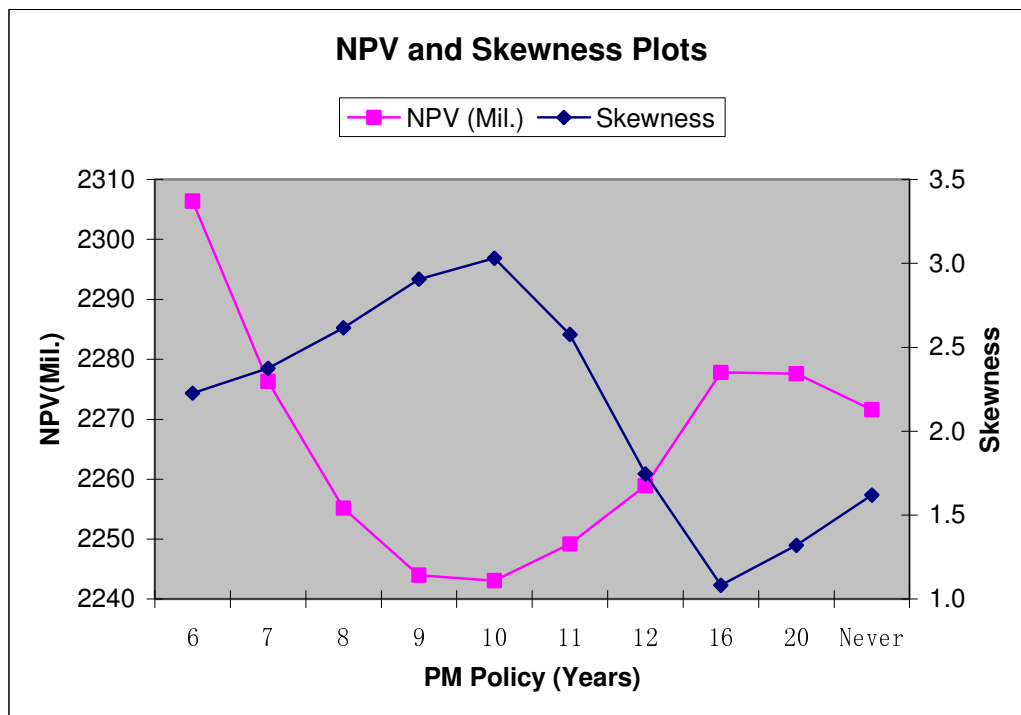
Figure 55. NPV and average skewness of 50 years for different maintenance policies

In addition to the comparison of cumulative failure values and the cumulative survival function values, the average skewness values over the 50 year life also can be compared, so as to assist the decision-making process as to which maintenance policy is preferable. Figure 55 shows the NPV cost and the corresponding average skewness values for each maintenance policy. As can be seen from Figure 55 the magnitude of the skewness value increases as the maintenance period increases from 6 years to 10 years and then decreases as we increase the maintenance period to 11 years or above. However, when the maintenance is longer than 16 years, there is a slight increase in the skewness value, as the expected NPV effective cost starts to decrease. These two phenomena are

believed to be closely related in the sense that when choosing among the last three maintenance policies (T_r=16 years to T_r=20 years and never do PM), the run-to-failure policy (never do PM) is preferred because it has a relatively smaller NPV cost.

Similarly, in comparing the two different maintenance policies $T_r = 9$ and $T_r = 10$, there is again no huge difference between the expected NPV cost achieved, and also there is no big difference in the average skewness. The average skewness values are 2.9064 and 3.0312 respectively. Hence, if we want to choose between these two maintenance policies based on the comparison of skewness values, even though $T_r = 10$ is more preferable to $T_r = 9$ because of it has larger positive skewness; however, the difference is small, so there is room for different philosophies without greatly affecting either expected NPV cost or downside risk. Still it is too hard to make judgment because the difference is almost negligible.

From this discussion we draw the following conclusion: Considering the requirement to minimize the NPV cost and still get a good reliability performance, if we want to choose between the two maintenance policies $T_r = 9$ and $T_r = 10$, then $T_r = 9$ is preferable to $T_r = 10$ because it has higher reliability performance (with cumulative survival probability of 0.9293) and smaller NPV cost value, and it also has roughly the same skewness number as does $T_r = 10$. However, the conclusion is based on the assumption that the cumulative failure value of 7% (the cdf for $T_r = 9$ is 0.0707) is acceptable to plant management. It is possible that plant management judges the value of

7% is too high for the consideration of risk/reliability. In that scenario, a shorter maintenance policy such as $T_r = 7$ or $T_r = 8$ may even be considered.

As has been discussed in the preceding section, the probability density functions (pdf) and the cumulative distribution functions (cdf) plots using the parameters acquired from the failure data with lognormal distribution and Weibull distribution are almost identical (Figure 46). The only difference between the two distributions is the hazard rate (failure rate), as shown in plot at the lower right of Figure 46. Also, from the analysis done in the preceding section, we know that the reliability performances using the two distributions are roughly the same with slightly differences.

However, when it comes to the system financial performance analysis, one may ask which distribution is preferable, lognormal distribution or Weibull distribution, or indeed if the choice of distributions makes little or any difference in the financial performance analysis?

Table 23

Comparison of expected NPV cost for all the PM policies over 35 years

PM (Years)	6	7	8	9	10	11	12	Never
NPV(Weibull) (Mil. $)	2186.6	2156.9	2140.7	2123.9	2118.0	2117.6	2116.9	2129.1
NPV(lognormal) (Mil. $)	2184.9	2153.7	2136.9	2120.3	2117.6	2120.1	2121.2	2127.7
cdf(Weibull)	0.0076	0.0196	0.0441	0.0890	0.1633	0.2744	0.4220	1
cdf(lognormal)	2.5e-4	0.0033	0.0200	0.0707	0.1715	0.3171	0.4823	1

As has been done in the preceding section, the financial performances will now be compared using the Weibull and lognormal distributions. To see only the effects of the two distributions in the calculation of NPV and hence the analysis of financial performances, a plant life of only 35 years is used rather than 50 years.

The expected NPV of the costs of each maintenance policy using the two distributions are given in Table 23. A rough observation of the numbers shows that no matter which distribution is used, the minimum expected NPV costs occurs at $T_r = 10$ years. A detailed comparison of the expected NPV costs shows that the minimum NPV costs from the two distributions are roughly the same ($2118.0M for Weibull and $2117.6M for lognormal). Also a comparison of the corresponding cdf values from the two distributions shows that they are roughly the same, with difference of around 1% for $T_r = 9$ years and $T_r = 10$ years.

Figure 56 gives a better of view of the comparison of NPV values. It is clear to see from this figure that the expected NPV cost attains its minimum at $T_r = 10$, for both distributions. Also the increasing/deceasing trends of the two tend to be the same: Expected NPV cost decreases with a PM period shorter than 10 years and increases afterwards with a longer PM period. However, a detailed comparison shows some significant differences in the NPV values, especially for $T_r = 9$ years and $T_r = 11$ years. For NPV values acquired using lognormal distribution, the NPV for $T_r = 9$ tends to be smaller than that of $T_r = 11$. On the other hand, for expected NPV cost obtained using the

Weibull distribution, it is the opposite; expected NPV cost for $T_r = 9$ is larger than that

for $T_r = 11$.
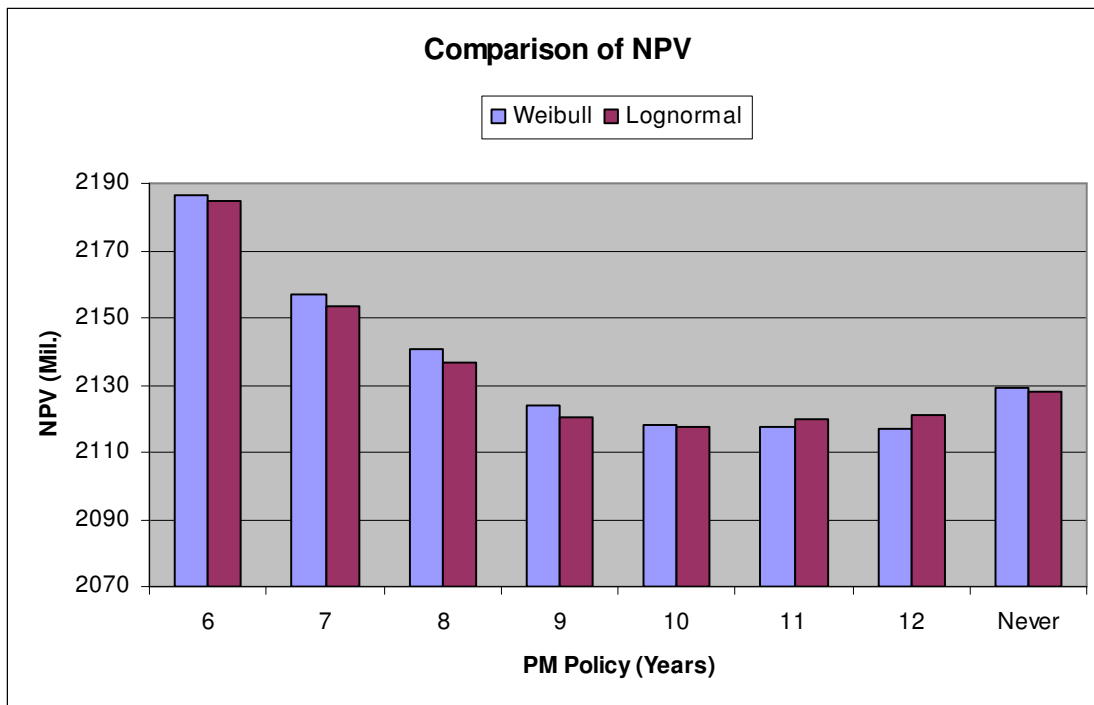
Figure 56. NPV costs for 35 years plant life, for different maintenance policies and

different failure distributions
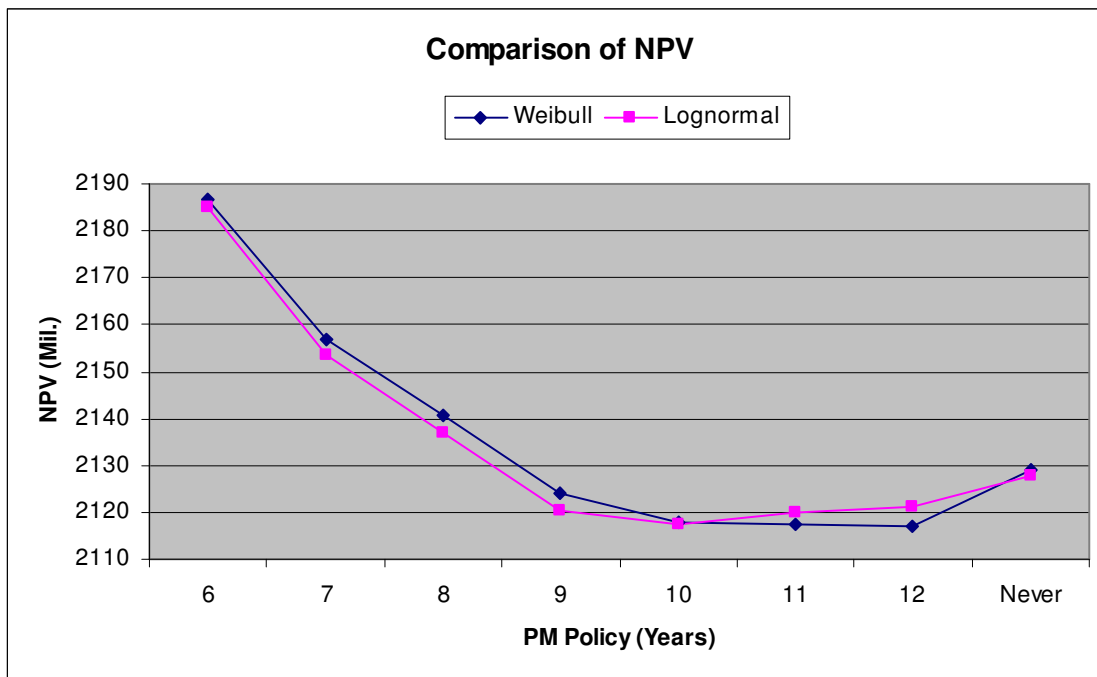
Figure 57. Comparison of expected NPV costs for 35 year plant life, different

maintenance policies, and different failure distributions

The trends of expected NPV costs for both distributions are shown in Figure 57. As can be clearly seen from the figure, the expected NPV cost acquired using the lognormal distribution tends to be less than that acquired using Weibull distribution, for replacement periods less than $T_r = 10$ years. Further, the expected NPV costs at $T_r = 10$ for the two distributions are almost the same. After that point ($T_r = 10$ years), the expected NPV cost acquired using Weibull distribution tends to be less than that acquired using lognormal distribution. This is easy to understand from the cdf and pdf plots for the two distributions, as can be found in Figure 46. That is, both cdf and pdf

values for the failures tend to be greater for Weibull distribution that those from lognormal distribution when $t < 10$ years and the trends become opposite afterwards. This means that the probability of system failure tends to be larger using Weibull distribution when $t < 10$ years, hence the expected NPV cost found using Weibull distribution is larger due to the higher failure costs. Similarly the NPV obtained using lognormal distribution is larger than that from the Weibull distribution, when $T_r > 10$ years.

When it comes making a decision as to which maintenance policy is better, from both reliability and financial point of view, $T_r = 9$ years is chosen as well when Weibull distribution instead of lognormal distribution is used in the analysis. This is because $T_r = 9$ years provides a high reliability performance (with cumulative survival probability of 0.9110 while the value for $T_r = 10$ years is 0.8367), and small expected NPV cost as well.

From the analysis done in this and the previous sections, we draw the following conclusion for the maintenance of the main generator system:

    i.   The reliability performance of the main generator system tends to be better with a shorter maintenance period.

    ii.   The financial performance (expected NPV cost) tends to be better when the replacement period is close to $T_r = 10$ years, but this minimum is relatively broad in that the associated expected NPV cost changes relatively little for changes of T_r on the order of a year or so.

iii.   Considering the requirement to minimize the NPV cost and still get a better reliability performance, if we want to choose between the two maintenance policies, $T_r = 9$ years is preferable to $T_r = 10$ years, because it has high reliability performance (with cumulative survival probability of 0.9293) and only a very slightly larger expected NPV cost. It also has large positive skewness which brings good financial performance as well.

iv.   The above conclusions are largely independent, from the perspective of both reliability performance and financial performance, of whether one uses the Weibull or lognormal distribution. The choice of distribution has little effect on the analysis of the system, and hence little effect on the selection of the preferred maintenance policy.

5.5 Applications of Entry-time Processes in PRA/GRA

From the preceding sections of this chapter we can see that entry-time processes can be applied to PM-based issues and to help make maintenance decisions from the aspects of both reliability and financial performance. Another possible application of the entry-time approach is to incorporate time-dependent failure rates, especially aging effects and maintenance policies, into PRA/GRA.

It is clear that system reliability performance measures such as failure probabilities and system availabilities can sometimes be used as important input for decision-making process, especially for PRA and GRA analyses. However, in classic PRA, constant

failure rates are applied to the fault tree and event tree analysis, and therefore aging effects and maintenance policies are not taken into account.

There is already some work done (for example, [17]) to incorporate aging effects into PRA, as introduced in the first chapter of the dissertation. However, the entry-time processes provide a different methodology at the system level that can generates time-dependent probabilities for the system as a whole. Also, entry-time processes allow time-dependent transition rates, which can include not only aging effects, but also time-dependent maintenance policies.

For the generator system discussed above, if we use the constant failure rate assumption as is being used in the current NPP PRA/GRA models when doing future reliability performance predictions, we would have a much lower failure probability (in state 3 and state 4) after around 5 years.

One may argue that the Bayesian updating [37] often used in analyzing reliability for NPPs accounts in some way for failure rate changes from past operational experience. Nonetheless, the associated drawback is that the PRA calculation of cdf, which is supposed to forecast the likelihood, actually only reflects the present experience. The associated shortcoming stems from the fact that in NPPs most PRA/GRA models are used not only for reflecting the current system status, but also for predicting the future system reliability performance so as to make adequate management decisions. For the most part, management decisions are made from the viewpoint of long-term system reliability rather than short-term performance, which requires not just consideration of past experience, but also consideration of system performance as it ages.

Consider a common scenario in a GRA model, for the above main generator system. In a typical GRA fault tree logic, the failure of a generator will lead directly to one of the tops of the fault tree (100% power loss). Without considering preventive maintenance, after 5 years the difference between a constant failure rate GRA model and a time-dependent failure rate model will be more than 2%. That amounts to a huge difference (up to 200MWe) in the generation loss calculation for a nuclear power plant with two 1200MW units.

Another advantage of this model is that not only aging effects are considered in the dynamic calculation, but also different preventive maintenance policies are integrated. The incorporation of entry-time processes with PRA/GRA models would not only permit the inclusion of aging effects, but also provide a methodology for evaluating the benefits of maintenance in controlling aging.

CHAPTER VI

CONCLUSIONS

The entry-time model was developed, assessed and applied to a case study for maintenance of main generator in nuclear power plants in the preceding chapters. The data and methodology issues are also addressed in the discussion.

In this chapter, the work is summarized to give a brief overview of the model and its applications in Section 6.1. Also the future research and application directions are discussed in Section 6.2.

6.1 Summary of the Work

The research has developed, assessed and demonstrated the applicability of a novel reliability methodology, centered about what we term as "entry-time processes," that has the potential to provide a significantly greater range of applicability and flexibility than traditional reliability tools for case studies related to equipment and components in nuclear power plants.

It has been shown that the entry-time methodology has particular potential for incorporation into case studies supporting plant planning, and related case studies, including such matters as the effects of component aging and the scheduling of inspections, tests and planned preventive maintenance activities. The potential for this type of application can only be further enhanced by what appears to be a movement toward obtaining improved estimates of equipment failure rates through first-principles consideration of the underlying causes of failure.

In this work, the entry-time model is defined and the integro-differential equations and its discrete algorithm are developed in the second chapter. In the third chapter, this discrete algorithm is verified by some analytically solvable hypothetical examples and by comparison to results from simulation. After that (Chapter III), the entry-time approach is applied to a real field NPP application, in a RIAM-based scenario. This application is based on data from the INPO-EPIX database (Sections 5.3 and 5.4) and followed by a discussion of possible applications of the entry-time approach to PRA and GRA model in NPP (Section 5.5). Also the applicability of the EPIX database is proved (In Chapter IV).

6.2 Future Research/Application Directions

As mentioned in the third chapter, further research needs to be done to compare the accuracy and efficiency of the entry-time methodology against simulations. A detailed analysis should be done as part of the future research about the error and "efforts" (computational efficiency) of the entry-time methodology and simulation. This is very important in choosing the calculation methodology when dealing with some 'rare event' problems. For example, for some catastrophic failure for a risk-related system, the probability of such failure is so rare that it is very difficult to capture in a simulation calculation, with a feasibly small number of sample paths. However, determination of the probability of such events is not particularly stressful for entry-time calculation. This could delineate a type of application for which the entry-time methodology has substantial advantages over traditional simulation approaches..

When dealing with different failure modes for the same system, when the failures are not independent, the "bad as old" assumption, as applied in Section 4.5, is invalid because of the data collection mechanism. Hence one might wish some alternative approach. The "good as new" assumption might be true, but would need to allow for infant mortality in the failure mode that was attempted to repair. An entry time model could accommodate that, but would need to allow for multiple entry times, one for each failure mode. This could be an important area of future research, when expanding the application of entry-time models for other applications.

One of the most important features of the entry-time approach is the inclusion of time-dependent failure rates. This permits inclusion of infant mortality, aging effects and maintenance policies in the analysis. As mentioned Chapter I that one of the drawbacks of the classis PRA/GRA models is that only constant failure rates are applied when setting up the event trees and fault trees.

Therefore, with the inclusion of time-dependent failure rates, the entry-time approach can be applied to set up dynamic event trees and dynamic fault trees and hence to build dynamic PRA/GRA models.

One possible way of doing that is to apply the entry-time model to a system or component where time-dependent failure rates are important, to obtain the dynamic reliability performance (such as time-dependent state probabilities) of the system/component. Once the state probabilities are acquired from the entry-time calculation, the evolution of the "states" can be identified as a function of time and other environmental parameters and hence a dynamic event tree for the system/component

performance can be set up, based on the results acquired from entry-time analysis. Then the dynamic event tree for the system/component can be fit into the comprehensive fault tree to construct a dynamic event tree for all systems. Using the same methodology as for constructing the dynamic event tree, the corresponding dynamic fault tree can be set up and used for PRA/GRA models and therefore can be used to quantify the dynamic performance of the systems.

Other than dynamic PRA/GRA applications, the entry-time approach can be applied mainly to the RIAM applications such as maintenance optimization and sensitivity/uncertainty analysis. In this dissertation an illustrative and relatively simple application to preventive maintenance decisions was presented. However, depending on the requirements of different applications, the general approach can be modified to obtain a more detailed analysis of systems or components.

REFERENCES

[1] Fleming KN. Markov models for evaluating risk-informed in-service inspection strategies for nuclear power plant piping systems. Reliab Eng Syst Saf 2004;83:27-45.

[2] Wang PKC. A maximum property of cauchy's problem for the multigroup neutron transport equation. Siam J Appl Math 1969;17:280-286.

[3] Devooght J, Smith C. Probabilistic reactor dynamics. Nucl Sci Eng Part I: 1992;111:229-240; Part II: 1992;111:241-256; Part III: 1992;112:101-113; Part IV: 1992;112:114-126.

[4] Klein D. An emerging fuel cycle renaissance? NRC Speech-S-07-044, http://adamswebsearch.nrc.gov/idmws/, accessed October,2007.

[5] Fasnacht J. Nuclear plant upratings--Enhancing implementation while reinforcing the viability of nuclear power, Nuclear News 2002;45: 44-45.

[6] Liming JK, Grantom CR. Risk-informed asset management (RIAM) for nuclear power plants. Trans Am Nucl Soc 2003; 88:55-56.

[7] Electric Power Research Institute. About nuclear asset/risk management. Palo Alto, CA: Electric Power Research Institute; 2004, URL: http://www.epri.com/targetDesc.asp?program=269074&value=04T023026&objid=2943 59, accessed October, 2006.

[8] Gregor F, Chockie A. Aging management and life extension in the US nuclear industry. Report No. 06:23. Seattle, WA: Chockie Group International, Inc.; 2006.

[9] Kadaka AC, Matsuo T. The nuclear industry's transition to risk-informed regulation and operation in the United States. Reliab Eng Syst Saf 2007;92:5-10.

[10] Keller W, Modarres M. A historical overview of probabilistic risk assessment development and its use in the nuclear power industry: a tribute to the late Professor Norman Carl Rasmussen. Reliab Eng Syst Saf 2005;89:271-285.

[11] Electric Power Research Institute. Introduction to simplified generation risk assessment modeling. Palo Alto, CA: Electric Power Research Institute; 2005, URL: http://www.epri.com/OrderableitemDesc.asp?product_id=000000000001007386&target nid=270758&value=05T061174&marketnid=270640&oitype=1&searchdate=1/26/2004, accessed October, 2006.

[12] U.S. Nuclear Regulatory Commission. Insights gained from aging research. NUREG/CR-5643.Washington, DC: U.S. Nuclear Regulatory Commission;1992.

[13] Campioni L, Scardovelli R, Vestrucci P. Optimized Monte Carlo simulations for system reliability analysis. Proceedings of PSAM 07 - ESREL'04, June 164-169, 2004, Probabilistic Safety Assessment and Management, p. 687-694. Berlin: Springer Verlag; 2004.

[14] Siu N. Risk assessment for dynamic systems: an overview. Reliab Eng Syst Saf. 1994;43:43-73.

[15] Izquierdo JM, Labeau PE. The stimulus-driven theory of probabilistic dynamics as a framework for probabilistic safety assessment, Proceedings of PSAM 07 - ESREL'04, June 14-18, 2004, Probabilistic Safety Assessment and Management, p. 687-694. Berlin: Springer Verlag; 2004.

[16] U.S. Nuclear Regulatory Commission. Aging data analysis and risk assessment development and demonstration study. NUREG/CR-5378. Washington, DC: U.S. Nuclear Regulatory Commission; 1992.

[17] Smith CL, Shah VN, Kao T, Apostolakis G. Incorporating aging effects into probabilistic risk assessment — a feasibility study utilizing reliability physics models. NUREG/CR-5632. Washington, DC: U.S. Nuclear Regulatory Commission; 1999.

[18] Gardiner CW. Handbook of stochastic methods for physics, chemistry and the natural sciences. New York : Springer-Verlag; 1983.

[19] CapassoV, Bakstein D. An introduction to continuous-time stochastic processes. New York: Birkhauser; 2003.

[20] Sigman K., Stationary marked point processes: an intuitive approach. Boca Raton, FL: Chapman & Hall; 1995.

[21] Cox DR. The analysis of non-Markovian stochastic processes by the inclusion of supplementary variables. Procs Camb Phil Soc 1955;51:433-41.

[22] Shilov GE, Gurevich BL. Integral, measure, and derivative: a unified approach. New York: Dover Publications;1978.

[23] Nelson P, Wang S. Dynamic reliability via computational solution of generalized state-transition equations for entry-time processes. Reliab Eng Syst Saf 2007;92:1281-1293.

[24] Gnedenko B, Ushakov I. Probabilistic reliability engineering. New York: Wiley-Interscience publication; 1993.

[25] Kuo W, Prasad VR, Tillman FA. Optimal reliability design, fundamentals and applications. Cambridge: Cambridge University Press; 2001.

[26] Lindqvist BH, Doksum KA. Mathematical and statistical methods in reliability. Singapore: World Scientific Publishing; 2003.

[27] Liming JK, Kee E. Main generator rotor replacement evaluation. Document No. 0PGP05-ZE-0001. Wadsworth, TX: STP Nuclear Operating Company; 2001.

[28] Electric Power Research Institute. Guidelines for application of the EPRI preventive maintenance basis, TR-112500. Palo Alto, CA: Electric Power Research Institute; 2000.

[29] Eide SA. Historical perspective on failure rates for US commercial reactor components. Reliab Eng Syst Saf 2003;80:123–132.

[30] U.S. Nuclear Regulatory Commission. http://www.nrc.gov, accessed October, 2007.

[31] U.S. Nuclear Regulatory Commission. Reactor safety study: an assessment of accident risks in US commercial nuclear power plants. WASH-1400 (NUREG 75/014) Washington, DC: U.S. Nuclear Regulatory Commission; 1975.

[32] PLG. Database for probabilistic risk assessment of light water nuclear power plants. Pickard, Lowe and Garrick, Inc., PLG-0500, Rev. 0; 1989 (proprietary).

[33] Minitab Software. http://www.minitab.com, accessed October, 2007.

[34] Anderson-Darling: A goodness of fit test for small samples assumptions, *Selected Topics in Assurance Related Technologies*, Volume 10, Number 5. (URL: http://src.alionscience.com/pdf/A_DTest.pdf, accessed October, 2007).

[35] Blank LT, Tarquin A, Blank L. Engineering economy. Columbus, OH: McGraw-Hill Science/Engineering/Math; 2002.

[36] Interest rate data. http://www.treasurydirect.gov/govt/rates/rates.htm, accessed February, 2008.

[37] Robert CP. The bayesian choice: from decision-theoretic foundations to computational implementation, New York: Springer; 2001.

APPENDIX A

SAMPLE FAILURE RECORDS FROM EPIX DATABASE

The EPIX database is queried using different search criteria to get records for component failures, as discussed in Section 4.2.

After appropriate SQL queries, we can find the following failure records for motors from the INPO-EPIX database. The structure of the data records can be seen from the following data segment:

DispositionedDate	DiscoveryDate	FailureEndDate	EstAgeAtFailure
12-Jul-00	16-May-99	22-Jun-99	690
12-Jul-00	16-May-99	22-Jun-99	690
04-Dec-00	22-Jun-99	24-Jun-99	3459
30-Dec-02	20-Dec-02	20-Dec-02	10623
21-Jan-03	03-Jan-03		10637
30-Dec-02	16-Dec-02	18-Dec-02	10619
04-Dec-03	27-Nov-03	28-Nov-03	10965
27-Feb-02	08-Feb-02		10308
16-Jan-01	13-Mar-00	01-Apr-00	9665
31-Jan-00	05-Jul-99	09-Jul-99	9413
27-Apr-02	07-Jan-01	07-Jan-01	6097
27-Apr-02	07-Jan-01	07-Jan-01	6097
19-Jun-98	14-Mar-98	14-Mar-98	7866
06-Oct-00	25-Apr-98	25-Apr-98	4830
23-Oct-03	03-Jan-03	04-Jan-03	6435
23-Feb-01	24-May-99	03-Jun-99	8550
04-Apr-03	17-Feb-03	20-Feb-03	4601
03-Jun-05	17-May-05	17-May-05	5789
30-Jul-04	06-May-04	06-May-04	11026
29-Apr-00	05-Mar-99	06-Mar-99	7121
10-Jun-03	18-Oct-02	30-May-03	10460
17-Jun-99	08-Feb-99	17-Feb-99	8466
11-Feb-02	21-Jan-02	22-Jan-02	10612
31-Mar-05	12-Jan-05	14-Jan-05	11699
22-Feb-00	07-Feb-00	07-Feb-00	10082
25-Aug-05	06-Feb-04	09-Feb-04	8717
22-Jun-05	03-Mar-04	04-Mar-04	9852
28-Apr-04	12-Mar-02	18-May-02	9130
22-Jun-05	18-May-02	19-May-02	9197

APPENDIX B

COMPLETE FAILURE DATA ANALYSIS TO CIRCUIT BREAKERS

AND MOTORS FOR SECTION 4.2

The results are shown below as a sequence of plots of data resulting from analyses
of generators of different model numbers and model types, as discussed in Section 4.2:

Distribution plots for circuit breakers:

Model number: DS 206; Type: K:

Weibull distribution plots:

Exponential distribution plots:

Distribution Overview Plot for CKTBRK_DS-206_K (Exponential)
LSXY Estimates-Complete Data

Normal distribution plots:

Distribution Overview Plot for CKTBRK_DS-206_K (Normal)
LSXY Estimates-Complete Data

Model number: DS 206; Type: S:

Weibull distribution plots:

Distribution Overview Plot for CKTBRK_DS-206_S (Weibull)
LSXY Estimates-Complete Data

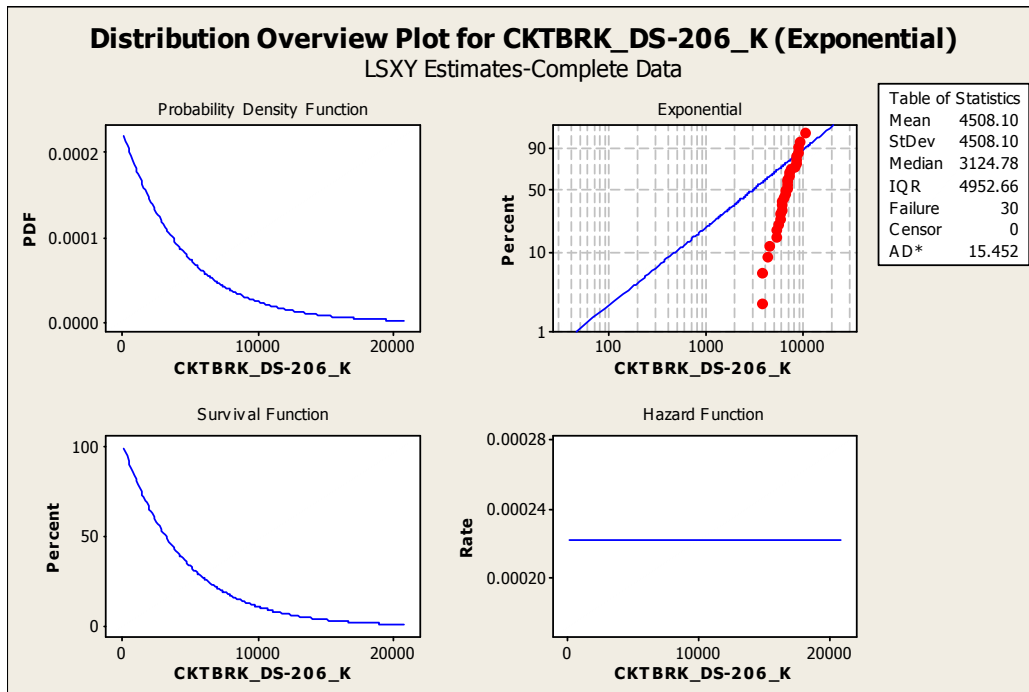| Table of Statistics	
Shape	0.995968
Scale	5535.98
Mean	5545.49
StDev	5567.95
Median	3831.56
IQR	6100.06
Failure	81
Censor	0
AD*	2.784
Correlation	0.937

Exponential distribution plots:

Distribution Overview Plot for CKTBRK_DS-206_S (Exponential)
LSXY Estimates-Complete Data

Table of Statistics	
Mean	3911.48
StDev	3911.48
Median	2711.23
IQR	4297.20
Failure	81
Censor	0
AD*	8.659
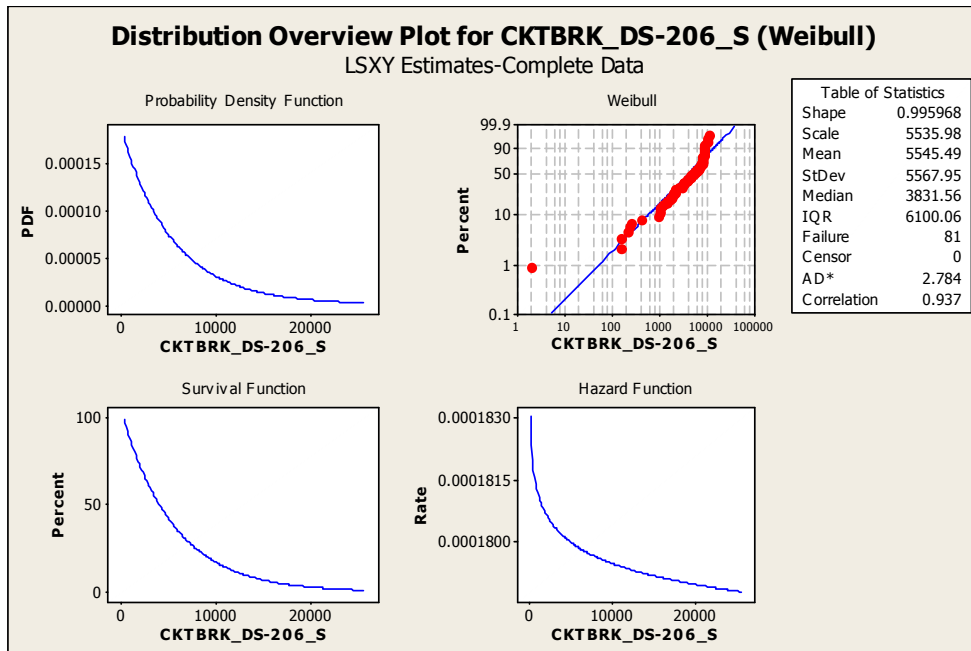
Normal distribution plots:

Model number: HFB3; Type: K:

Weibull distribution plots:

Exponential distribution plots:

Distribution Overview Plot for CKTBRK_HFB3_K (Exponential)
LSXY Estimates-Complete Data

Normal distribution plots:

Distribution Overview Plot for CKTBRK_HFB3_K (Normal)
LSXY Estimates-Complete Data

Model number: HFB3; Type: S:
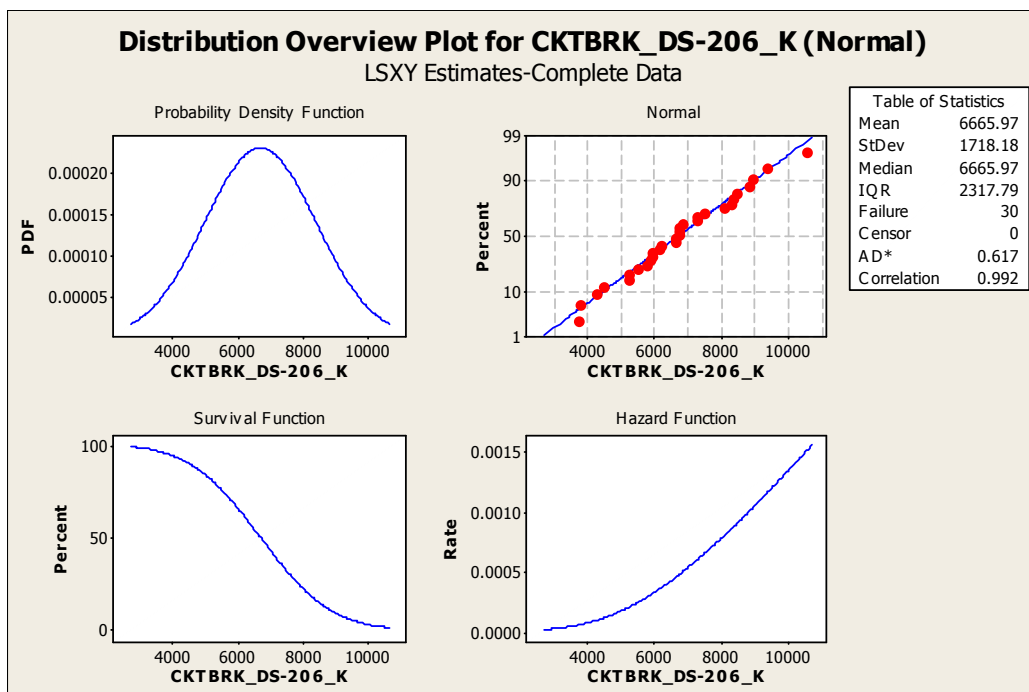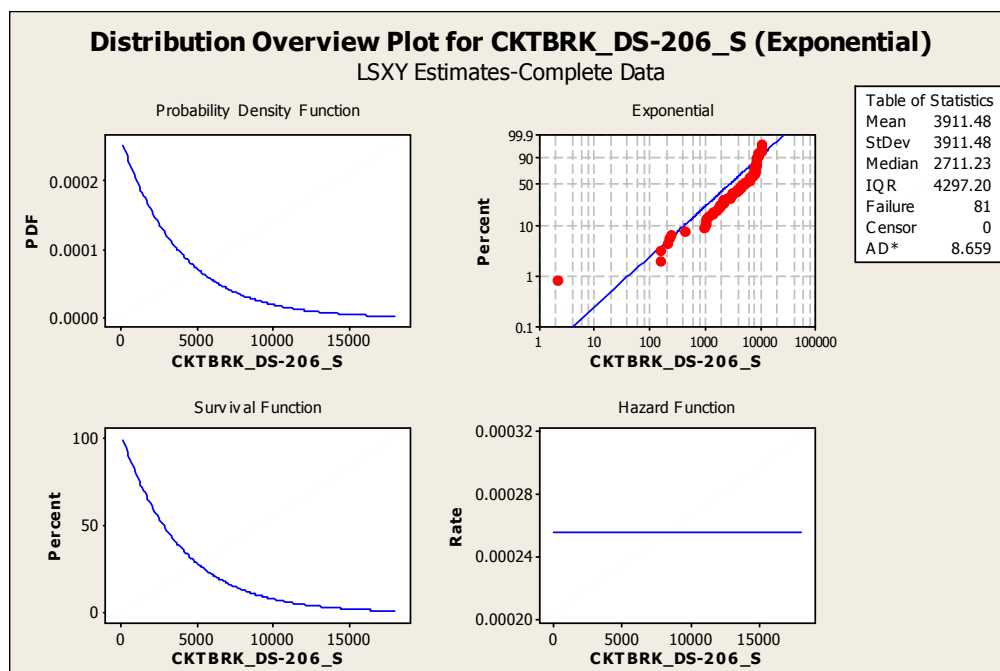
Weibull distribution plots:

Exponentail distribution plots:

Normal distribution plots:

Distribution Overview Plot for CKTBRK_HFB3_S (Normal)
LSXY Estimates-Complete Data

Table of Statistics
Mean 6239.08
StDev 2199.67
Median 6239.08
IQR 2967.31
Failure 106
Censor 0
AD* 0.740
Correlation 0.990
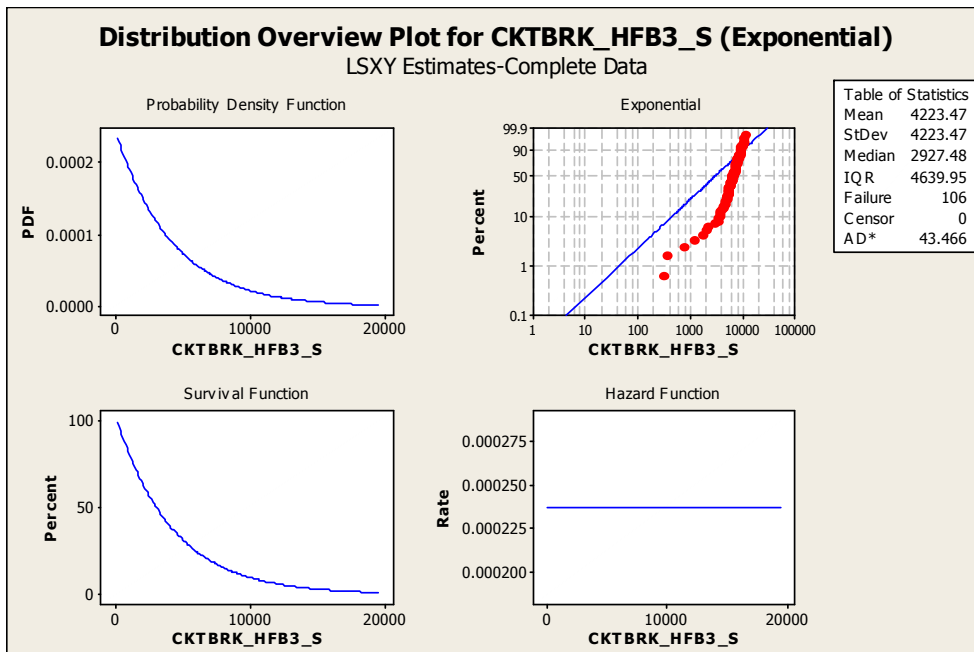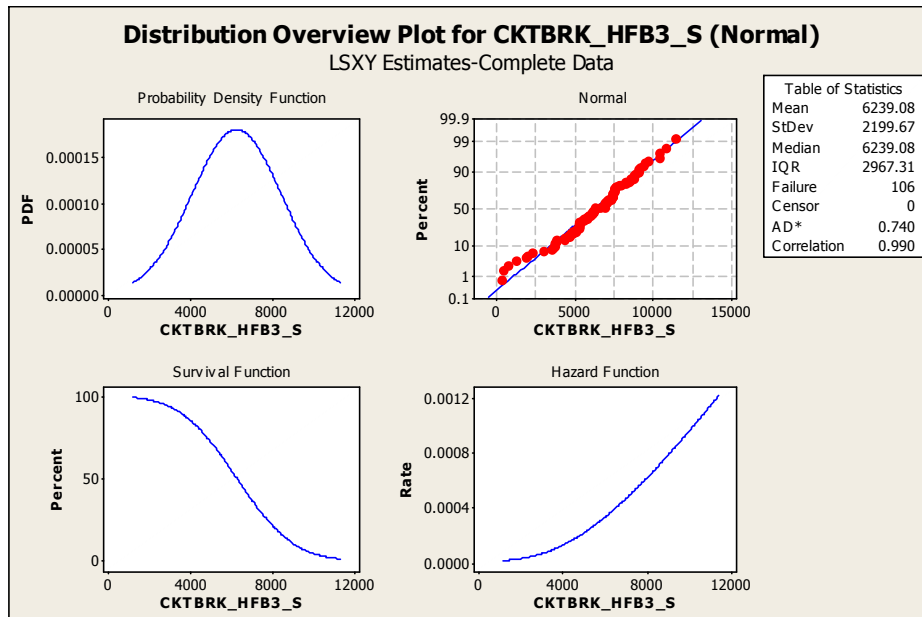
Distribution plots for motors:

Model number: CS VSS; Type: S:

Weibull distribution plots:

Distribution Overview Plot for MOTOR_CS-VSS_S (Weibull)
LSXY Estimates-Complete Data

Table of Statistics
Shape 1.18089
Scale 6067.75
Mean 5731.90
StDev 4871.36
Median 4448.72
IQR 5888.55
Failure 23
Censor 0
AD* 1.515
Correlation 0.954

Exponential distribution plots:

Distribution Overview Plot for MOTOR_CS-VSS_S (Exponential)
LSXY Estimates-Complete Data

Normal distribution plots:

Distribution Overview Plot for MOTOR_CS-VSS_S (Normal)
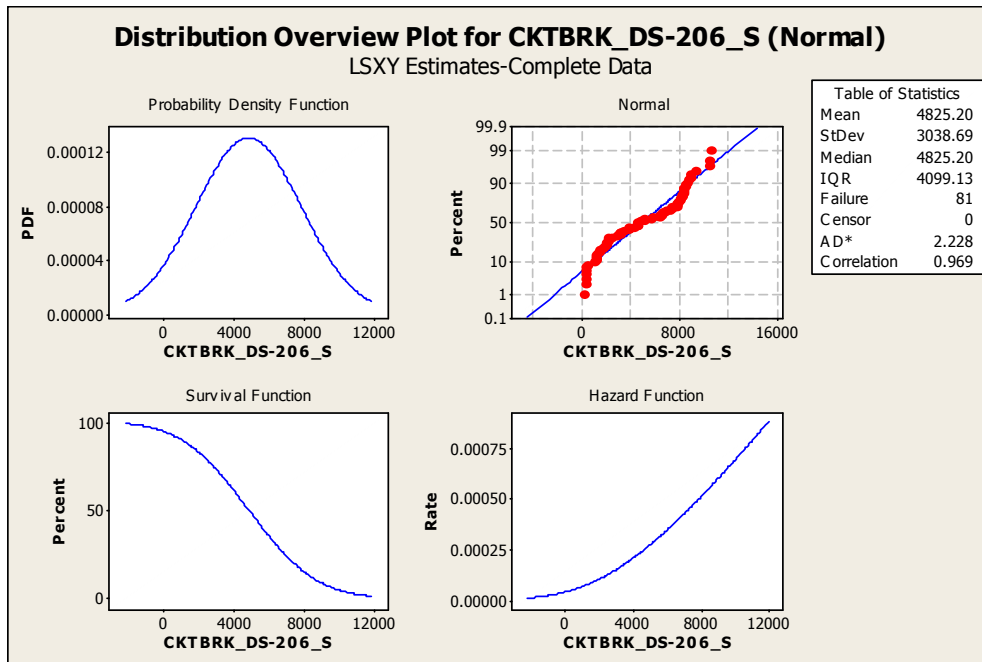LSXY Estimates-Complete Data
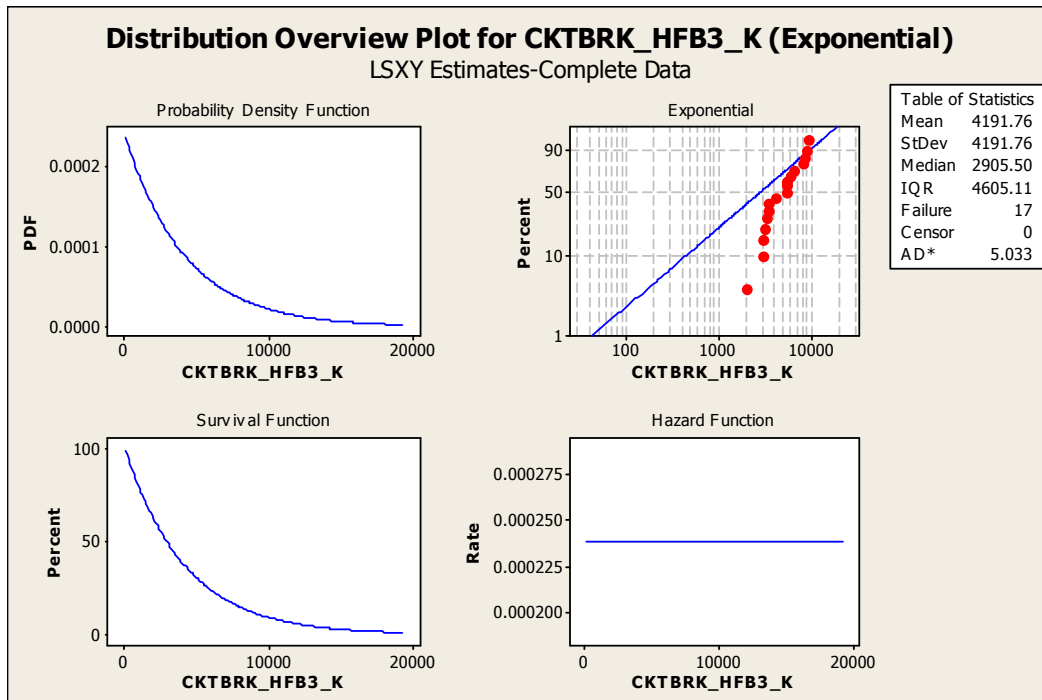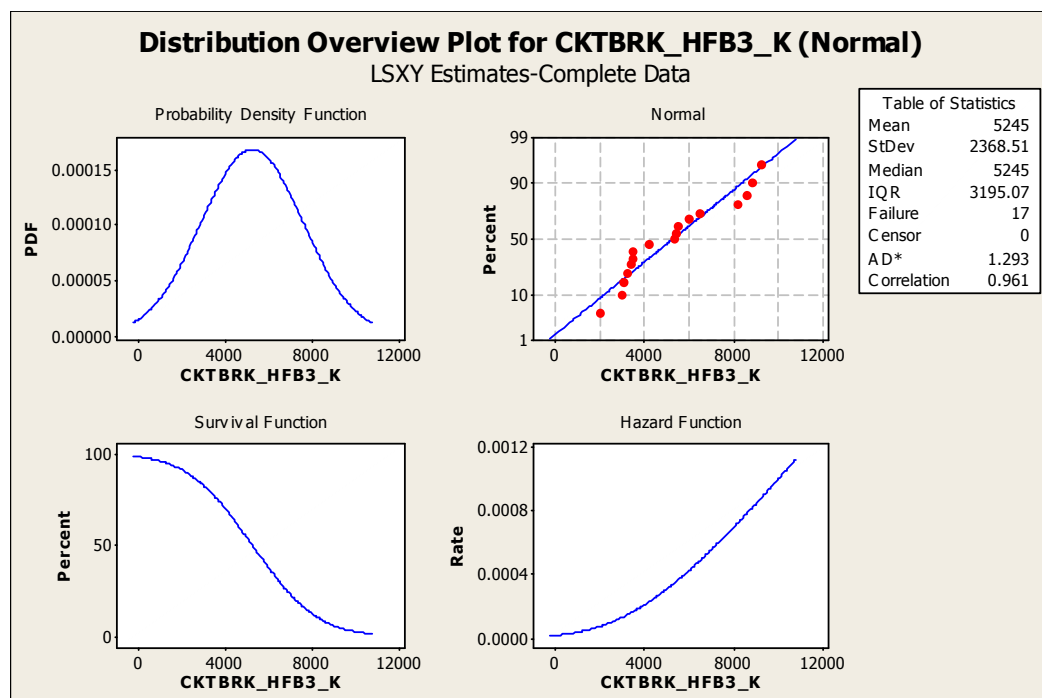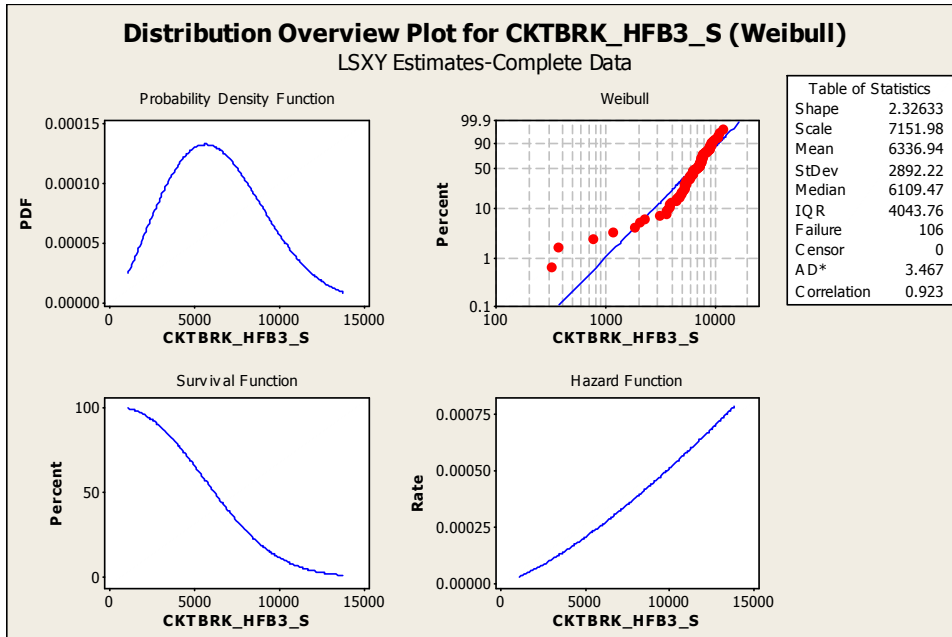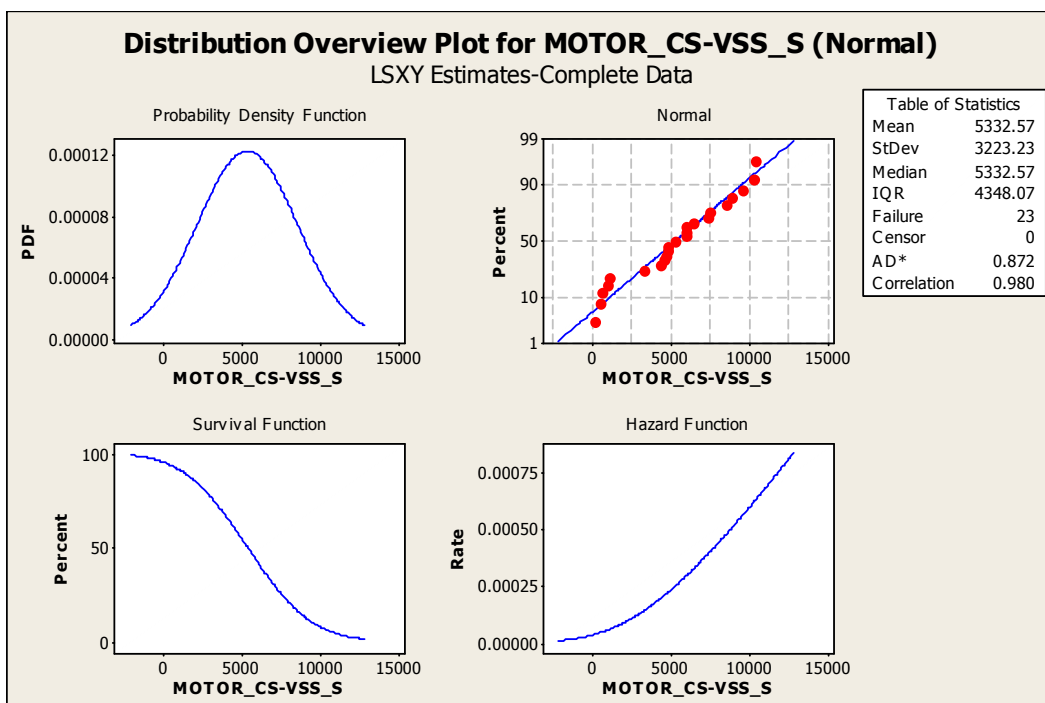
Model number: TBDP; Type: S:

Weibull distribution plots:

Exponential distribution plots:

Normal distribution plots:

Distribution Overview Plot for MOTOR_TBDP_S (Normal)
LSXY Estimates-Complete Data
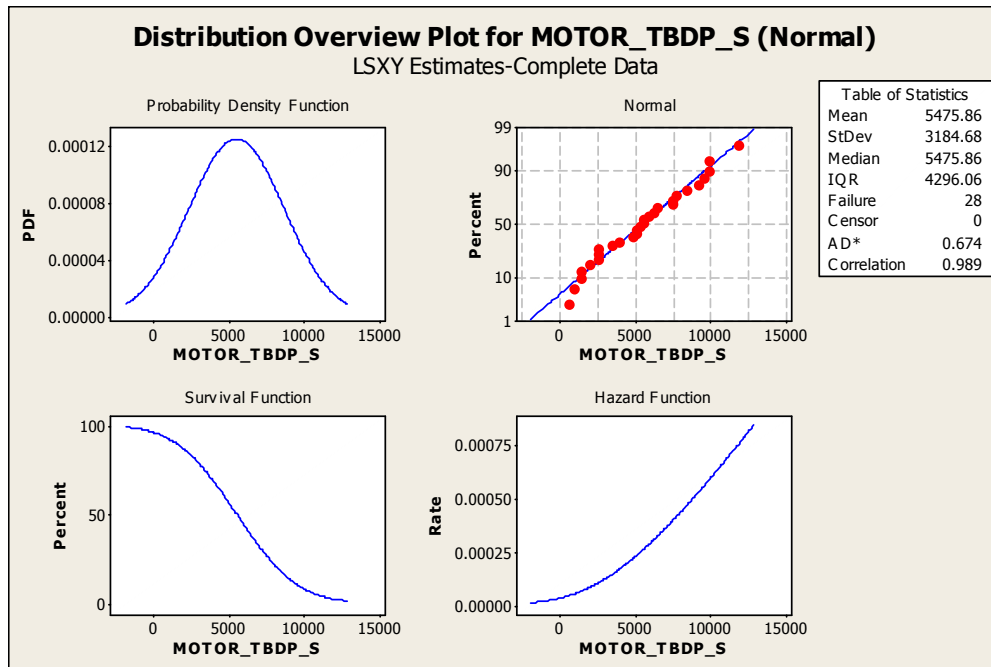
Model number: FTYPE AN; Type: S:

Weibull distribution plots:

Distribution Overview Plot for MOTOR_FTYPE-AN_S (Weibull)
LSXY Estimates-Complete Data

Exponential distribution plots:

Distribution Overview Plot for MOTOR_FTYPE-AN_S (Exponential)

Normal distribution plots:

Distribution Overview Plot for MOTOR_FTYPE-AN_S (Normal)
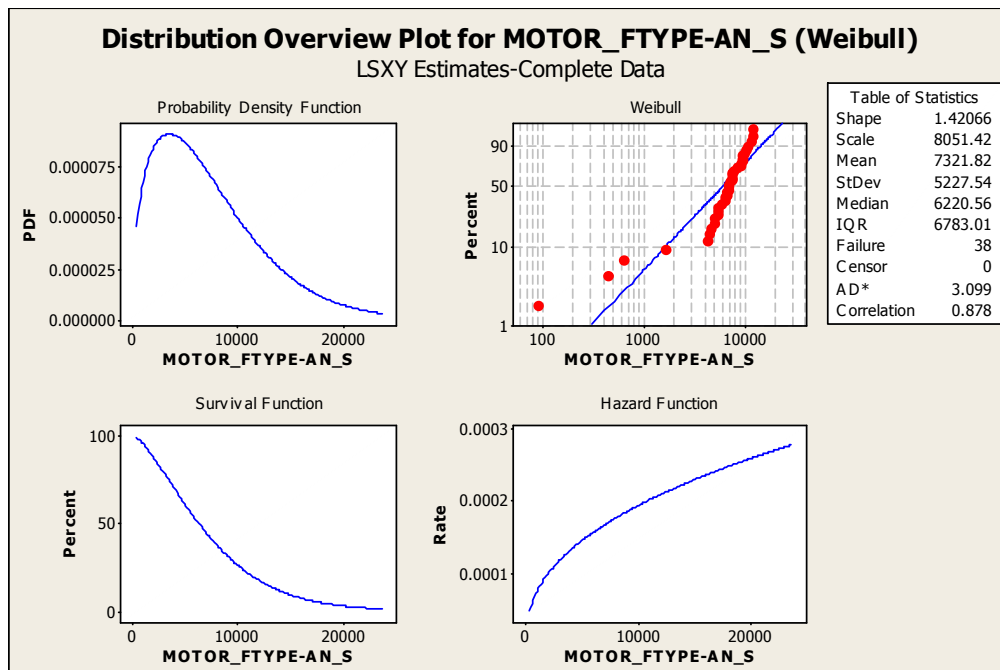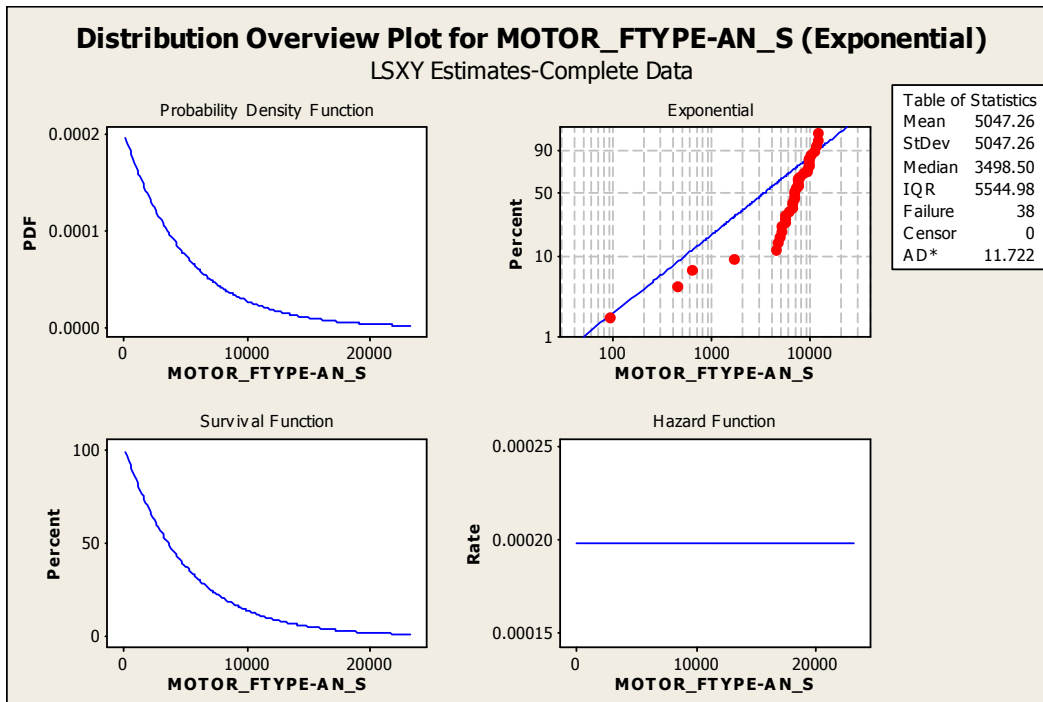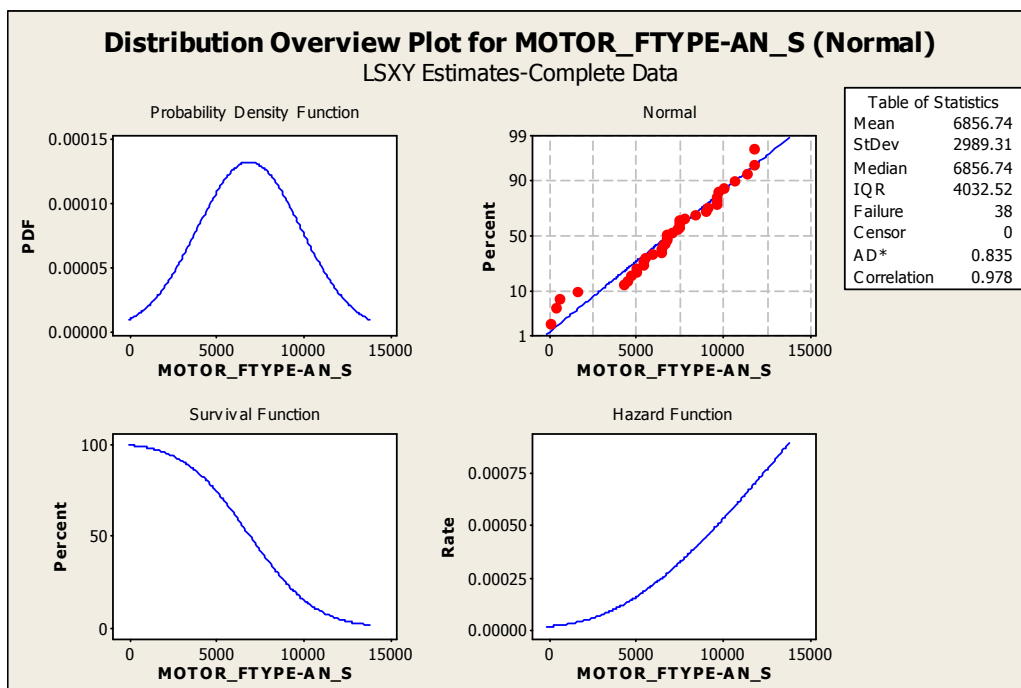
APPENDIX C

COMPLETE FAILURE DATA RECORDS FOR MAIN GENERATOR

(ARBITRARY CENSORING PROCEDURE APPLIED)

The failure records for main generators manufactured by Westinghouse are queried from the EPIX database, as discussed in Section 4.5. The data are then analyzed using Mintitab. The following table shows the data used in Minitab using the arbitrary censoring procedure.

EstAgeAtFailure_MG_WH_1	EstAgeAtFailure_MG_WH_2
*	649
649	1797
1797	2196
2196	2202
2202	2216
2216	2234
2234	2238
2238	2238
2238	2257
2257	2387
2387	2632
2632	2684
2684	2690
2690	2715
2715	3221
3221	3231
3231	3321
3321	3367
3367	3385
3385	3387
3387	3464
3464	3494
3494	3530
3530	3586
3586	3597
3597	3602

EstAgeAtFailure_MG_WH_1	EstAgeAtFailure_MG_WH_2
3602	3655
3655	3677
3677	3717
3717	3844
3844	3940
3940	3975
3975	3986
3986	4006
4006	4006
4006	4011
4011	4030
4030	4072
4072	4086
4086	4244
4244	4294
4294	4372
4372	4377
4377	4453
4453	4465
4465	4494
4494	4520
4520	4564
4564	4619
4619	4623
4623	4641
4641	4725
4725	4742
4742	4762
4762	4854
4854	4854
4854	5011
5011	5051
5051	5064
5064	5122
5122	5157
5157	5200
5200	5270
5270	5357
5357	5404
5404	5476
5476	5781
5781	5883

EstAgeAtFailure_MG_WH_1	EstAgeAtFailure_MG_WH_2
5883	5986
5986	5996
5996	6054
6054	6439
6439	6576
6576	6611
6611	6637
6637	6805
6805	6816
6816	7239
7239	7347
7347	7865
7865	8774
8774	9000
9000	9347
9347	9538
9538	9698
9698	9732
9732	10308
10308	10487
10487	10534
10534	10650
10650	10686
10686	10812
10812	10829
10829	10841
10841	10916
10916	11197
11197	11359
11359	11778
11778	11864
11864	12384
12384	*

APPENDIX D

DATA CENSORING METHODS

The data queried from the database can be interpreted as different observations, as discussed in Section 4.4. The different observations correspond to different "censoring schemes" in MiniTab. In this appendix, some examples are given to show the connections between observations and "censoring schemes"

In MiniTab, the user can input the data using different "censoring schemes". Here the table below shows how the censoring scheme is related to the observation of data:

Here Table D-1 shows the different types of observations that are supported by the current version of MiniTab [33].

Table D-1

Different types of observations

Type of observation	Description	Example
Exact failure time	You know **exactly** when the failure occurred.	The fan failed at exactly 500 days.
Right censored	You only know that the failure occurred **after** a particular time.	The fan had not yet failed at 500 days.
Left censored	You only know that the failure occurred **before** a particular time.	The fan failed sometime before 500 days.
Interval censored	You only know that the failure occurred **between** two particular times.	The fan failed sometime between 475 and 500 days.

From Table D-1, we know we may have different types of observations. Then when using the MiniTab software to do reliability analysis to the data, we have different censoring methods corresponding to those observations. Table D-2 shows how to input the observed data into MiniTab software using different censoring methods (here "*" means missing data):

Table D-2

Examples of MiniTab input corresponding to different types of observations:

Start	End	
*	10000	Left censored at 10000 hours.
10000	20000	
20000	30000	
30000	30000	Exact failures at 30000 hours.
30000	40000	
40000	50000	
50000	50000	
50000	60000	Interval censored between 50000 and 60000 hours.
60000	70000	
70000	80000	
80000	90000	
90000	*	Right censored at 90000 hours.

Table D-3

Sample failure data (Estimated age at failure) from the EPIX database

Age at Failure
3494
3975
4006
4011
4244
4372
4377
4453
4520
5051
5883

Here Table D-3 shows some sample failure data acquired from the database.In our analysis, we use two different data interpretation schemes in the analysis of the failure data. Scheme 1 is "discovery by inspection" in which we assume the failures occurred in between two inspections. Hence the MiniTab input data for the above failure records (Table D-3) can be found in Table D-4.

Table D-4

Method 1 "discovery by inspection" procedure

Start	End
*	3494
3494	3975
3975	4006
4006	4011
4011	4244
4244	4372
4372	4377
4377	4453
4453	4520
4520	5051
5051	5883
5883	*

Method 2 is "discovery by alarm, with no censoring" in which we assume all failures are exact, which means they are discovered immediately after the failures. Hence the MiniTab input data using this censoring procedure for the above failure records (Table D-3) can be found in Table D-5.

Table D-5

Method 2 "discovery by alarm, with no censoring" procedure (Assume all failures are exact)

Start	End
3494	3494
3975	3975
4006	4006
4011	4011
4244	4244
4372	4372
4377	4377
4453	4453
4520	4520
5051	5051
5883	5883

APPENDIX E

DETAILED COST/REVENUE TABLE (USED IN SECTION 5.2)

Unit Capacity(MW)	1200				
Electricity Price ($/MWh)	40				
Recovery time for PM (Year)	0.3				
Recovery time for N-C failure (Year)	0.2		PM	N-C Failure	C Failure
Recovery time for C failure (year)	0.8	O&M Change factor	1/5	1/6	1/4
		Per day	Per Year		
	Fuel cost	$100,000	$36,500,000		
State 1(running)	O&M	$400,000	$146,000,000		
	Power Generation	$1,152,000	$420,480,000		
	Net Profit	$652,000	$237,980,000		
		Per day	Per recovery time	Per Year	
	O&M	480,000	N/A	$175,200,000	
State 2(PM State)	Power Generation	0	0	$0	
	Components costs	N/A	10,000,000	$33,333,333	
	Net Profit		N/A	$(208,533,333.33)	
		Per day	Per recovery time	Per Year	
	O&M	466,667	N/A	$170,333,333	
State 3(Noncatastrophic Failure)	Power Generation	0	0	$0	
	Components costs	N/A	5,000,000	$25,000,000	
	Net Profit		N/A	$(195,333,333.33)	
		Per day	Per recovery time	Per Year	
	O&M	500,000	N/A	$182,500,000	
State 4(Catastrophic Failure)	Power Generation	0	0	$0	
	Components costs	N/A	20,000,000	$25,000,000	
	Net Profit		N/A	$(207,500,000.00)	

APPENDIX F

CODES USED IN THE ENTRY-TIME ANALYSIS OF THE MAIN

GENERATOR RELIABILITY PERFORMANCE IN SECTION 5.3

Entry_time_Main.m:

```
%Program Name: Entry_time_Main.m
%Program function: This is the main entry of the entry-time process code
%Program NOTE: This is a revision of the initial program
%Program by: Eric Wang
%Program Date: 06/01/2007
%%%%%%%%%%%%%Revision History%%%%%%%%%%%%%%%%
%Revision Date%%%%%Revision reason%%%%%%%%%%%%%%%
%06/01/2007: Program initial setup
%07/30/2007: Use this program for the Main Generator Example
%          This example uses lognormal dis. rather than Weibull Dist.
%
%%%%%%%%End of Revision History%%%%%%%%%%
%%
%%%%%%%%%%%%%%%%%%%%%%%%%%%% Functions List %%%%%%%%
%Function Name%%%%%%%%%%%Function usage %%%%%%%%%%%%
%lambda0: Differential transition probability at entry time zero
%Lambda:  Cumulative transition probability
%
%
%%%%%%%%%%%%%%%End of Functions List%%%%%%%%%%%%%
%%
%%%%%%%%%%%%%%%Definition of states%%%%%%%%%%%%%%
%% State 1: System is in normal running state
%% State 2: System is down for preventive maintenance
%% State 3: System is down due to non-catastrophic failure
%% State 4: System is down due to catastrophic failure
%% Note that: 95% the failure is non-catastrophic and 5% is catastrophic
home;clear all;close all;
global I N Delt N_r n_c_nc n_c_c n_p mu sigma beta eta
Time0=clock;
disp(sprintf('The program starts at: %s\n',time_display(0)));
disp(sprintf('Program running, please stand by...\n'));
Pdiag_Save_name='Pdiag_Save_10';Figure_Name='Plot_10';
I=4;    %Number of states
N=350;   %Number of time stpes
```

```
Terminal_time=35;    %Termial calendar time
T_r=15;        % Max time between maintenances
t_c_nc=0.2;  % Time for non-catastrophic corrective maintenance
t_c_c=0.8;   % Time for catastrophic corrective maintenance
t_p=0.4;       % Time for preventive maintenance
P_ini=[1,0,0,0];    %Initial probability the system is in each state
mu=4510.22/365;
sigma=919.001/365;
beta=5.853;
eta=4851/365;
%%%%%%%Change the parameters above for
calculation%%%%%%%%%%%%%%%%
Delt=Terminal_time/N; %Time step
N_r=T_r/Delt;      % Max no. of time steps between maintenances
n_c_nc=t_c_nc/Delt;     % No. of time steps for non-catastrophic CM
n_c_c=t_c_c/Delt;      % No. of time steps for catastrophic CM
n_p=t_p/Delt;     % No. of time steps for preventive maintenance
T=Terminal_time;
for i=1:I   %Initialize the P matrix: P{i}(m,n)=P_i(m,n) in equations
   P{i}=zeros(N+1,N+1);
   P{i}(1,1)=P_ini(i);
end
disp(sprintf('Now starting entry-time calculation...\n'));
for n=1:N       % Calendar time index of probability being computed
   Time_loop_start=clock;
   disp(sprintf('Now calculating N=%d, and %d loop(s) remaining...\n',n,N-n));
   disp(sprintf('This loop starts at: %s\n',time_display(0)));
   for m=1:n   % Entry time index of probability being computed
      for i=1:I   % State index of probability being computed
         Delp=0; % Initialize transitions from earlier times
         for j=1:I
            Delp=Delp+Delt*lambda0(j,i,1,n)*P{i}(1,n);
         end
         for mp=1:m-1  % Loop to obtain transitions from all earlier entry times
            for j=1:I % Loop over all states, including state being computed
               DelLambda=Lambda(j,i,mp,n+1)-Lambda(j,i,mp+1,n+1);
               Delp=Delp+(P{i}(mp+1,n)-P{i}(mp,n))*DelLambda;
            end
         end
         P{i}(m,n+1)=P{i}(m,n)-Delp;
      end
   end
   % Calculate next probabilities along diagonal, for all states
   for i=1:I   % Next diagonal update
```

```
      Delp1=0;
      Delp2=0;
      for j=1:I
         Delp1=Delp1+Delt*lambda0(i,j,1,n+1)*P{j}(1,n);
         Delp2=Delp2+Delt*lambda0(j,i,1,n+1)*P{i}(1,n);
      end
      for mp=1:m-1
         for j=1:I
            DelLambda1=Lambda(i,j,mp,n+1)-Lambda(i,j,mp+1,n+1);
            DelLambda2=Lambda(j,i,mp,n+1)-Lambda(j,i,mp+1,n+1);
            Delp1=Delp1+(P{j}(mp+1,n)-P{j}(mp,n))*DelLambda1;
            Delp2=Delp2+(P{i}(mp+1,n)-P{i}(mp,n))*DelLambda2;
         end
      end
      P{i}(n+1,n+1)=P{i}(n,n)+(Delp1-Delp2);
   end
   time_used_loop=etime(clock,Time_loop_start);
if time_used_loop>60
   disp_loop_running_time=sprintf('Total time used for the loop is %f minutes\n
\n',time_used_loop/60);
else
   disp_loop_running_time=sprintf('Total time used for the loop is %f seconds\n
\n',time_used_loop);
end
disp(sprintf('This loop ends at: %s\n',time_display(0)));
disp(disp_loop_running_time);
end
for i=1:I
   Pdiag{i}=diag(P{i});
end
save(Pdiag_Save_name,'Pdiag');
t=linspace(0,T,N+1);
figure(1);
hold on;
subplot(4,1,1)
hold on
plot(t,Pdiag{1},'-'); % Probability of first state
xlabel('Time (years)')
ylabel('P_1')
subplot(4,1,2)
hold on
plot(t,Pdiag{2},'-'); % Probability of second state
xlabel('Time (years)')
ylabel('P_2')
```

```
subplot(4,1,3)
hold on
plot(t,Pdiag{3},'-'); % Probability of third state
xlabel('Time (years)')
ylabel('P_3')
subplot(4,1,4)
hold on
plot(t,Pdiag{4},'-'); % Probability of Fourth state
xlabel('Time (years)')
ylabel('P_4')
saveas(1,Figure_Name,'fig');
time_used_total=etime(clock,Time0);
if time_used_total>60
    disp_total_running_time=sprintf('Total time used for the program is %f
minutes\n',time_used_total/60);
else
    disp_total_running_time=sprintf('Total time used for the program is %f
seconds\n',time_used_total);
end
disp(sprintf('The program ends at: %s\n',time_display(0)));
disp(disp_total_running_time);
```

lambda0.m:

```
%Program Name: lambda0.m
%Program function: Subroutine for differential transition probability at
%entry time zero
%Program by: Eric Wang
%Program Date: 06/01/2007
%%%%%%%%%%Revision History%%%%%%%%%%%
%Revision Date%%%%%%%Revision reason%%%%%%%%%%
%06/01/2007: Program initial setup
%
%
%
%%%%%%%%%End of Revision History%%%%%%%%
%%
%%%%%%% Functions List %%%%%%%%%%%%%
%Function Name%%%%%%%Function usage %%%%%%%%%
%NONE
%
%
%
```

```
%%%%%%%End of Functions List%%%%%%%%%%%%
%%
function lambda0=lambda0(i,j,m,n)
global I N Delt N_r n_c_nc n_c_c n_p mu sigma beta eta
lambda0=0;
if i==2&j==1
   if n-m<=N_r & n-m+1>N_r
      lambda0=1.0/Delt;
   end
elseif i==3&j==1
   if n>m
lambda=beta/eta*((n-m)*Delt/eta)^(beta-1)*0.95;
   end
elseif i==4&j==1
   if n>m
 lambda=beta/eta*((n-m)*Delt/eta)^(beta-1)*0.05;
   end
elseif i==1&j==2
   if n-m<=n_p& n-m+1>n_p
      lambda0=1.0/Delt;
   end
elseif i==1&j==3
   if n-m<=n_c_nc& n-m+1>n_c_nc
      lambda0=1.0/Delt;
   end
elseif i==1&j==4
   if n-m<=n_c_c& n-m+1>n_c_c
      lambda0=1.0/Delt;
   end
end
```

VITA

Name: Shuwen Wang

Permanent Address: 3133 TAMU

Nuclear Engineering Department

Texas A&M University

College Station, TX, 77843-3133

Email: EricXWang@gmail.com

Education: B.S., Nuclear Engineering, Shanghai Jiao Tong University, 2001

M.E., Nuclear Engineering, Texas A&M University, 2005

Ph.D., Nuclear Engineering, Texas A&M University, 2008